Studies on Selective Partial Oxidation of Methane and Light Alkanes on Solid Metal Oxide Catalysts

Kenji Wada

1992

Studies on Selective Partial Oxidation of Methane and Light Alkanes on Solid Metal Oxide Catalysts

Kenji Wada

1992

Acknowledgements

The studies presented in this thesis are the summaries of the author's work carried out during 1986-1991 at the Department of Hydrocarbon Chemistry, Faculty of Engineering, Kyoto University.

The author would like to express his sincerest gratitude to Professor Yoshihisa Watanabe for his invaluable guidance, suggestions, innumerous instructions and encouragement throughout the course of these studies. Heartfelt thanks go to Professor Toshimitsu Suzuki of Kansai University for giving the author so much instructions, suggestions and encouragement. Thanks are also due to Associate Professor Take-aki Mitsudo and Dr. Teruyuki Kondo for their heartfelt discussions. The author is also grateful to Dr. Tsunehiro Tanaka, Dr. Hiroshi Segawa, and Mr. Hisao Yoshida for the instruction of some experiments and helpful suggestions, and to Dr. Bunsho Ohtani for his kind advice. He also wishes to express his gratitude to Associate Professor Yasushi Tsuji of Gifu University. He is deeply indebted to Associate Professor Kouichi Miura, Messrs. Kazuhiro Mae and Jun-ichi Hayashi of Research Laboratory of Carbonaceous Resources Conversion Technology, Kyoto University for measuring BET surface areas. He thanks Dr. Yoshio Hatanaka of Unocal Japan for providing several rare earth oxides. It is his great pleasure to thank Messrs. Hiroyuki Ohme, Masahide Shima, Kiyomi Yoshida, Fumio Saitoh and Tsuyoshi Takatani for their collaborations and lively discussions, and all members of the research group of Professor Yoshihisa Watanabe.

Finally, the author would like to give his greatest thanks to his parents and brother for their continuous encouragement and support throughout the present studies.

December 1991

Kenji Wada

Contents

Preface

Background

Now we greatly rely on petroleum as the raw materials of chemical feedstocks and energy sources. Most of crude oil reserves are, however, located in the specific areas of the world, such as the Middle East, and the price of crude oil sometimes has been affected by the political situation. In addition, predicted shortage in the supply of crude oil in the near future prompts us to develop an alternative resource to petroleum.

Recently, a new industrial system, so-called 'C_1-chemistry', where methane is one of the fundamental materials as well as syngas, has been attracted much attentions.[1] Methane is the principal component of natural gas, often over 90 mol% of its hydrocarbon fraction, and mainly used as a fuel. Other hydrocarbon components are separated and used as resources of chemical feedstocks. Natural gas is expected to be one of widely reserved and abundant resources. Reserves of natural gas, however, are often located in too remote areas from the place of consumers, and transportation of long distance of liquified natural gas is economically quite inefficient. New conversion technology of methane to transportable liquid fuels is therefore of great importance.

In addition to the use as a fuel, methane is used as a raw material to be converted into syngas and methanol.[2] Mobil Corp. has developed the processes for producing gasoline and light alkenes from methanol.[3] The process for methanol synthesis includes two step reactions.[2] The first step is a high temperature steam reforming of methane into syngas over the NiO/Al_2O_3 catalyst, and the second is a low temperature methanol synthesis, for example over the $Cu/ZnO/Al_2O_3$ catalyst. The first step, however, is a highly endothermic reaction. The requirement of energy input at a high temperature and the complicated equipments make this process economically disadvantageous. Therefore an alternative way of utilizing natural gas is now in progress. The direct conversion of not only methane but also other light alkanes such as ethane and propane into more valuable compounds is an attractive process because of its economical merits.

Numbers of attempts of selective conversion of simple light alkanes under mild conditions have been carried out, and most of them have

focused on methane activation. However, surprisingly few attempts of direct conversion of light alkanes have been successful,[2] mainly because of their high molecular stabilities (see Table 1).[4]

Table 1. Characteristics of light alkanes[4]

RH molecules	R	D_{R-H}[a] (kJ·mol^{-1})	IP[b] (eV)	PA[c] (eV)	pKa
CH_4	CH_3	435	12.7	5.3	40
C_2H_6	C_2H_5	410	11.5	5.6	42
C_3H_8	*n*-C_3H_7	410	11.1	6.1	-
C_3H_8	*iso*-C_3H_7	397	-	-	44

[a] C-H bond dissociation energy.

[b] Ionization potential

[c] Proton affinity.

Partial Oxidation of Methane into Oxygen-containing Chemicals

Obviously the one-step conversion of methane into more useful chemicals by partial oxidation would be the better way to utilize the natural gas reserves than the syngas process. Partial oxidation of methane to methanol or methanal is thermodynamically favored, but deep oxidation to carbon oxides is more favorable. Therefore a high temperature is required to give methanol or methanal selectively under the kinetic control conditions.[2]

	ΔG (at 700 K, kJ·mol^{-1})	
$CH_4 + 1/2O_2 \longrightarrow CH_3CHO$	-92	(1)
$CH_4 + O_2 \longrightarrow HCHO + H_2O$	-293	(2)
$CH_4 + 3/2O_2 \longrightarrow CO + 2H_2O$	-569	(3)
$CH_4 + 2O_2 \longrightarrow CO_2 + 2H_2O$	-791	(4)

Partial oxidation of methane using molecular oxygen as an oxidant[2] has been studied by many researchers ever since early 1920s.[5,6] The reaction was usually performed on severe conditions, at a high temperature under high pressure. The first commercial attempt has been developed in Germany during the 1940s.[7] The process using a solid oxide based catalyst has also been developed. The catalyst most widely studied is molybdenum oxide based one. Several multicomponent oxides based on molybdenum oxide such as $Fe_2O_3 \cdot (MoO_3)_3$ were reported to be excellent catalysts by the researchers in ICI England.[8] The reaction was typically operated at *ca.* 5 MPa and at around 750 K, and the yield of methanol reached 1.4%. Recent processes over the noble metal loaded catalysts[9] or the solid oxide catalysts[10] afforded methanal in the yield of 5 8%. Addition of a small amount of dimethyl ether or organic halides increased the yield of methanal in these studies. Although some of these processes exhibited the high yields with the high selectivities for the formation of methanol and methanal, only few of them were actually put into practical use, because of their ineffectiveness in economy, complicated engineering, and hazards of explosion.

Selective partial oxidation of methane at atmospheric pressure was studied over the MoO_3/SiO_2 and MoO_3/Cab-O-Sil catalysts using N_2O as an oxidizing reagent by Lunsford et al.[11,12] The methane conversion of 26.7% and the combined selectivity for methanol and methanal of 98.9% were achieved at 823 K. They proposed that O^- anion radical produced by the decomposition of N_2O would be the active species on the catalyst surface. Partial oxidation of ethane with N_2O selectively yielded ethanal and ethene.[14] Some of the key species, e.g. $CH_3\cdot$, O^- and CH_3O^-, have been detected by IR and ESR measurements. It is generally accepted that O^- species on the catalyst surface is responsible for the selective C-H activation of light alkanes.[2] Later, the O^- species was found to be able to react with methane even below a room temperature.[13] Although these process can convert methane and ethane selectively into oxygen-containing chemicals in high yields, N_2O is prohibitively expensive to use on the industrial scale.

Formation of the proposed active oxygen species, O^-, from molecular oxygen is considered to be possible on the surface of the supported MoO_3 or V_2O_5 catalysts having M=O double bond.[2] The studies using molecular oxygen or air as an oxidant have been investigated mainly on the supported MoO_3 catalysts. Pitchai and Klier[2] investigated

the reaction on MoO_3/silica-alumina in the presence of steam, and reported that methanal was formed in the highest selectivity of 47% in the reaction at 873 K with high CH_4/O_2 ratio of 17.5. The yield of methanal was, however, very low, and only amounted to 0.3%. The attempts over aluminosilicates,[15] Y-type zeolite[16] and $FeNbO_4 \cdot B_2O_3$[17] were not successful to convert methane selectively to oxygen-containing chemicals in high yields.

Photocatalytic Oxidation of Light Alkanes

Photocatalysis using metal oxide catalysts is one of the fields of current interest because of its potential ability for a photoenergy conversion and the selectivity in the reactions that can not be achieved in the thermal catalytic reactions.[18] If the reaction proceeds with visible light irradiation in high efficiency, it should be more attractive from the viewpoint of effective utilization of the sun light. The studies on photocatalytic reactions over solid metal oxides have been extended to selective partial oxidation of alkanes leading to more valuable compounds.[19-29]

The possibility of formation of O^- spec.es by photoactivation of supported metal oxides and solid oxide semiconductors is now generally accepted. Kazansky and co-workers have investigated the reaction of methane with surface O^- species produced by γ-irradiation or UV irradiation over V^{5+}/SiO_2. They reported the formation of carbon oxides together with a small amount of methanal.[21] Ever since the pioneer work of Kazansky et al., many researchers have tried selective photo-oxidation of methane and other light alkanes at an ambient temperature over the various catalysts.[22-30] Most of them, however, resulted in the predominant formation of carbon oxides. Although only few studies have been reported to be successful until now,[22] the photocatalytic reactions would be one of the promising approach to achieve the selective activation of light alkanes, since the potential performances of the photocatalysis of the partial oxidation are expected to be very high.[19]

Catalytic Oxidative Coupling Reactions using Methane

One of the recent topics in the field of C_1-chemistry is production of ethane and ethene by oxidative coupling of methane.[31] The direct thermal

conversion of methane to ethane and ethene is a quite inefficient endothermic process, and requires a very high temperature to obtain a significant conversion of methane. Thermodynamic constraints can be surmounted in the oxidative system because of the reaction to be exothermic.

	ΔG (at 1000 K, kJ·mol^{-1})	
$2CH_4 \longrightarrow C_2H_6 + H_2$	+71	(5)
$2CH_4 + 1/2O_2 \longrightarrow C_2H_6 + H_2O$	-160	(6)

Keller and Bhasin[32] of Union Carbide examined the coupling of methane over a series of metal oxide catalysts at atmospheric pressure using a cyclic reaction system to minimize deep oxidation of the products. In their study, a lattice oxygen of the catalyst converted methane to higher hydrocarbons in the absence of molecular oxygen at 873 - 1273 K. The reduced oxide catalyst was re-oxidized in a stream of air without feeding methane. Oxides of Mn, Cd and Tl were the excellent catalysts. After the pioneering work of Keller and Bhasin, oxidative coupling of methane has attracted much attention and a large number of catalytic systems have been developed.[33-50] Hinsen and Baerns[33] studied oxidative coupling of methane in a continuous flow of the reaction gas containing both methane and oxygen. They found that a silica supported PbO catalyst showed the high selectivity for ethane and ethane (C_2 compounds) approaching 72%. The basic oxide catalyst such as Li-doped magnesium oxide[34,35] and rare earth oxide[36,37] showed excellent activities and selectivities for the formation of C_2 compounds in the flow system at 923 - 1023 K. An anion radical, O^-, was considered to be active and selective oxygen species. The selectivity for C_2 compounds has reached over 70% at a significant level of methane conversion.[31] Although there are still numbers of difficult problems such as high reaction temperatures to be put into the practical use, oxidative coupling of methane has provided a new route to the production of more valuable hydrocarbons starting from methane.

In addition to oxidative 'homo' couping of methane, cross coupling between methane and other hydrocarbons, so called 'oxidative methylation' has been developed by researchers of USSR in late 1970s.[51,52] Methane reacted with hydrocarbons having a methyl group flanking to the electron withdrawing groups, such as toluene and acetonitrile, in the

presence of the oxides of Mo, Bi and Zn promoted with alkali and alkaline earth metals. Details of the catalyst and the procedure, however, have not been well disclosed. Oxidative methylation of toluene yielded ethylbenzene, styrene and benzene together with carbon oxides and hydrogen. Acrylonitrile was formed from methane and acetonitrile. These processes seem to have a possibility to provide a new route to utilize natural gas.

Survey of This Thesis

The purpose of this thesis is to evolve the new methodology for activation of stable C-H bond in light akanes, especially that of methane, by selective partial oxidation over the solid oxide catalysts. As described above, although direct partial oxidation of light alkanes into oxygen-containing chemicals is quite attractive target of the study, it seems very difficult to selectively obtain desired products under mild conditions by the usual heterogeneous catalysis in the thermal reaction.[2] Photocatalytic processes at an ambient temperature have often resulted in deep oxidation,[19] probably because most of the products could not desorb from the surface of the catalyst before suffering from deep oxidation. The present author therefore examined photocatalytic oxidation of light alkanes into oxygen-containing chemicals at elevated temperatures so that the surface species desorb promptly from the catalyst.

In the studies of oxidative dimerization of methane, the reactant gas mixture has been usually diluted with an inert gas such as He or N_2 to avert the risk of explosion.[31] But none of the studies have carried out the reaction using chemically reactive diluent, such as carbon dioxide. Thus the present author examined effects of employing carbon dioxide as a diluent of the reactant gas for oxidative dimerization of methane. The present author then investigated the activities of the group IIA and IIIB metal oxide based catalysts for oxidative methylation of toluene with methane, because they have been reported to be excellent for oxidative coupling of methane.[34-36] Oxidative methylation of simple light alkane, ethane, with methane was also examined over the rare earth oxide based catalysts.

This thesis consists of two parts. Part I, which encompasses chapters 1 to 4, deals with selective photocatalytic oxidation using the supported molybdenum oxide catalysts[53,54] and the solid oxide semiconductors, mainly the zinc oxide catalysts,[55] in the presence of

molecular oxygen. The first example of selective photocatalytic partial oxidation of methane to methanal is presented in this part. The author found that elevated reaction temperatures up to 450 - 550 K induced drastic increases in the catalytic activities and selectivities for the partial oxidation of methane, ethane and propane. Chapter 3 deals with effects of loading of various metal oxides to the parent zinc oxide catalysts in order to improve the selectivity of methane oxidation.[55] Furthermore, chapter 4 extended the investigation of photocatalytic oxidation of propene at an elevated temperature.

Part II, which is composed of chapters 5 to 7, deals with the new thermal catalytic reactions with methane in the presence of molecular oxygen, the oxidative coupling reactions of hydrocarbons with methane over various basic solid metal oxide catalysts. In chapter 5, effects of the use of carbon dioxide as a reactive diluent of the reactant gas mixture on oxidative coupling of methane are described. The activities and selectivities of several group IIA and IIIB metal oxide based catalysts were found to be improved.[56] Effects of methods of preparation of the catalysts are discussed. Chapter 6 deals with the oxidative cross-coupling of methane (oxidative methylation) with toluene to form styrene and ethylbenzene using the alkali and alkaline metal halide loaded rare earth oxide catalysts at around 1023 K.[57,58] Studies on the production of propane and propene by oxidative methylation of ethane with methane are described in chapter 7. Several rare earth oxides were found to be the excellent catalysts for this reaction.

References

1 D.L. King, J.A. Cusumano and R.L. Garten,
Catal. Rev.-Sci. Eng., 23, **1981**, 233.

2 R. Pitchai and K. Klier,
Catal. Rev.-Sci. Eng., 28 (1), **1986**, 13.

3 C.D. Chang and A.J. Silvestri, *J. Catal., 47*, **1977**, 249.
C.D. Chang, *Catal. Rev.-Sci. Eng., 26*, **1984**, 323.

4 A.E Shilov, *Activation of Saturated Hydrocarbons by Transition Metal Complexes,* D. Reidel Publishing Company, Holland, **1984**.

5 D.M. Newitt and A.E. Haffner,
Proc. Royal Soc. London, Ser. A, 134, **1932**, 591.

6 H.D. Gasser and N.R. Hunter, *Chem. Rev., 85,* **1985**, 235.

7 M.M. Holm and E.H. Reich, *Fiat Report No. 1085,* Office of Military Government of Germany, March 31, **1947**, in Ref. 2.

8 D.A. Dowden and G.T. Walker, U.K. Patent 1244001, **1971**, in Ref. 2.

9 R.S. Mann et al., *CA, 90*, 22254w.

10 A.Ya. Averbukh et al., *CA, 92*, 93839t, 58174a.

11 H.F. Liu, M. Iwamoto and J.H. Lunsford,
J. Chem. Soc., Chem. Commun., **1982**, 78.

12 H.F. Liu, R.S. Liu, K.W. Liew, R.E. Johnson and J.H. Lunsford,
J. Am. Chem. Soc., 106, **1984**, 4117.

13 T. Tashiro, T. Ito and K. Doi,
J. Chem. Soc., Faraday Trans., 86 (7), **1990**, 1139.

14 L. Mendelovici and J.H. Lunsford, *J. Catal., 94,* **1985**, 37.

15 B.M. Ershov, P.M. Stadnik and V.I. Gomanai, *Katal. Katal., Akad Nauk Ukr. SSR Respub. Mezhvedom Sb, 3,* **1967**, 111 in Ref. 2.

16 I.P Mukhlenov, A.R. Vilenslii and A. Ya. Averbukh, *Izv. Vyssh. Ucheb. Zaved., Khim. Khim. Tekhnol., 13,* **1970**, 1636, in Ref. 2.

17 K. Otsuka, T. Komatsu, K. Jinno, Y. Uragami and A. Morikawa,
Proc. 9th. Congr. Catal. Calgary, **1988**, 915.

18 M. Grätzel, *Energy Resourse through Photocatalysis and Catalyis,* Academic Press, New York, **1983**.

19 M. Formenti and S.J. Teichner, *Catalysis,*
The Chemical Society, London, *2*, 87, **1978**.

20 R.I. Bickley, *Catalysis,* The Chemical Society, London, *5,* 308, **1982**.

21 S.L. Kaliaguine, B.N. Shelimov and V.B. Kazansky,
J. Catal., 55, **1978**, 384.

22 M.D. Ward, J.F. Brazdil, S.P. Mehandru and A.B. Anderson, *J. Phys. Chem., 91*, **1987**, 6515.
23 K. Marcinkowska, S. Kaliaguine and P.C. Roberge, *J. Catal., 90*, **1984**, 49.
24 S.F. Gerasimov, *React. Kinet. Catal. Lett., 32(1),* **1986**, 57.
25 W. Hill, B.N. Shelimov and V.B. Kazansky, *J. Chem. Soc., Faraday Trans. 1, 83 (3)*, **1987**, 2381.
26 K. Marcinkowska, S. Kaliaguine and P.C. Roberge, *Proc. 9th. Congr. Catal. Calgary*, **1988**, 521.
27 N. Djeghri, M. Formenti, F. Juillet and S.J. Teichner, *Faraday Discuss. Chem. Soc., 58*, **1984**, 185.
28 M. Daroux, D. Klvana, M. Duran and M. Bideau, *Can. J. Chem. Eng., 63*, **1985**, 668.
29 K.R. Thampi, J. Kiwi and M. Grätzel, *Catal. Lett.,* **1989**, 109.
30 M. Grätzel, K.R. Thampi and J. Kiwi, *J. Phys. Chem., 93,* **1989**, 4128.
31 for a review, J.S. Lee and S.T. Oyama, *Catal. Rev.-Sci. Eng., 30 (2),* **1988**, 249.
32 G.E. Keller and M.M Bhasin, *J. Catal., 73,* **1982**, 9.
33 W. Hinsen, W. Bytyn and M. Baerns, *Proc. 8th. Congr. Catal. Weinheim*, **1984**, 581.
34 T. Ito, J.X. Wang, G.H. Lin and J.H. Lunsford, *J. Am. Chem. Soc., 107,* **1985**, 5062.
35 C.H. Lin, T. Ito, J.X. Wang and J.H. Lunsford, *J. Am. Chem. Soc., 109,* **1987**, 4808.
36 K. Otsuka, K. Jinno and A. Morikawa, *Chem. Lett.,* **1985**, 499.
37 K. Otsuka, *Sekiyu Gakkaishi, 30,* **1987**, 385.
38 T. Imai and T. Tagawa, *J. Chem. Soc., Chem. Commun.,* **1986**, 52.
39 K. Aika, T. Moriyama, N. Takasaki and E. Iwamatsu, *J. Chem. Soc., Chem. Commun.,* **1986**, 1210.
40 A. Morikawa, N. Takasaki, E. Iwamatsu and K. Aika, *Chem. Lett.,* **1986**, 1165.
41 K. Asami, S. Hashimoto, T. Shikada, K. Fujimoto and H. Tominaga, *Chem. Lett.,* **1986**, 1233.
42 I. Matsuura, Y. Utsumi, M. Nakai and T. Doi, *Chem. Lett.,* **1986**, 1981.
43 N. Yamagata, K. Tanaka, S. Sasaki and S. Okazaki, *Chem. Lett.,* **1987**, 81.

44 K. Otsuka and T. Komatsu,
J. Chem. Soc., Chem. Commun., **1987**, 388.
45 K. Otsuka, Y. Shimizu and T. Komatsu, *Chem. Lett,* **1987**, 1835.
46 E. Iwamatsu, T. Moriyama, N. Takasaki and K. Aika,
J. Chem. Soc., Chem. Commun., **1987**, 19.
47 K. Machida and M. Enyo,
J. Chem. Soc., Chem. Commun., **1987**, 1639.
48 K. Fujimoto, S. Hashimoto, K. Asami and H. Tominaga,
Chem. Lett., **1987**, 2157.
49 J.M. Thomas, X. Kuan and J. Stachurski,
J. Chem. Soc., Chem. Commun., **1988**, 162.
50 J.E. France, A. Shamsi and M.Q. Ahsan,
Energy & Fuels, 2, **1988**, 235.
51 Kh.E. Kcheyan, O.M. Revenko and A.N. Shatalova,
Proc. -World Pet. Congress., 11(4), **1984**, 465, and references therein.
52 N. Yakovich, L.P. Bokareva and A.G.Kostyuk,
Pr-va Krupnotonnazhn, Prouktov Neftekhimii, M., **1979**, 37
in *Chem Abstr., 93,* **1980**, 7755d.
53 T. Suzuki, K. Wada, M. Shima and Y. Watanabe,
J. Chem. Soc., Chem. Commun., **1990**, 1059.
54 K. Wada, K. Yoshida, Y. Watanabe and T. Suzuki,
Appl. Catal., 74, **1991**, L1.
55 K. Wada, K. Yoshida, Y. Watanabe and T. Suzuki,
J. Chem. Soc. Chem. Commun., **1991**, 726.
56 T. Suzuki, K. Wada and Y. Watanabe, *Appl. Catal., 59,* **1990**, 213.
57 T. Suzuki, K. Wada and Y. Watanabe, *Appl. Catal., 53,* **1989**, L19.
58 T. Suzuki, K. Wada and Y. Watanabe,
Ind. Eng. Chem. Res., 30, **1991**, 1719.

Part I

Selective Activation of C-H Bond in Light Alkanes via Photocatalytic Partial Oxidation using Metal Oxide Catalysts at Elevated Temperatures

Chapter 1

Selective Photocatalytic Oxidation of Methane and Light Alkanes to Oxygen-containing Chemicals using Silica Supported Molybdenum Oxide Catalysts

Abstract

Photocatalytic partial oxidation of methane, ethane and propane was performed over supported molybdenum oxide catalysts at elevated temperatures using a fluidized bed flow type reaction system under UV irradiation. The MoO_3/SiO_2 catalysts showed the activities for selective photo-oxidation of light alkanes to form oxygen-containing chemicals at 450 500 K, whereas the reactions at an ambient temperature gave only very small amounts of the products. The 4.4 wt.% MoO_3 loaded catalyst gave methanal from methane in the highest yield of 19 $\mu mol \cdot h^{-1}$ together with a small amount of methanol at 503 K. Formation of carbon oxides was not observed. The reactions required UV irradiation of a wavelength shorter than 300 nm. The yield of methanal was greatly affected by the reaction temperature, the loading level of MoO_3, and the light intensity. Photo-oxidation of ethane and propane also selectively gave the corresponding aldehydes and ketones in higher yields (~80 $\mu mol \cdot h^{-1}$). Active sites on the surface seemed to come from terminal tetrahedrally coordinated Mo=O groups in multilayers of molybdenum species, on the basis of XPS, UV and XRD studies. The photocatalytic oxidation was considered to be initiated by the formation of surface charge transfer complex, Mo^{5+}-O^-.

Introduction

Direct conversion of light alkanes over solid oxide catalysts has attracted much attention and has been studied for many years. However, the functionalization of unactivated C-H bond in light alkanes, especially methane, is very difficult. Known processes to utilize such alkanes under severe conditions at higher temperatures under high

pressure, are usually nonselective. Therefore only few attempts to convert methane and ethane directly into oxygen-containing chemicals with high selectivities have been successful.[1]

Photocatalytic oxidation of methane or ethane over solid oxide catalysts has been studied extensively.[2-9] Kaliaguine et al.[2] have investigated the reactions of methane and ethane with hole centers generated by γ-irradiation of metal complexes (e.g. V^{5+}-O^-) dispersed on silica, and reported the formation of carbon dioxide as the main product together with a small amount of methanal. They proposed that the reaction was initiated by O^- anion radical. Photoinduced reactions of methane with molybdenum oxide supported on silica in the absence of oxygen were reported to give small amounts of C_2 and C_3 hydrocarbons.[3] Ward et al.[4] reported selective photo-oxidation of methane over the silica supported MoO_3 or $CuMoO_4$ catalysts. The reactions performed at 313 - 373 K yielded a small amount of methanol without deep oxidation, but methanal was not obtained. Photo-oxidation of a higher alkane, propane, on the supported molybdenum oxide catalysts has been investigated.[10,11] In these studies, the reaction was carried out at an ambient temperature, and produced ethanal, propanal and acetone together with large amounts of carbon oxides.

Photo-oxidation of light alkanes over n-type solid oxide semiconductors has been also studied.[5-8] Photoinduced reaction of ethane with molecular oxygen over TiO_2 gave ethanal with the selectivity of 18% at the ethane conversion of 0.6%. Oxidation of methane was not successful.[5] Grätzel et al.[6] investigated photo-thermal oxidation of methane over TiO_2, and reported that an increase in the reaction temperature to 473 K enhanced the formation of carbon monoxide which was not observed at 320 K. They also reported the reaction on TiO_2 promoted with MoO_3 or heteropolymetalates such as $(SiW_{12}O_{40})^{-4}$.[7] The reactions afforded predominantly carbon monoxide. However, none of oxygen-containing chemicals such as methanol and methanal was obtained. Recently, theoretical studies have been done in addition to the experimental ones.[4,12]

In the present chapter, selective photo-oxidation of light alkanes, from methane to propane, into corresponding aldehydes and ketones on supported molybdenum oxide catalysts is described.[13,14] The reactions over various catalysts under varieties of reaction conditions were carried

out. The possible reaction paths and active surface species are briefly discussed.

Experimental Section

Materials

Typical silica supported molybdenum oxide catalysts, without any remarks in the text, were prepared by an usual pore volume impregnation method. Silica gel (Alfa, surface area; 300 $m^2.g^{-1}$, mean particle size; 10 μm, pore volume; 1.6 $cm^3.g^{-1}$), γ-alumina (Nishio), low alumina (Shokubai Kasei, alumina; 13%) or high alumina (Shokubai Kasei, alumina; 29%) was impregnated overnight in an aqueous solution of ammonium heptamolybdate followed by vacuum evaporation at 323 K. The pH of the pristine solution was 6. Where necessary, pH was adjusted to 1 or 11 by adding an aqueous solution of HNO_3 or NH_4OH, respectively. The dried catalyst was then calcined in air at 823 K for 120 min. Other MoO_3/SiO_2 catalysts were prepared by the following procedure, an equilibrium adsorption method. Support (2 g) was impregnated in 100 cm^3 of an aqueous solution of ammonium heptamolybdate (0.007 M) for 72 h with vigorous stirring. The pH of the solution was adjusted with dilute HNO_3 and NH_4OH solutions. The basic solution was colorless, but solutions at pH 1 and 5.5 colored yellow and faint yellow, respectively. After filtration and washing with 5 cm^3 of distilled water, the dried residual solid was calcined in the same manner applied in the usual impregnation method. One of the MoO_3/SiO_2 was prepared as follows: the vapor of $Mo(CO)_6$ was introduced into the vessel containing dried silica gel. The $Mo(CO)_6$-adsorbed silica gel was subjected to UV irradiation in a stream of air for 30 min, and then calcined in air at 823 K for 120 min. A part of molybdenum oxide loaded on the support was reported to be lost during the calcination in air at the high temperature above 823 K.[1] Therefore amounts of molybdenum containing in MoO_3/SiO_2 catalysts after the calcination at 823 K were measured by the atomic absorption analysis. In the measurements, molybdenum oxide was leached out from the catalyst with a dilute NH_4OH solution. The catalysts mounted in the reaction apparatus were again subjected to *in situ* calcination in a

stream of air at 823 K for 120 min, and then UV irradiation at the same temperature as the reaction in air for 30 min.

Highly purified methane (> 99.9%, including ethane less than 0.01% and none of other higher hydrocarbons) was used without any further purification. The delivered ethane including a small amount of CO_2 and H_2O was slowly passed over a column filled with pulverized fused potassium hydroxide and molecular sieves-5A, and then fed to the reactor. Propane, helium and oxygen were used as received.

Apparatus and Procedures

The reaction was carried out using an upstream fluidized bed flow reactor equipped with a preheater and a window for UV irradiation (10 mm x 20 mm, inner thickness; 1 mm), as illustrated in Figure 1. The reactant gas mixture was passed through the preheater (maximum temperature; 823 K) to maintain the temperature of the fluidized catalyst bed. There were variations in the temperature of *ca.* 15 K between the top and the bottom of the catalyst bed. UV irradiation was performed using 3 types of high pressure mercury vapor lamp; 200 W one (arc length; 150 mm, further designated as lamp A), 75 W one (Toshiba Rikagaku Inc., arc length; 15 mm, lamp B) and 200 W one (arc length; 75 mm, lamp C). Relative intensity of the light flux into the catalyst bed was measured by the chemical actinometry using ferric ammonium oxalate, and estimated to be 1 : 1 : 3 for lamps A : B : C. These values contained considerable errors ranging 20%, because of the lack of accuracy in the measurements. The reaction was carried out typically with 0.025 g of the catalyst, 7.5 mmol·h^{-1} of alkane. For oxidation of methane, W/F of 0.62 g·h·mol^{-1}, space velocity of 10000 h^{-1} and the ratio CH_4 : O_2 : He of 6 : 2 : 25 were employed. The oxidation conditions of ethane and propane were as follows: W/F; 0.71 g·h·mol^{-1}, space velocity; 8200 h^{-1}, alkane feed rate; 7.5 mmol·h^{-1}, C_2H_6 : O_2 : He; 6 : 1 : 21 or C_3H_8 : O_2 : He; 3 : 1 : 10. Liquid products from oxidation of methane, ethane and propane were collected in a trap filled with distilled water at 273 K, in an acetone trap at 195 K and in a methanol trap at 195 K, respectively. Gaseous products were collected in gas sampling bags. After a certain reaction period, the feed of gas mixture was stopped, and the outlet was closed. Then the catalyst bed was cooled down to a room temperature, and flushed with argon (5 cm^3·min^{-1}) for 10 min. Again the catalyst bed was heated in a stream of

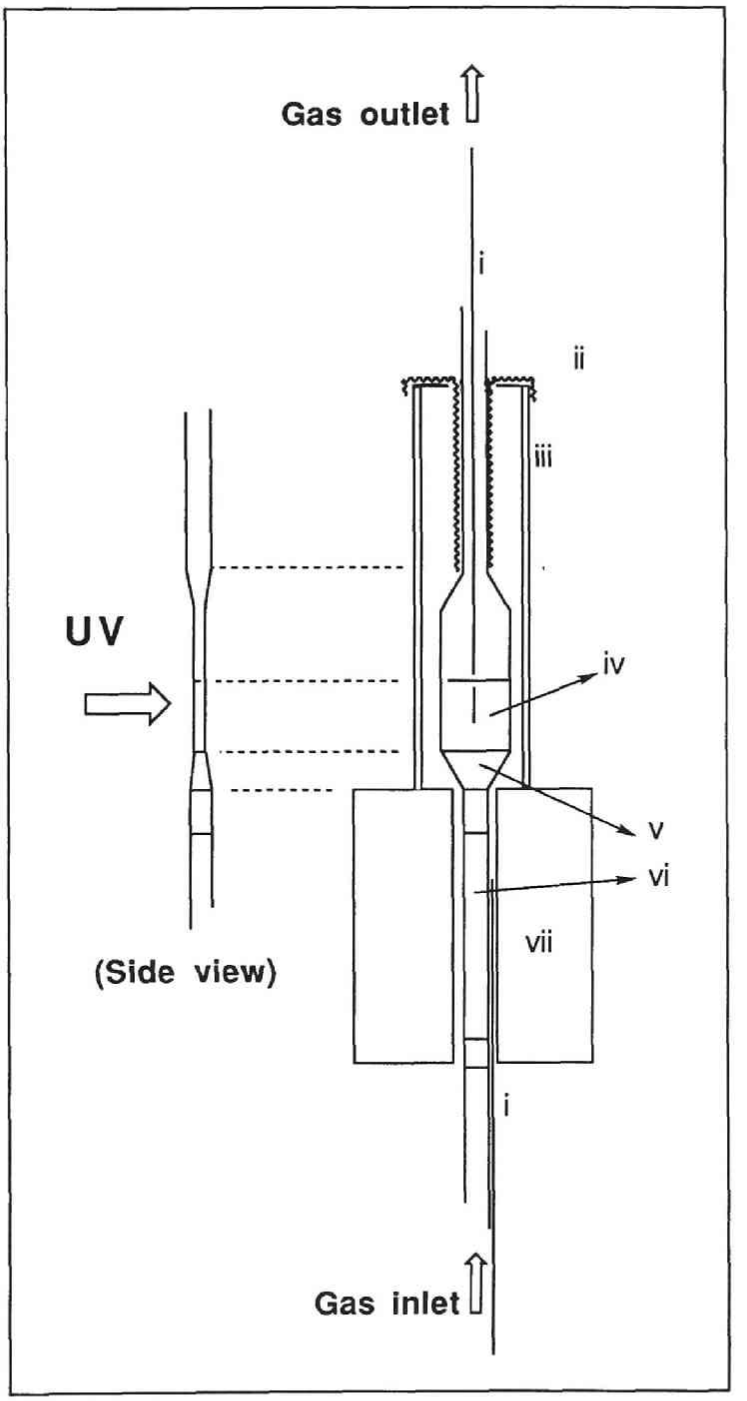

Figure 1. A part of experimental apparatus for photo-oxidation of alkanes: (i) thermocouples, (ii) aluminium foil cover, (iii) quartz glass tube cover, (iv) fluidized catalyst bed, (v) silica sand (22-60 mesh), (vi) silica sand (>22 mesh), (vii) electric furnace.

argon (5 $cm^3 \cdot min^{-1}$, 27.5 $K \cdot min^{-1}$) up to 823 K without irradiation, and then kept for 10 min. An effluent gas was passed through the cold trap and collected into a gas sampling bag.

Analysis

The products were analyzed using gas chromatography: a Porapak-Q column at 353 K with an FID for C_1 - C_4 hydrocarbons and at 433 K for methanol, ethanal and ethanol; a Porapak-N column at 433 K with an FID for acetone and propanal; a TSG-1 on Shimarite-F column, distributed from Shimadzu Co. Ltd., at 393 K with a TCD for methanal; a molecular sieves-5A column at 323 K with a TCD for oxygen; and an active carbon column at 323 K with a TCD for H_2, CO and CO_2.

An atomic absorption analysis was carried out using an AA-8200 atomic absorption / flame emission spectrometer (Nippon Jarrell Ash Inc.). BET surface area of the catalysts was measured with a BELSORP 28, a microprocessor-controled automatic system using N_2 at 77 K, from BEL Japan Inc. An X-ray diffraction study was performed using a RIGAKU Geigerflex with Kα-ray of copper in the range $5° < 2\theta < 70°$.

UV-visible diffuse reflectance spectra were measured with a Shimadzu model MPS-2000 multipurpose spectrophotometer, in which reflected beams were gathered by an integrating sphere (50 mm inner diameter). A UV cell (10 mm x 40 mm, 1 mm inner thickness) equipped with a branched chamber and a stop valve was used in order to avoid any contact with moisture. The catalyst submitted for the measurement was heated in the branched chamber at 573 K under atmospheric pressure for 30 min, then evacuated at 823 K for 30 min followed by the treatment under 150 torr (1 torr; 133.3 $N \cdot m^{-2}$) of oxygen at 823 K for 120 min. Then the catalyst was transferred into the UV cell, and measured *in vacuo*. Magnesium oxide (Wako) as used as a reflectance standard. All the spectra are modified in terms of the Kubelka-Munk function,[15]

$$F(R'_{\infty,sample}) = \frac{(1 - R'_{\infty,sample})^2}{2R'_{\infty,sample}}$$

The reflectance value of the sample, $R'_{\infty,sample}$, is experimentally determined from reflectance of the catalyst relative to MgO standard,

$$R'_{\infty,sample} = \left[\frac{R'_{\infty,sample}}{R'_{\infty,MgO}}\right] \times R'_{\infty,MgO}$$

where $R'_{\infty,MgO}$ is defined to be 1.

XPS (X-ray photoelectron spectroscopy) spectra of the MoO_3/SiO_2 catalysts were acquired using a Perkin-Elmer 5500 MT system equipped with a hemispherical energy analyzer. The catalyst pretreated in air at 823 K for 2 h was mounted on indium foil and then transferred to an XPS analyzer chamber. The residual gas pressure in the chamber during data acquisition was less than 1×10^{-8} torr. XPS spectra were measured at a room temperature using Mg $K\alpha_{1,2}$-ray radiation (15 kV, 400 W). The extent of dispersion of supported molybdenum species was estimated on the basis of relative peak area intensities of Mo(3p3) (398.2 eV), Mo($3d_{5/2}$) (232.7 eV), Mo($3d_{3/2}$) (235.9 eV), Si(2p) (103.3 eV), O(1s) (531.1 eV), and C(1s) (285.0 eV). The electron take off angle was set at 45 deg. Spectral accumulation time was approximately 40 min for Mo(3p3) and 10 min for Si(2s) lines. Binding energies were referenced to the Si(2p) level for the catalyst support, SiO_2.

Results

Characterization of the Catalysts

Figure 2 shows XRD patterns of the impregnated MoO_3/SiO_2 catalysts at various loading levels. A pattern common to all the samples could be identified as poorly crystalline silica gel. For the catalyst loaded with 13 wt.% of MoO_3, peaks attributed to a crystalline MoO_3 appeared. They were further developed with an increase in a loading level. This clearly indicates formation of a large crystallite of MoO_3 on the surface of the catalysts at a higher loading level.

Figure 3 shows UV diffuse reflectance spectra of some of the silica supported MoO_3 catalysts. A major absorption band around 240 250 nm together with a shoulder peak around 280 nm was detected for the MoO_3 (2.5 wt.%)/SiO_2 catalyst (iii) and 4.4 wt.% loaded one (ii). On the other hand, the MoO_3 (21 wt.%) loaded catalyst exhibited the strong absorption band around 300 nm, in addition to that around 240 nm. Absorption at 280 nm was not confirmed on this catalyst, probably due to overlapping with the predominant band at 300 nm. The spectra of the catalysts

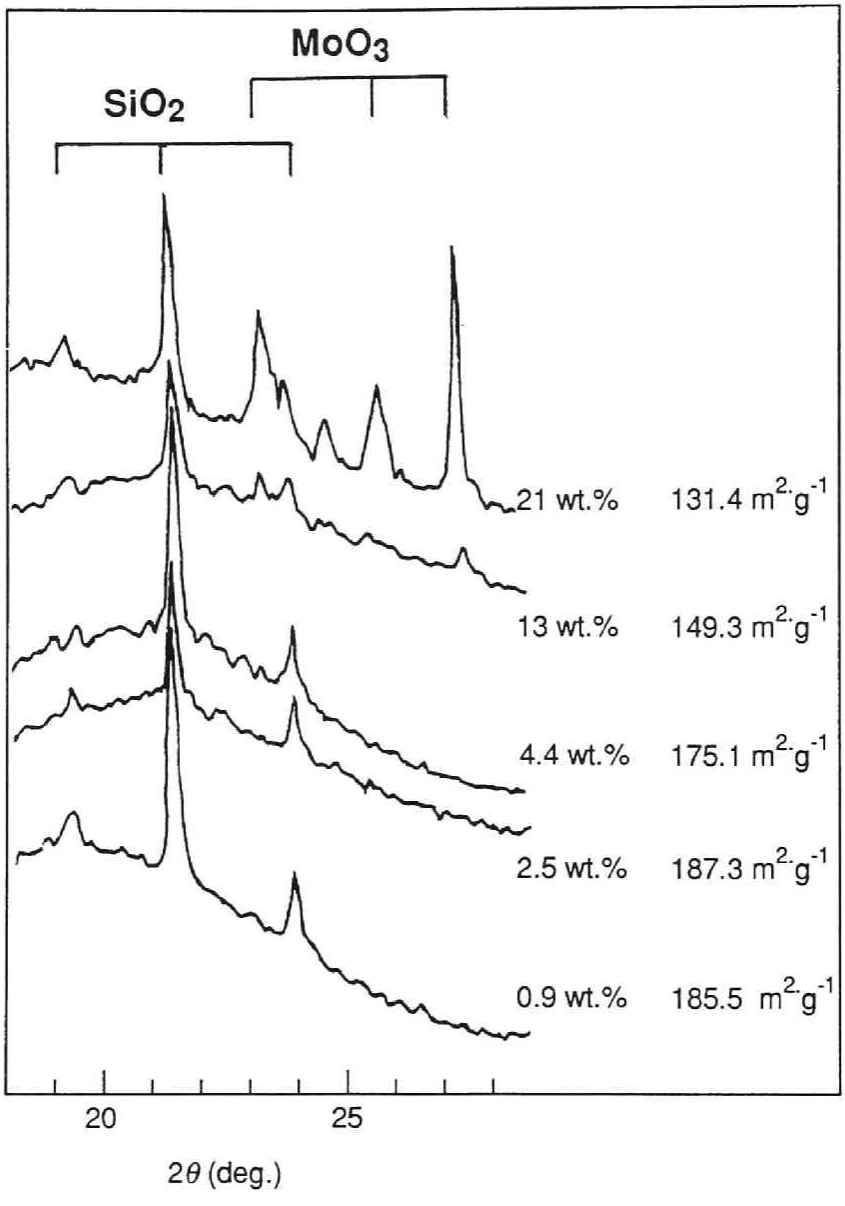

Figure 2. XRD patterns and BET surface areas of the MoO_3/SiO_2 catalysts prepared by the impregnation method of various loading levels.

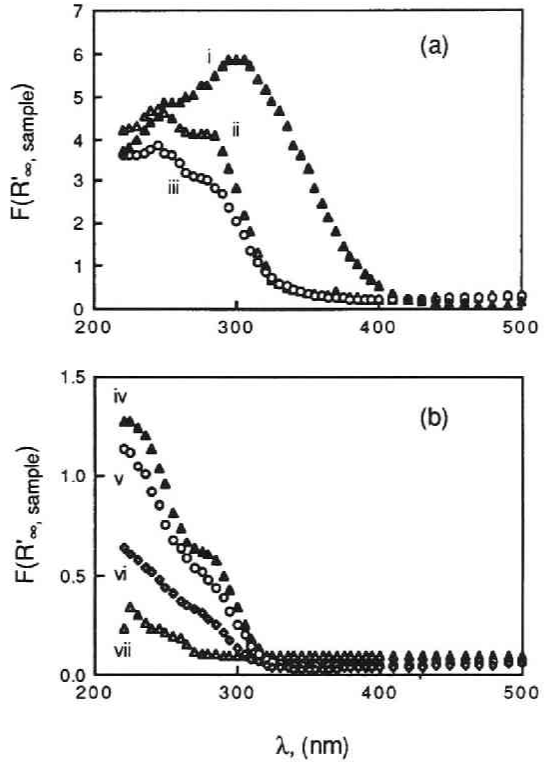

Figure 3. UV diffuse reflectance spectra of the MoO_3/SiO_2 catalysts prepared by the (a) impregnation method at pH = 6 of (i) 21 wt.%, (ii) 4.4 wt.%, (iii) 2.5 wt.% loading, and (b) equilibrium adsorption method from the solution at (iv) pH = 1, (v) pH = 5.5, (vi) pH = 11. (vii) = SiO_2 support.

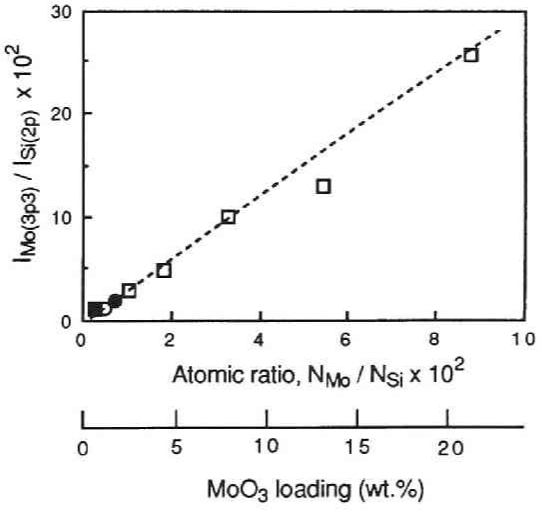

Figure 4. The XPS intensity ratio $I_{Mo(3p3)} / I_{Si(2p)}$ as a function of overall atomic ratio of Mo and Si of the MoO_3/SiO_2 catalysts prepared by the (□) impregnation method, (●) equilibrium adsorption method at pH = 1, (○) pH = 5.5, and (■) pH =11.

prepared by the equilibrium adsorption method from acidic and neutral solutions showed absorption bands around 240 nm and 280 nm, whereas the catalyst prepared at pH 11 showed very weak absorptions. It should be noted that the moisture exposed MoO_3(2.5 wt.%)/SiO_2 catalyst showed a new strong absorption band around 320 - 330 nm.

In Figure 4, the ratio of the XPS intensities of the Mo(3p3) and Si(2s), $I_{Mo(3p3)}/I_{Si(2s)}$, of the MoO_3/SiO_2 catalysts are plotted as a function of the overall atomic ratio (N_{Mo}/N_{Si}). The $I_{Mo(3p3)}/I_{Si(2s)}$ curve for the catalyst prepared by the impregnation method at pH 6 can be represented as a straight line passing through the data of the 2.5 wt.% loaded catalyst to the 21 wt.% loaded one. It is generally accepted that the straight line of $I_{Mo(3p3)}/I_{Si(2s)}$ versus N_{Mo}/N_{Si} passing through the origin can be interpreted as the formation of well dispersed species on the surface. The XRD analysis of Figure 2, however, clearly shows the formation of the crystallite of MoO_3 on the catalyst surface containing Mo above 5.4 mol%. These results seem to suggest Mo segregation or formation of multilayer species on the surface of the support even with the catalyst in low Mo content. The data obtained with the catalysts prepared by the equilibrium adsorption method at pH 5.5 and pH 1 also correspond to the $I_{Mo(3p3)}/I_{Si(2s)}$ line of the samples prepared by the impregnation method. On the other hand, the catalyst prepared at pH 11 showed higher observability of Mo against the content of Mo ($I_{Mo(3p3)}/I_{Si(2s)}$; 1.1×10^{-2} where N_{Mo}/N_{Si}; 0.29×10^{-2}) than the impregnated catalysts. This suggests that the Mo species on the catalyst prepared by the equilibrium adsorption method at pH 11 was more dispersed than those on other catalysts.

Photo-oxidation of Methane over Supported Molybdenum Oxide Catalysts

Table 1 shows the results ot the photocatalytic oxidation of methane at 450 - 500 K on various supported molybdenum oxide catalysts during the first 120 min. Loading levels of MoO_3 onto SiO_2 support in the following Tables and Figures are calculated based on the atomic adsorption analysis of the calcined catalysts at 823 K, while those of the catalysts other than MoO_3/SiO_2 in Table 1 are calculated on the basis of the content of Mo in the impregnating solutions. The amounts of Mo species on the catalyst would more or less decrease during the

Table 1. Photoinduced partial oxidation of methane on various supported molybdenum catalysts[a]

Run	Catalyst	Cat. wt. (g)	Loading (wt.%)	Temp.[b] (K)	Yield(μmol·h^{-1}) HCHO	MeOH
1	None[c]		-	-	n.d.	n.d.
2	None		-		n.d.	n.d.
3	SiO_2[d]	0.050	-	463	trace	n.d.
4	MoO_3/SiO_2	0.025	4.4	493	5.8	0.2
5	MoO_3/Low Alumina	0.025	5.0[e]	473	trace	n.d.
6	MoO_3/High Alumina	0.025	5.0[e]	503	trace	trace
7	MoO_3/Al_2O_3	0.025	5.0[e]	493	trace	trace
8	$H_3PMo_{12}O_{40}/SiO_2$[d]	0.050	10[e]	493	2.2	0.4
9	MoO_3	0.180	-	503	trace	n.d.
10	Na_2MoO_4	0.250	-	493	trace	n.d.

[a] CH_4 feed rate = 7.5 mmol·h^{-1}, $CH_4 : O_2 : He = 6 : 2 : 25$, any trace amount of carbon dioxide was not detected, lamp = A (200 W, arc length = 150 mm), n.d. = not detected.

[b] Temperature at the centre of the catalyst bed.

[c] Without UV irradiation.

[d] $CH_4 : O_2 : He = 2 : 3 : 17$.

[e] Calculated from the amounts of the additives in impregnating solutions.

activation. Products were methanal and methanol. Any trace amounts of carbon oxides were not observed unless otherwise noted. Formation of formic acid was not detected by GC analysis. Blank reactions in the absence of a catalyst at a preheater temperature of 823 K with or without UV irradiation did not give any oxidation products. This ruled out the possibility of dark oxidation on the reactor wall up to 823 K, and proved that the reaction was not photochemical. The reaction performed on silica gel showed that a trace amount of methanal obtained in the catalytic run was due to the support. A silica supported molybdenum oxide catalyst (5.0 wt.% to the support, 4.4 wt.% after the pretreatment in a stream of air, see experimental section) afforded 5.8 $\mu mol \cdot h^{-1}$ (0.75 $mol \cdot (Mo\text{-}mol \cdot h)^{-1}$) of methanal along with 0.2 $\mu mol \cdot h^{-1}$ of methanol. The catalyst bed was fluidized to give uniform irradiation to all the catalyst particles through the window. The apparent irradiation area was *ca.* 1 cm^2. The color of the catalyst remained white during the reaction. Molybdenum oxide loaded on a different support, such as low alumina, high alumina and γ-alumina, produced only a trace or none of the oxidation products, indicating that strong interactions between molybdenum species and the support, which modified the nature of surface active sites. Since uniform fluidization of the catalyst particles in the reaction cell was not achieved with these three catalysts, apparent irradiation area was fairly decreased. The catalyst particles were rather spouted than fluidized. Heteropolyoxyanions such as $PMo_{12}O_{40}^{3-}$ have been known to be photoactive for oxidation of alcohols and alkanes.[7,18] In our study, a silica supported $H_3PMo_{12}O_{40}$(10 wt.%) catalyst gave methanal in the yield of 2.2 $\mu mol \cdot h^{-1}$. On the other hand, bulk of MoO_3 or Na_2MoO_4 did not show any catalytic activities.

We compared catalytic activities of silica supported MoO_3 prepared by the usual impregnation method with those by the equilibrium adsorption method using $(NH_4)_6Mo_7O_{24}$ solutions at different pH. Table 2 summarizes the results. As shown in runs 11 - 13, both the catalysts impregnated from an acidic and a basic solution contained smaller amounts of Mo species after the activation, and gave methanal in lower yields than that prepared from the solution of pH 6.

With the catalysts prepared by the equilibrium adsorption method at various pH, loading levels of MoO_3 decreased in following order, pH 1 (1.8 wt.%) < 5.5 (1.2 wt.%) < 11 (0.7 wt.%). Among them, the catalyst prepared at pH 1 was one of the most excellent catalysts. Methanal was

Table 2. Effects of the preparation methods of the silica supported MoO_3 catalysts[a]

Run	Preparation (pH[b])		Loading (wt.%)	Temp.[c] (K)	Yield(μmol·h^{-1}) HCHO	MeOH
11	Impregnation	(1)	2.9	473	2.5	0.2
12		(6)	4.4	463	4.9	0.2
13		(11)	2.6	473	2.6	0.2
14	Equilibrium Adsorption	(1)	1.8	473	4.4	0.3
15		(5.5)	1.2	473	3.6	trace
16		(11)	0.7	473	0.7	n.d.
17	$Mo(CO)_6$ Adsorption		1.8	493	2.7	0.2

[a] Amount of catalyst = 0.025 g, W/F = 0.62 g·h·mol^{-1}, space verocity = 10000 h^{-1}, CH_4 feed rate = 7.5 mmol.h^{-1}, $CH_4 : O_2 : He = 6 : 2 : 25$, any trace amount of carbon dioxide was not detected, lamp = A (200 W, arc length = 150 mm), n.d. = not detected.

[b] Acidity of impregnating solutions.

[c] Temperature at the centre of the catalyst bed.

selectively obtained in the yield of 4.4 $\mu mol \cdot h^{-1}$. On the other hand, the catalyst prepared from the solution at pH 6 showed the highest intrinsic activity for methanal formation (the yields of the products per unit loading amount of MoO_3, 2.7 $mol \cdot (Mo\text{-}mol \cdot h)^{-1}$), while the catalyst from acidic solution showed lower value, 2.2 $mol \cdot (Mo\text{-}mol \cdot h)^{-1}$. The molybdenum species on the catalyst prepared by the impregnation at pH 11 was inferior in the intrinsic activity, 1.4 $mol \cdot (Mo\text{-}mol \cdot h)^{-1}$. The MoO_3/SiO_2 catalyst prepared by adsorption of $Mo(CO)_6$ vapor, including 1.8 wt.% of MoO_3, afforded methanal in the yield of 2.7 $\mu mol \cdot h^{-1}$.

Figure 5 shows effects of the reaction temperature on the yield of methanal over the silica supported MoO_3(4.4 wt.%) catalyst prepared by the usual impregnation method. Yields of the products markedly increased above 440 K, and then leveled off at around 450 - 500 K. Although Ward et al.[4] reported the production of methanol at around 320 K on MoO_3/SiO_2, the reaction in our study at 318 K gave none of the products. The elevation of the catalyst bed temperature was required to activate the catalyst to produce methanal and methanol in significant yields. After the reaction at 320 K, the catalyst bed temperature was raised up to 823 K in a stream of argon, but oxygen-containing chemicals did not evolve at all. The color of the catalyst, which was white before the reactant gas was introduced, became blue after the reactions at the temperatures below 440 K, whereas it remained white after the reaction at higher temperatures.

Table 3 summarizes effects of several factors of reaction conditions, e.g. intensity of UV irradiation. The reaction did not take place at all without UV irradiation at 523 K. The result of the reaction with UV irradiation through a Pyrex filter (passes >300 nm) suggests that a wavelength shorter than 300 nm is required to activate the MoO_3/SiO_2 catalyst. We tried to examine rewards of fluidization of the catalyst bed by restricting the movement of the catalyst particles using a quartz wool plug. The apparent irradiation area was reduced to *ca.* 0.5 cm^2. Movement of the particle was limited. The yield of methanal in this case was reduced to 2.2 $\mu mol \cdot h^{-1}$, indicating that fluidization of the catalyst bed is quite advantageous by virtue of increasing the irradiation area.

When incident light flux into the catalyst bed was tripled by the use of lamp C, yields of the products increased. The highest yield of methanal (19 $\mu mol \cdot h^{-1}$, 2.5 $mol \cdot (Mo\text{-}mol \cdot h)^{-1}$) was obtained at 503 K. In

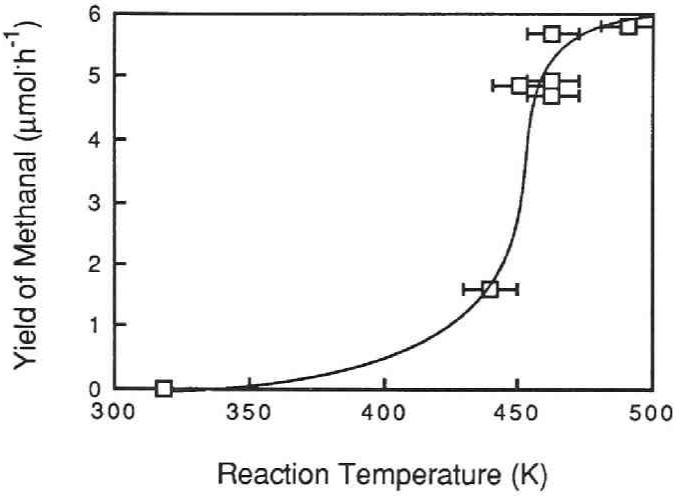

Figure 5. The yield of methanal at various reaction temperatures over the MoO_3(4.4 wt.%)/SiO_2 catalyst using lamp A (200 W, arc length = 150 mm). Amount of catalyst = 0.025 g, CH_4 feed rate = 7.5 mmol·h^{-1}, CH_4 : O_2 : He = 6 : 2 : 25, W/F = 0.62 g·h·mol^{-1}.

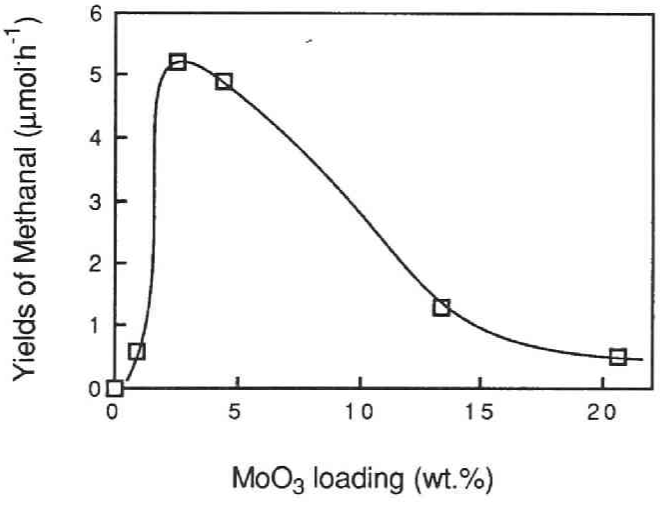

Figure 6. The yield of methanal at 463 K over the MoO_3/SiO_2 catalysts of various loading levels prepared by impregnation method using lamp A (200 W, arc length = 150 mm). Amount of catalyst = 0.025 g, CH_4 feed rate = 7.5 mmol·h^{-1}, CH_4 : O_2 : He = 6 : 2 : 25, W/F = 0.62 g·h·mol^{-1}.

Table 3. Photoinduced partial oxidation of methane over the MoO_3(4.4 wt.%)/SiO_2 catalysts prepared by the impregnation method[a]

Run	Lamp[b]	Temp.[c] (K)	Yield(μmol·h^{-1}) HCHO	MeOH	CO
18	-	523	n.d.	n.d.	n.d.
3	A	493	5.8	0.2	n.d.
19[d]	A	463	2.8	0.2	n.d.
20[d,e]	A	463	trace	n.d.	n.d.
21[f]	A	473	2.2	trace	n.d.
22	C	483	11	0.4	n.d.
23	C	503	19	0.7	6

a Amount of catalyst = 0.025 g, W/F = 0.62 g·h·mol^{-1}, space verocity = 10000 h^{-1}, CH_4 feed rate = 7.5 mmol·h^{-1}, CH_4 : O_2 : He = 6 : 2 : 25, n.d. = not detected, any trace amount of carbon dioxide was not detected.

b A: 200 W (arc length = 150 mm) Hg lamp,
C: 200 W (arc length = 75 mm) Hg lamp.

c Temperature at the centre of the catalyst bed.

d Amount of catalyst = 0.050 g, CH_4 : O_2 : He = 2 : 3 : 17, amount of loaded MoO_3 = 7.9 wt.%.

e Irradiated through the Pyrex filter.

f Fixed catalyst bed.

Table 4. Selective photo-oxidation of ethane into ethanal and methanal over the MoO_3(2.5 wt.%)/SiO_2[a]

Run	Lamp[b]	Cat. Wt. (g)	Temp.[c] (K)	Yield(μmol·h^{-1}) CH_3CHO	C_2H_5OH	HCHO	CO	CO_2
24		0.025	483	n.d.	n.d.	n.d.	n.d.	trace
25	B	0.025	463	14	0.7	4.0	n.d.	trace
26	B	0.014	463	6.6	0.7	1.6	n.d.	n.d.
27	B	0.051	463	17	1.2	3.2	n.d.	4
28	C	0.025	493	38	3.1	20	trace	7
29[d]	C	0.025	493	60	2.3	22	trace	5

[a] Amount of catalyst = 0.025 g, W/F = 0.71 g·h·mol^{-1}, ethane feed rate = 7.5 mmol·h^{-1}, C_2H_6 : O_2 : He = 6 : 1 : 21, space velocity = 8200 h^{-1}, n.d. = not detected.

[b] B: 75 W (arc length = 15 mm), C: 200 W (arc length = 75 mm) Hg lamp.

[c] Temperature at the center of the catalyst bed.

[d] Ethane feed rate = 19 mmol·h^{-1}, oxygen feed rate = 2.5 mmol·h^{-1}.

addition, 6 $\mu mol \cdot h^{-1}$ of carbon monoxide was formed. Carbon monoxide might be formed by the decomposition of methanal, that may occur under somewhat severe conditions, under UV irradiation or at a high reaction temperature. Formation of hydrogen could not be confirmed, since the low concentration of hydrogen in the feed including helium was not detectable. The enhanced yields indicate that active species formation on the catalyst by photons was not saturated, and yields of the products increases almost in proportion to the intensity of light flux under these conditions.

As illustrated in Figure 6, the yield of methanal changed with variations in loading levels of MoO_3 on silica. The highest yield of methanal was obtained with the 2.5 wt.% loaded catalyst. Further increase in the loading of MoO_3 decreased the yield of methanal.

Photo-oxidation of Ethane under Various Reaction Conditions

Photo-oxidation of ethane was examined on the silica supported MoO_3 (2.5 wt.%) catalyst, which showed the highest activity for selective photo-oxidation of methane. Results during the first 60 min are shown in Table 4. An apparent irradiation area of the fluidized catalyst bed (0.025 g) was kept *ca.* 1 cm^2. Products were ethanal and methanal together with small amounts of ethene, ethanol and carbon dioxide. Formation of acetic acid was not observed by GC analysis. The reaction without a catalyst at a preheater temperature of 823 K gave only a trace amounts of carbon dioxide, and none of oxygen-containing compounds. The reaction without UV irradiation gave none of the products. Under irradiation using lamp B, the MoO_3/SiO_2 catalyst afforded 14 $\mu mol \cdot h^{-1}$ of ethanal and 4.0 $\mu mol \cdot h^{-1}$ of methanal together with small amounts of ethanol and carbon dioxide. Selectivity for useful oxygen-containing chemicals was more than 90%. The rate of oxidation in a unit time did not change during a prolonged run for 5 h.

With a decrease in the amount of the catalyst from 0.025 g to 0.014 g, yields of the products decreased to one-half. On the other hand, slightly higher yields of the products were obtained with a doubled amount of the catalyst (see runs 25 - 27). An efficient UV irradiation area decreased in proportion to the amount of the catalyst less than 0.025 g, whereas it slightly increased with 0.051 g of the catalyst. Yields of the

products depended on the efficient irradiation area, in other word, number of photons reached into the catalyst.

When the light flux increased by the use of lamp C, the yields of the products increased. Ethanal and methanal were formed at 493 K in the yields of 38 $\mu mol \cdot h^{-1}$ and 20 $\mu mol \cdot h^{-1}$, respectively. Optimization of the reaction conditions drew the highest yields of ethanal (60 $\mu mol \cdot h^{-1}$) and methanal (22 $\mu mol \cdot h^{-1}$). The combined yield of carbon oxides was *ca.* 5 $\mu mol \cdot h^{-1}$, implying the high selectivity for oxygen-containing compounds over 96%.

Figure 7 shows the yields of the products at various catalyst bed temperatures under UV irradiation using both lamp B and C. With a 75 W mercury lamp, only 1.2 $\mu mol \cdot h^{-1}$ of ethanal was obtained without preheating. Formation of ethanal was markedly enhanced above 400 K, and the yield leveled off around 475 500 K. The amount of produced carbon dioxide did not exceed 3 $\mu mol \cdot h^{-1}$. With the 200 W mercury lamp, the yield of ethanal showed the maximum value at 493 K. Further increases in the reaction temperature decreased the ethanal formation, whereas the yield of methanal markedly increased. The yield of carbon dioxide also leveled off above 473 K at approximately 6 $\mu mol \cdot h^{-1}$. These results indicate that the catalyst bed temperature around 450 - 500 K is preferable for the selective formation of ethanal.

We examined the presence of adsorbed species on the surface of the catalyst by raising the catalyst bed temperature to 823 K under a flow of argon. None of the desorbed products were observed from the catalyst used for the reactions in the dark or without preheating. From the catalyst after the reaction at around 500 K for 60 min, a very small amount of carbon dioxide (less than 0.5 μmol) was formed together with ethane. A trace amount of ethene evolved, too.

We examined effects of partial pressure of the reactant in the reaction mixture on the MoO_3(2.5 wt.%)/SiO_2 catalyst prepared by the impregnation method. Figure 8 shows the yields of the products and the ethane conversion at various partial pressure of ethane, P_{ethane}, with constant partial pressures of the other components and constant W/F. The conversion of ethane increased markedly with an increase in P_{ethane} over the range up to *ca.* 20 kPa, and gradually at higher levels of P_{ethane}. Higher partial pressure of ethane was favorable for selective formation of ethanal.

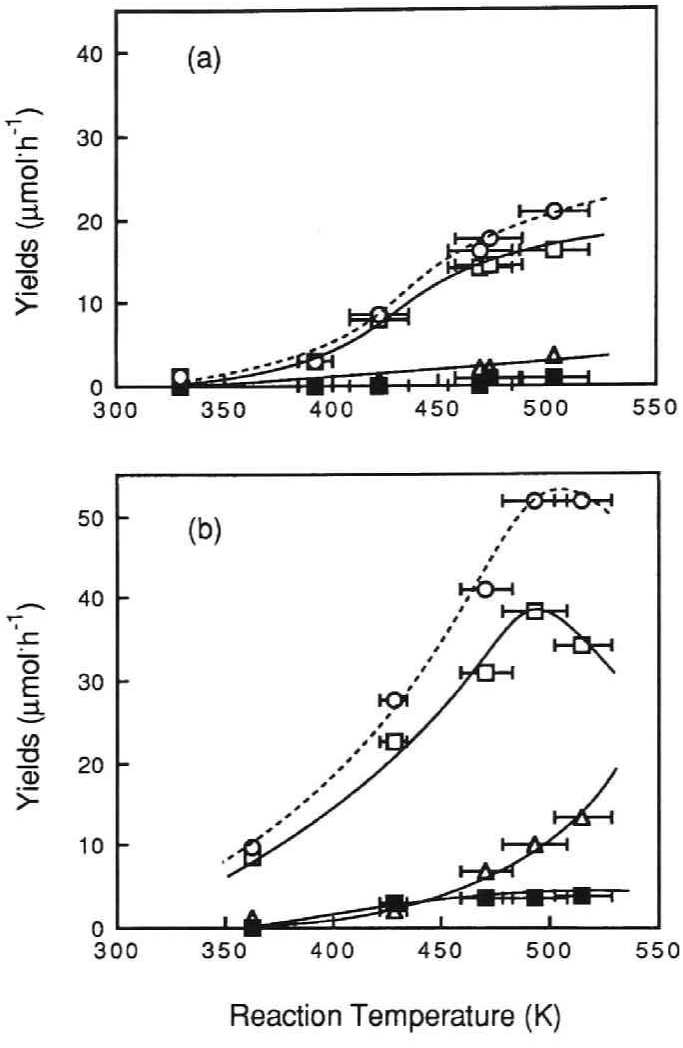

Figure 7. The products yields over the MoO_3(2.5 wt.%)/SiO_2 catalyst at various catalyst bed temperatures with UV irradiation (a) by the 75 W mercury vapor lamp (arc length = 15 mm), and (b) by the 200 W one (arc length = 75 mm). The yields of (□) CH_3CHO, (△) HCHO (x 1/2), and (■) CO_2 (x 1/2), and (○) conversion of C_2H_6. Amount of catalyst = 0.025 g, C_2H_6 feed rate = 7.5 mmol·h^{-1}, C_2H_6 : O_2 : He = 6 : 1 : 21, W/F = 0.71 g·h·mol^{-1}.

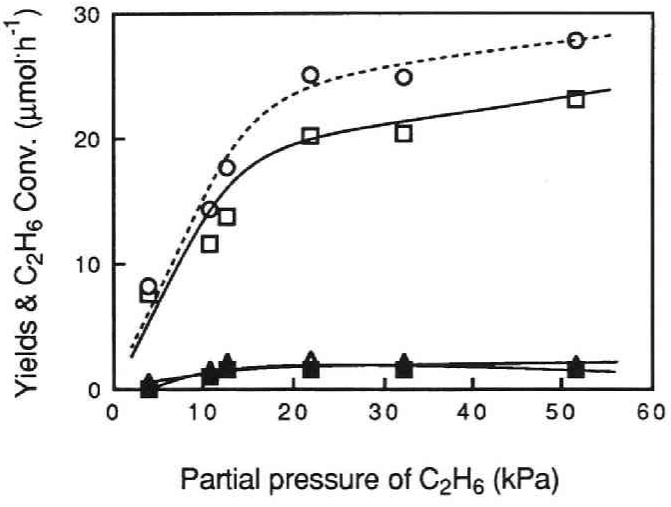

Figure 8. Effects of partial pressure of ethane over impregnated MoO_3(2.5 wt.%)/SiO_2 on ethane conversion (○), yields of ethanal (□), methanal (△) and CO_2 (■) (x 1/2) at 473 K using lamp B (75 W, arc length = 15 mm), P_{oxygen} = 7.2 kPa.

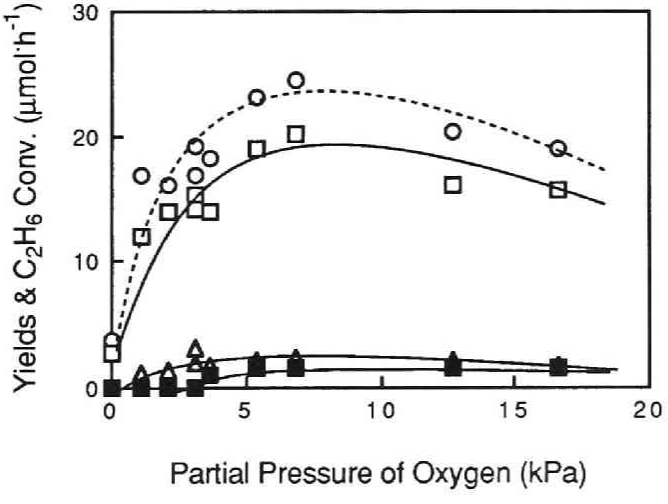

Figure 9. Effects of partial pressure of oxygen over impregnated MoO_3(2.5 wt.%)/SiO_2 on ethane conversion (○), yields of ethanal (□), methanal (△) and CO_2 (■) (x 1/2) at 473 K using lamp B (75 W, arc length = 15 mm), P_{ethane} = 22 kPa.

Another variable examined was partial pressure of oxygen, P_{oxygen}. Figure 9 illustrates effects of P_{oxygen}. With increasing P_{oxygen} up to *ca.* 5 kPa, ethane conversion and yields of ethanal markedly increased. With further increase in P_{oxygen}, however, conversion of ethane and yields of aldehydes gradually decreased. It should be noted that deep oxidation of ethane to carbon oxides was not enhanced furthermore by an increase in P_{oxygen} above 5 kPa. Partial pressure of oxygen suitable for formation of ethanal was 5 kPa. On the other hand, the reaction in the absence of oxygen yielded 2.7 $\mu mol \cdot h^{-1}$ of ethanal together with small amounts of ethene and ethanol during first 60 min. The yields promptly decreased with time on stream. After the reaction without molecular oxygen for several hours, the color of the catalyst changed to grayish blue-green.

Photo-oxidation of Propane

Photo-oxidation of propane on MoO_3/SiO_2 has been performed by Marcinkowska et al.[11,12] at an ambient temperature, and they reported formation of ethanal, propanal and acetone together with large amounts of CO and CO_2. Thus the reaction was low in the selectivity for useful products.

We examined photo-oxidation of propane as well as methane and ethane at an elevated temperature on MoO_3(2.5 wt.%)/SiO_2, and the results are shown in Table 5. The products were propanal, acetone and ethanal together with small amounts of methanal and carbon dioxide. Formation of carbon monoxide, propenal and carboxylic acids was not observed by GC analysis. None of the products was obtained in the reaction without UV irradiation. The reaction in the absence of the catalyst at the preheater temperature of 723 K gave only a trace amount of carbon dioxide.

Irradiation using lamp B at around 470 K gave *ca.* 20 $\mu mol \cdot h^{-1}$ of the oxygen-containing products. The reaction using lamp C generally afforded higher yields of the products. For example, at 493 K, 15 $\mu mol \cdot h^{-1}$ of propanal, 9.8 $\mu mol \cdot h^{-1}$ of acetone and 15 $\mu mol \cdot h^{-1}$ of ethanal were formed. Only 3 $\mu mol \cdot h^{-1}$ of carbon dioxide was detected in the effluent gas, suggesting the high selectivity for oxygen-containing chemicals. The yields in a unit time did not change during the prolonged run for 7 h.

Table 5. Selective photo-oxidation of propane over the MoO_3(2.5 wt%)/SiO_2 catalyst[a]

Run	Lamp[b]	Temp.[c] (K)	Yield(μmol·h^{-1})				
			C_2H_5CHO	$(CH_3)_2CO$	CH_3CHO	CO	CO_2
30		550	n.d.	n.d.	n.d.	n.d.	trace
31	B	471	8.1	5.0	6.3	n.d.	1
32	B	516	10	7.0	6.1	n.d.	3
33	C	493	15	9.8	15	n.d.	3
34[d]	C	493	16	10	16	n.d.	3

a Amount of catalyst = 0.025 g, W/F = 0.71 g·h·mol^{-1}, C_3H_8 feed rate = 7.5 mmol·h^{-1}, C_3H_8 : O_2 : He = 3 : 1 : 10, space velocity = 8200 h^{-1}, n.d. = not detected.

b B: 75 W (arc length = 15 mm), C: 200 W (arc length = 75 mm) Hg lamp.

c Temperature at the center of the catalyst bed.

d Prolonged run of 6 - 7 h.

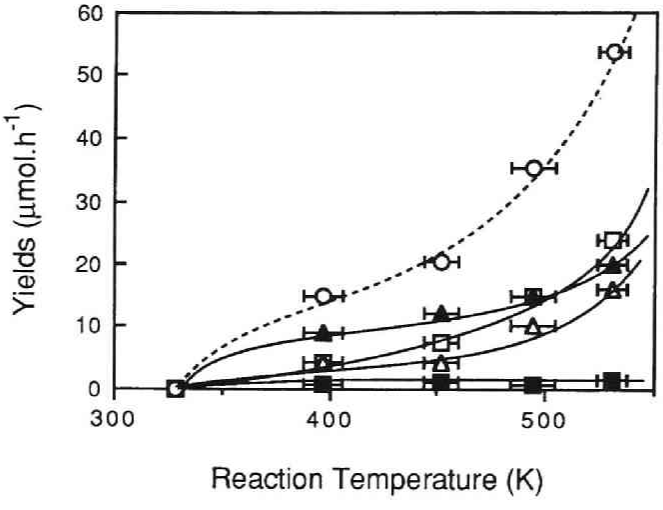

Figure 10. Photo-oxidation of propane at various catalyst bed temperature on impregnated MoO_3(2.5 wt.%)/SiO_2 using lamp C (200 W, arc length = 75 mm). Amount of catalyst = 0.025 g, C_3H_8 feed rate = 7.5 mmol·h^{-1}, C_3H_8 : O_2 : He = 3 : 1 : 10, W/F = 0.71 g·h·mol^{-1}. The yields of (□) propanal, (△) acetone, (▲) ethanal, (■) CO_2 (x 1/3), and (○) C_3H_8 conversion.

Heating the catalyst bed to 823 K after the completion of the reaction for 3 h at 493 K afforded 0.7 μmol of carbon dioxide together with trace amounts of propene, ethane, ethene and unreacted propane. Ethanal, propanal and acetone were not detected by the GC analysis.

Figure 10 shows the yields of the products at various catalyst bed temperatures under UV irradiation using lamp C. Whereas only trace amounts of products were formed without preheating (319 K), the highest yields of propanal 24 $\mu mol \cdot h^{-1}$, acetone 16 $\mu mol \cdot h^{-1}$ and ethanal 20 $\mu mol \cdot h^{-1}$ were achieved at around 530 K. It should be noted that ethanal, a C-C bond dissociated product, was formed at relatively lower temperatures of 400 - 450 K, while predominant formation of methanal was observed in the photo-oxidation of ethane at the higher temperature (see above). The amount of carbon dioxide in the effluent gas did not exceed 5 $\mu mol \cdot h^{-1}$. Even if the evolved carbon dioxide after the reaction was formed by deep oxidation of propane, high selectivity for useful products was achieved in our reaction system.

Discussion

Correlation between the UV-absorption λ max and the co-ordination state of metal ions is usually accepted. In the present study, the MoO_3(2.5 wt.%)/SiO_2 catalyst showed the absorption bands with maxima around 240 250 nm and 280 nm. The absorption bands below 300 nm could be attributed to Mo^{6+} species in tetrahedral coordination, as generally accepted.[16] The bands around 240 nm and 280 nm have been assigned to $3t_2 \leftarrow 2t_1$ and to $3t_2 \leftarrow t_1$ transition, respectively, in the tetrahedrally coordinated molybdenum species.[17] Marcinkowska et al.[10] attributed this band to an oxomolybdenum dimer or a tetrahedrally coordinated molybdenum ion in terminal position of a polymeric layer. They attributed the band around 240 nm to monomeric molybdenum species.

The absorption band of a wavelength above 300 nm often has ben attributed to the Mo species in octahedral coordination.[16] XRD study revealed the formation of large crystallite of MoO_3 on the surface of the MoO_3(21 wt.%)/SiO_2 catalyst. Therefore the band around 300 nm, which was newly observed with this catalyst, could be attributed to octahedrally coordinated species.

Photo-oxidation of methane did not proceed without irradiation of wavelength below 300 nm. In the study of Marcinkowska et al.[10], photo-oxidation of propane gave the products under UV irradiation of a wavelength above 280 nm. Provided that the catalyst was activated by light of wavelength corresponding to its adsorption band in the UV region, catalytically active species therefore would be provided from tetrahedrally coordinated species at least absorbing UV at around 280 nm.

Results of the reactions with the catalysts prepared by different methods and/or at different pH gave information on the active molybdenum species. The influence of pH in the impregnation on the structure and properties of MoO_3/SiO_2 has been studied extensively.[19,20] The molybdenum species prepared in an aqueous solution of ammonium heptamolybdate should be monomeric MoO_4^{2-} under basic conditions, while a variety of polymeric species exists at a lower pH value (see eq.(1) and (2)).[21-23]

$$(Mo_7O_{24})^{6-} + 4H_2O \rightleftharpoons 7(MoO_4)^{2-} + 8H^+ \quad (2<pH<6) \qquad (1)$$

$$(Mo_7O_{24})^{6-} + 3H^+ + HMoO_4^- \rightleftharpoons Mo_8O_{26}^{4-} + 2H_2O \quad (pH<2) \qquad (2)$$

It has been reported that monolayer type molybdenum species would be formed at low loading levels when the pH of the solution was lower than the isoelectric point of the support, typically pH 2 for silica.[24] The interaction between molybdate and silica would be weak at higher pH values. Formation of islands of molybdenum oxide have been proposed on the surface of the catalyst prepared from a neutral solution. The changes in the state of MoO_3 on the surface might affect photocatalytic reactions.

The catalysts prepared by the equilibrium adsorption method in the basic solution was revealed to contain much highly dispersed surface molybdenum species than those prepared from basic and neutral solutions by XPS study. But the loading level of MoO_3 was very low, 0.7%, and the catalyst did not show significant activity. On the other hand, the catalysts prepared from the solution at lower pH contained the larger amount of MoO_3, and showed higher intrinsic activities. The

intrinsic activity of molybdenum species depend not only on the method of catalyst preparation but also on the loading levels of MoO_3. As shown in Figure 6, the MoO_3(2.5 wt.%) loaded catalyst exhibited the maximum intrinsic activity for methanal formation. The intrinsic activity decreased with a further increase in the loading level of MoO_3. These results suggest that the less dispersed molybdenum species, but not large crystallite of MoO_3, are responsible for the high activities, which should include the terminal doubly bonded tetrahedral molybdenum species responsible for the absorption band at 280 nm in the UV spectra.

In a previous study on the photo-oxidation over n-type solid semiconductors, active oxygen species have been proposed as neutral atomic oxygen originated from molecular O_2.[5] On the other hand, Gerasimov[9] has showed that in photo-oxidation of methane with molecular oxygen on V^{5+}/SiO_2 at an ambient temperature, molecular oxygen could not be direct source of CO_2, which was a sole product of the reaction, at the initial stage of the reaction. Recent study on photo-oxidation of propene revealed the direct participation of the lattice oxygen.[25]

As described above, photo-oxidation of ethane in the absence of oxygen selectively gave a small amount of ethanal at the initial stage of the reaction. Thus it is reasonable to consider the source of oxygen in ethanal to be a lattice oxygen of molybdenum oxide, although the present study did not include an experiment with labeled oxygen. On the other hand, conversion of ethane was much influenced with P_{oxygen}, as shown in Figure 9. This suggests that molecular oxygen promotes the reaction significantly.

The results in our present study, despite of the higher reaction temperature, did agree with the mechanism proposed by Kazansky et al.[2] in its outline. They proposed the mechanisms of photocatalytic oxidation of CH_4 and C_2H_6 over V^{5+}/SiO_2 catalyst at an ambient temperature. The probable mechanism of photo-oxidation of ethane over molybdenum oxide on silica is illustrated in Scheme I on the basis of the mechanisms proposed by Kazansky et al. The reaction with methane or propane may proceed in a similar manner. This mechanism requires the presence of surface doubly bonded $Mo^{6+}O^{2-}$ species. The first step involves activation of a lattice oxygen by UV irradiation, resulting in the formation of charge transfer complex. An alkane is adsorbed on the photoactivated O^- species and subjected to the activation of its C-H bond.

Kazansky et al. have suggested that a hydrogen is abstracted by a bridged lattice oxygen. Abstraction of hydrogen by other electron rich oxygen species may be possible. Then molecular oxygen is adsorbed onto a molybdenum ion that can provide an electron to oxygen. Following the formation of aldehydes and/or ketones together with re-oxidation of surface species, the photo-catalytic cycle is completed. A similar mechanism has been proposed for propane oxidation.[10] The mechanism in Scheme I requires molecular oxygen to form aldehydes and ketones, and oxygen atom in ethanal is originated from the lattice oxygen.

The reaction without oxygen gave a small amount of ethanal as the main product. The direct formation of ethanal can be explained by the participation of the lattice oxygen species, e.g. O^{2-}, in place of molecular oxygen (see Scheme I). In this case, the reduced-state molybdenum species are formed and kept not to be re-oxidized, resulting in rapid deactivation in the course of the reaction.

The most characteristic feature in our procedure is irradiation at high temperatures to obtain the high yields with high selectivities of aldehydes. A higher temperature may primarily promote desorption of the oxygenated products from the catalyst. At an ambient temperature, the color of the catalysts promptly turned blue during the reaction. Blue coloration of the catalysts is probably due to "molybdenum blue" species in non-stoichiometric reduced state.[3] Bluish coloration was observed after the reaction without molecular oxygen. Although adsorption of water or other species on the supported molybdenum oxide catalyst could change its color, the catalyst seems to be partially reduced at a lower temperature due to slow re-oxidation process. Providing that the reaction mainly proceeds as shown in Scheme I, the re-oxidation process includes simultaneous abstraction of another hydrogen from activated alkane, and cleaverage of metal-oxygen bond. It is reasonable that these elemental processes are affected by the reaction temperature, resulting in changing rate of re-oxidation. Enhanced release of the products and the rate of re-oxidation of molybdenum oxide might increase turnover frequency of overall reaction.

Effects of partial pressure of alkane or oxygen can well be interpreted, if the following steps that simplifies the processes in Scheme I, are assumed.

Scheme 1.

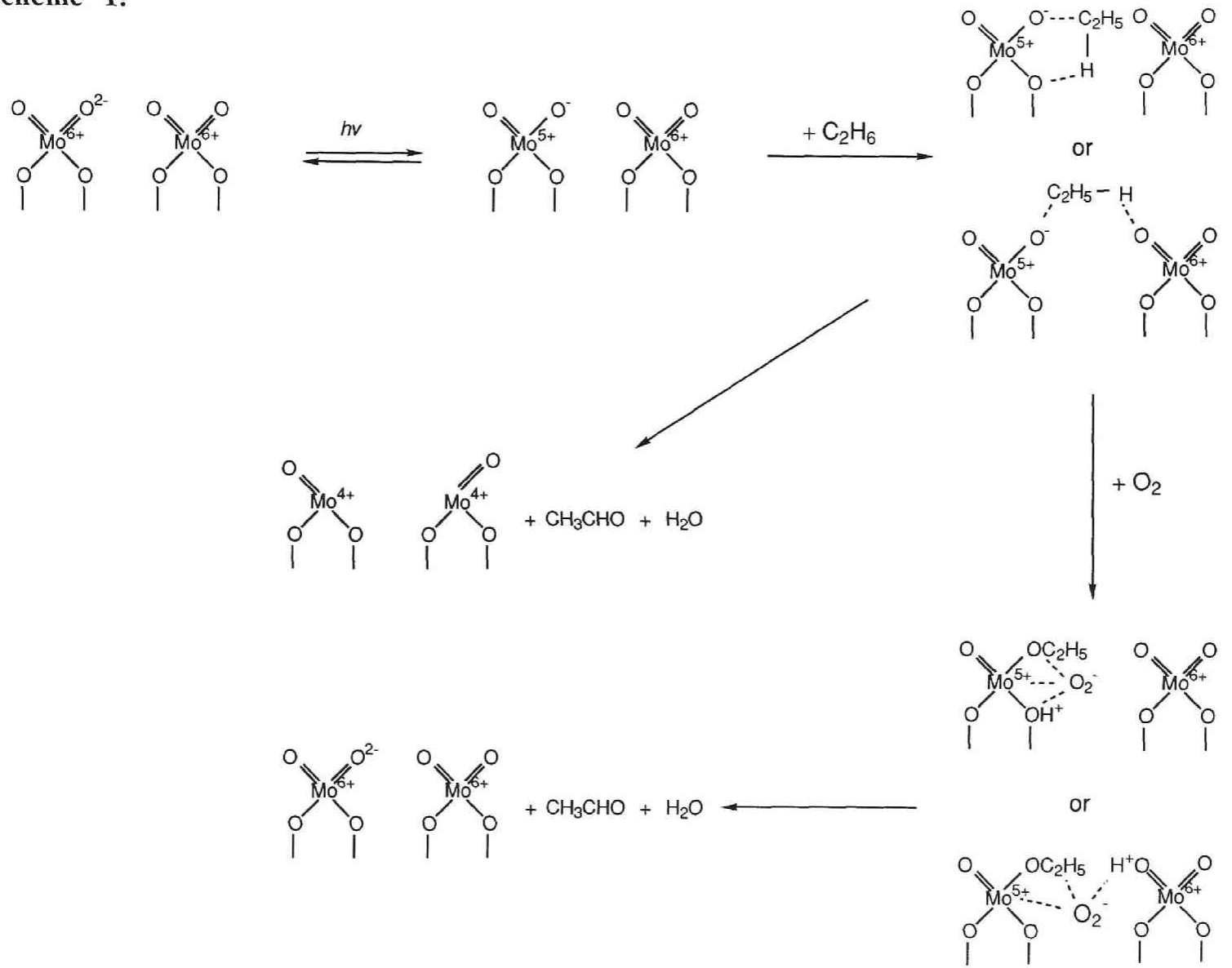

$$\underset{\underline{1}}{Mo{=}O} \underset{k_d}{\overset{h\nu}{\rightleftharpoons}} \underset{\underline{2}}{(Mo{=}O)^*} \xrightarrow{+C_2H_6,\ k_1} \underset{\underline{3}}{(Mo{=}O)\cdot C_2H_6} \xrightarrow{+O_2,\ k_2} Mo{=}O + CH_3CHO + H_2O \qquad (3)$$

Neglecting that interaction among adsorbed species on the catalyst surface, and assuming that the each steps of adsorption of ethane and desorption of the products are irreversible, the rate equation for formation of activated Mo species, 2, can be expressed as follows:

$$\frac{d[S_2]}{dt} = c\, I_{UV}[S'_1] \quad k_d[S_2] \quad k_1[S_2]P_{ethane} \qquad (4)$$

And the rate equation for the formation of the surface species 3 in Scheme 1 should be

$$\frac{d[S_3]}{dt} = k_1[S_2]P_{ethane} \quad k_2[S_3]P_{oxygen} \qquad (5)$$

where $[S_2]$, $[S_3]$ are the concentrations of surface species 2 and 3, respectively. And k_d is a rate constant of any deactivation of photo-excited species. I_{UV} represents the intensity of light, and c is a coefficient. The rate constant for respective steps are designated as k_1, k_2. P_{ethane} and P_{oxygen} should be nearly constant during the reaction in the flow type reactor, since the conversion of alkane and oxygen are very low. $[S'_1]$ is the concentration of vacant site on the surface.

$$\frac{d[S'_1]}{dt} = \quad c\, I_{UV}[S'_1] + k_d[S_2] + k_2[S_3]P_{oxygen} \qquad (6)$$

$$[S'_1] = [S_1] - [S_2] - [S_3] \qquad (7)$$

$[S_1]$ is an initial concentration of the surface species that can be activated by light. Providing that the stationary concentration of surface species 2, 3 and the number of vacant site are constant during the reaction, $d[S'_1]/dt$, $d[S_2]/dt$ and $d[S_3]/dt$ should be zero. Therefore $[S_3]$ is written as follows:

$$[S_3] = \frac{c\, I_{UV} k_1 P_{ethane} [S_1]}{k_2 P_{oxygen}(k_d + c\, I_{UV} + k_1 P_{ethane}) + k_1 P_{ethane} c\, I_{UV}} \quad (9)$$

When a sufficient amount of photon is infused on the catalysts, the rate of photo-oxidation of ethane is given as eq. (10), if formation of the products from 3 along with the simultaneous re-oxidation of Mo ion is rate determining:

$$-\frac{dP_{ethane}}{dt} = k_2 P_{oxygen}[S_3]$$
$$= \frac{c\, I_{UV} k_1 k_2 P_{ethane} P_{oxygen} [S_1]}{k_2 P_{oxygen}(k_d + c\, I_{UV} + k_1 P_{ethane}) + k_1 P_{ethane} c\, I_{UV}} \quad (10)$$

where $cI_{UV}k_1/(k_d + cI_{UV})k_2$ is estimated to be *ca.* 0.11, on the basis of the tangent of the curve of the ethane conversion shown in Figure 8 an 9 at around P_{ethane} or $P_{oxygen} = 0$.

The plots of eq. (10) against P_{ethane} and P_{oxygen} exhibits approximately similar profiles to those shown in Figures 8 and 9 at low P_{ethane} or P_{oxygen}. As shown in Figure 9, ethane conversion showed maximum at P_{oxygen} at 7 kPa, probably due to the limited amount of photon infused into the catalyst bed. Decreases in ethane conversion at a higher P_{oxygen} can be understood if one assumes adsorption of oxygen onto the catalyst surface, which has been known to occur even in the dark to a small extent on V^{5+}/SiO_2.[25] This would interfere the photo-adsorption of ethane, and therefore oxidation of ethane would be somewhat suppressed.

Unclear aspects of the reaction mechanism lie on the formation of C-C bond cleaved products, methanal or ethanal. The amount of methanal increased with increasing the temperature. On the other hand, in photo-oxidation of propane, formation of ethanal was pronounced at a lower temperature (see Figure 10). However, lesser amounts of 'C_1' compounds, carbon oxides and methanal, were found than predicted stoichiometric amounts. There seems to occur formation of new C-C bond on the surface in a similar manner as oligomerization of alkenes on $MoO3/SiO_2$, although this process has been reported to be suppressed in the presence of oxygen.[26,27] Acceptable explanations for our results are still not attained yet.

In conclusion, the selective photocatalytic oxidation of light alkanes to aldehydes, including the first example of selective formation of methanal from methane, could be achieved by using the MoO_3/SiO_2 catalysts at 450 - 500 K irradiation with UV light.

References

1 P. Pitchai and K. Klier, *Catal. Rev.-Sci. Eng., 28 (1),* **1986**, 13.

2 S.L. Kaliaguine, B.N. Shelimov and V.B. Kazansky, *J. Catal., 55*, **1978**, 384.

3 W. Hill, B.N. Shelimov and V.B. Kazansky, *J. Chem. Soc., Faraday Trans. 1, 83 (3)*, **1987**, 2381.

4 M.D. Ward, J.F. Brazdil, S.P. Mehandru and A.B. Anderson, *J. Phys. Chem., 91*, **1987**, 6515.

5 N. Djeghri, M. Formenti, F. Juillet and S.J. Techner, *Faraday Discuss. Chem. Soc., 58*, **1984**, 185.

6 K.R. Thampi, J. Kiwi and M. Grätzel, *Catal. Lett.,* **1989**, 109.

7 M. Grätzel, K.R. Thampi and J. Kiwi, *J. Phys. Chem., 93*, **1989**, 4128.

8 M. Daroux, D. Klvana, M. Duran and M. Bideau, *Can. J. Chem. Eng., 63*, **1985**, 668.

9 S.F. Gerasimov, *React. Kinet. Catal. Lett., 32 (1)*, **1986**, 57.

10 K. Marcinkowska, S. Kaliaguine and P.C. Roberge, *J. Catal., 90*, **1984**, 49.

11 K. Marcinkowska, S. Kaliaguine and P.C. Roberge, *Proc. 9th. Congr. Catal. Calgary, 4*, **1988**, 521.

12 P. Mehandru, B. Anderson, F. Bradzil and K. Grasselli, *J. Phys. Chem., 91*, **1987**, 2930.

13 T. Suzuki, K. Wada, M. Shima and Y. Watanabe, *J. Chem. Soc., Chem. Commun.,* **1990**, 1059.

14 K. Wada, K. Yoshida, Y. Watanabe and T. Suzuki, *Appl. Catal., 74*, **1991**, L1.

15 G. Kortüm, *Reflectance Spectroscopy*, Springer-Verlag, Berlin, **1969**, 183.

16 Y. Iwasawa and S. Ogasawara, *J. Chem. Soc., Faraday Trans. 1, 75*, **1979**, 1465.

17 M. Wolfsberg and L. Helmholz, *J. Chem. Phys., 20*, **1952**, 837.

18 M.D. Ward, J.F. Brazdil and R.K. Grasselli, *J. Phys. Chem., 88*, **1984**, 4210: T. Baba, H. Watanabe and Y. Ono, *J. Phys. Chem., 87*, **1983**, 2406: J.R. Darwent, *J. Chem. Soc., Chem. Commun.*, **1982**, 798: C.L. Hill and D.A. Bouchard, *J. Am. Chem. Soc., 107*, **1985**, 5148: A. Hiskia and E. Papaconstantinou, *Polyhedron, 7*, **1988**, 477.

19 H.M. Ismail, C.R. Theocharis and M.I. Zaki, *J. Chem. Soc., Faraday Trans. 1, 83*, **1987**, 2835, and the references therein.

20 R.L. Cordero, F,J,G, Llambias and A.L. Agudo, *Appl. Catal., 74*, **1991**, 125.

21 H. Jeziorowski and H. Köninger, *J. Phys. Chem., 83*, **1979**, 116.

22 L. Wang and W.K. Hall, *J. Catal., 77*, **1982**, 232.

23 P.Gajardo, P. Grange and B. Delmon, *J. Phys. Chem., 83*, **1979**, 1771: P. Gajardo, D. Pirotte, P. Grange and B. Delmon, *J. Phys. Chem., 83*, **1979**, 1780.

24 G.A. Parks, *Chem. Rev., 65*, **1965**, 177.

25 S. Yoshida, T. Tanaka, M. Okada and T. Funabiki, *J. Chem. Soc., Faraday Trans. 1, 80*, **1984**, 119.

26 M. Anpo, M. Kondo, S. Coluccia, C. Louis and M. Che, *J. Am. Chem. Soc., 111*, **1989**, 8791.
M. Anpo, M. Kondo, Y. Kubokawa, C. Louis and M. Che, *J. Chem. Soc., Faraday Trans. 1, 84*, **1988**, 2771.

27 T. Nakajima, H. Miyata and Y. Kubokawa, *Bull. Chem. Soc. Jpn., 55*, **1982**, 609: H. Miyata, T. Nakajima and Y. Kubokawa, *J. Catal., 69*, **1981**, 292: H. Miyata, M. Wakamiya and Y. Kubokawa, *J. Catal., 34*, **1974**, 117.

Chapter 2

Selective Photo-oxidation of Light Alkanes using Solid Oxide Semiconductors

Abstract

Photocatalytic activities of n-type solid metal oxide semiconductors for the oxidation of light alkanes from methane to propane were examined at 450 500 K. Activities of the zinc oxide catalysts for photo-oxidation of alkanes were greatly enhanced by the elevation of the catalyst bed temperature to *ca.* 500 K. Ethanal was formed in the highest yield of 84 $\mu mol \cdot h^{-1}$ with the selectivity of *ca.* 75% with 0.25 g of zinc oxide at 493 K under the conditions employed. Photo-oxidation of propane under similar conditions gave 57 $\mu mol \cdot h^{-1}$ of propanal and 56 $\mu mol \cdot h^{-1}$ of acetone, respectively, with the combined selectivity over 75%. The reaction of methane over zinc oxide yielded a small amount of methanal (4.7 $\mu mol \cdot h^{-1}$) together with a large amount of CO_2, and the selectivity for methanal was low (*ca.* 10 %). UV irradiation was indispensable for the reactions, and only very small amounts of the products were formed in the reactions at an ambient temperature. The yields of the products were depended on the method of the preparation of the zinc oxide catalysts. Photocatalytic activities of titanium oxides for the oxidation of ethane and propane decreased with increasing the reaction temperatures, while that for methane oxidation increased.

Introduction

The activation of C-H bonds in simple light alkanes, especially methane, for their selective oxidation into oxygen-containing chemicals is a subject of current interest.[1] The studies on photo-oxidation of light alkanes, including methane, have been carried out either on supported surface metal oxides[2-7] and n-type solid semiconductors.[8-11] However, only few studies on selective formation of oxygen-containing chemicals from light alkanes ($<C_3$) were successful.[2] Kazansky and co-workers[3] showed that O^- anion radial species reacted with methane and ethane to form a small amount of methanal together with a large amount of carbon oxides on various supported metal oxide, e.g. V_2O_5. The O^- species were formed by γ- and UV irradiation. Formenti et al. reported photoinduced oxidation of C_2 - C_6 alkanes on TiO_2 at an ambient temperature.[8] Oxidation of methane was not successful in their

study. Photo-thermal oxidation of methane has once been investigated on TiO_2 by Grätzel et al.[9] Selectivity for carbon monoxide was enhanced at a higher reaction temperature, whereas only carbon dioxide was formed at an ambient temperature. On the other hand, catalytic activities of ZnO have been investigated for the photo-oxidation of higher alkanes,[12] alkenes[13,14], CO.[15,16]

The first examples of selective photo-oxidation of light alkanes, including methane, with oxygen to form oxygen-containing chemicals have been described in chapter 1 using molybdenum oxide supported on silica at the catalyst bed temperature of 450 - 550 K.[17,18]

In the present chapter, we wish to describe increasing effects of the catalyst bed temperature on photo-oxidation of light alkanes, methane, ethane and propane, on various n-type solid oxide semiconductors having absorption bands in UV-visible region.

Experimental Section

Materials

Two kinds of zinc oxide catalysts were delivered from Mitsuwa Pure Chemicals Co. Ltd. One was white fine powder, designated as ZnO-A, and the other was yellow grain, ZnO-C. Zinc oxide from Wako Pure Chemical Industry Ltd. was named ZnO-B. One of zinc oxide catalysts, ZnO-D, was prepared by thermal decomposition of zinc oxalate at 1023 K for 1 h in a stream of dried air and then for 1 h under argon.[19] A silica supported zinc oxide catalyst was prepared by impregnating an aqueous solution of zinc acetate onto silica gel (Alfa, surface area is 300 $m^2.g^{-1}$, 200 mesh under) followed by vacuum evaporation at 323 K. The dried solid was calcined in a stream of air at 823 K for 2 h. Characteristics of these catalysts are listed in Table 4. Titanium oxides in anatase form and rutil form delivered from Wako. The other TiO_2, P-25, was used as received. A JRC-TIO-1, one of TiO_2 samples, was acquired from the Catalysis Society of Japan. The JRC-TIO-1 has been announced to be anatase form including 3.63% of SO_3, and having surface area of 76.2 $m^2.g^{-1}$. Other metal oxides were delivered from Wako and used as received. All the catalysts were subjected to *in situ* calcination in the reaction cell at 823 K for 2 h, and following UV irradiation at the same temperature as the reaction temperature (typically 493 K) in dried air for 0.5 h.

Highly purified methane (> 99.9%, including ethane less than 0.01 % and none of other higher hydrocarbons) was used as received. Ethane containing small amounts of CO_2 and H_2O was purified by passing through a column filled with pulverized fused potassium hydroxide and molecular sieves-5A, and then fed to the reactor. Propane, helium and oxygen were used without any further purification.

Apparatus and Procedure

An upstream flow type fixed bed reactor, which is illustrated in Figure 1, was used for the reaction. The reactor is made by quartz glass and has an window for UV irradiation (10 x 20 mm; inner thickness = 1 mm). A quartz glass tube (35 mm o.d.) was equipped to cover the whole reactor. The temperature of the catalyst bed was maintained uniformly by passing heated air around the reactor. UV irradiation was performed by the use of a high pressure mercury vapor lamp (200 W, arc length; 75 mm) with an water filter. The typical reaction conditions are as follows: amount of catalyst; 0.25 g, feed rate of alkane; 7.5 $mmol \cdot h^{-1}$, the molar ratio alkane : O_2 : He; 3 : 1 : 10, W/F; 7.1 $g \cdot h \cdot mol^{-1}$. Liquid products carried with an effluent gas were collected by passing it into an ice-water trap at 273 K for the products of methane oxidation, an acetone trap at 195 K for those of ethane oxidation and a methanol trap at 195 K for the products with C_3H_8. Gaseous products passed through the cold traps were collected into gas sampling bags. After the completion of the reactions, the inlet and outlet of the reactor were closed, and the reactor was quickly cooled down to a room temperature. After the catalyst bed was flushed with argon (5 $cm^3 \cdot min^{-1}$) for 10 min, the catalyst bed was again heated in a stream of argon (5 $cm^3 \cdot min^{-1}$) at a rate of 27.5 $K \cdot min^{-1}$ to 823 K without UV irradiation, and then hold it for 10 min at 823 K. The effluent gas was passed through the cold trap and collected into a gas sampling bag.

Analysis

BET surface area of the catalysts was measured by use of a BELSORP 28 from BEL Japan Inc., a microprocessor-controled automatic system using N_2. An X-ray diffraction study was performed using a RIGAKU Geigerflex with Kα-ray of Copper in the range of $5° < 2\theta < 70°$. A Shimadzu model MPS-2000 multipurpose spectrophotometer was used to measure UV-visible diffuse reflectance spectra. Spectra were recorded over the range of 190 - 700 nm against a MgO (Wako) reference, using an integrating sphere of 50 mm inner diameter. The apparent shape and size of the catalysts were observed with a JEOL JSM-T100 scanning electron microscope (SEM). The products were analyzed by gas chromatography: a Porapak-Q column at 353 K with FID for C_1 - C_4 hydrocarbons and at 433 K for methanol, ethanal and ethanol; a Porapak-N column at 433 K with FID for acetone and propanal; a TSG-1 on Shimarite-F column, distributed from Shimadzu Co. Ltd., at 393 K with TCD for methanal; a molecular sieves-5A column at 323 K with TCD for oxygen; and an active carbon column at 323 K with TCD for H_2, CO and CO_2 (detection limit; carbon oxides ~ 0.002 vol.%, aldehydes and alcohols ~0.1%).

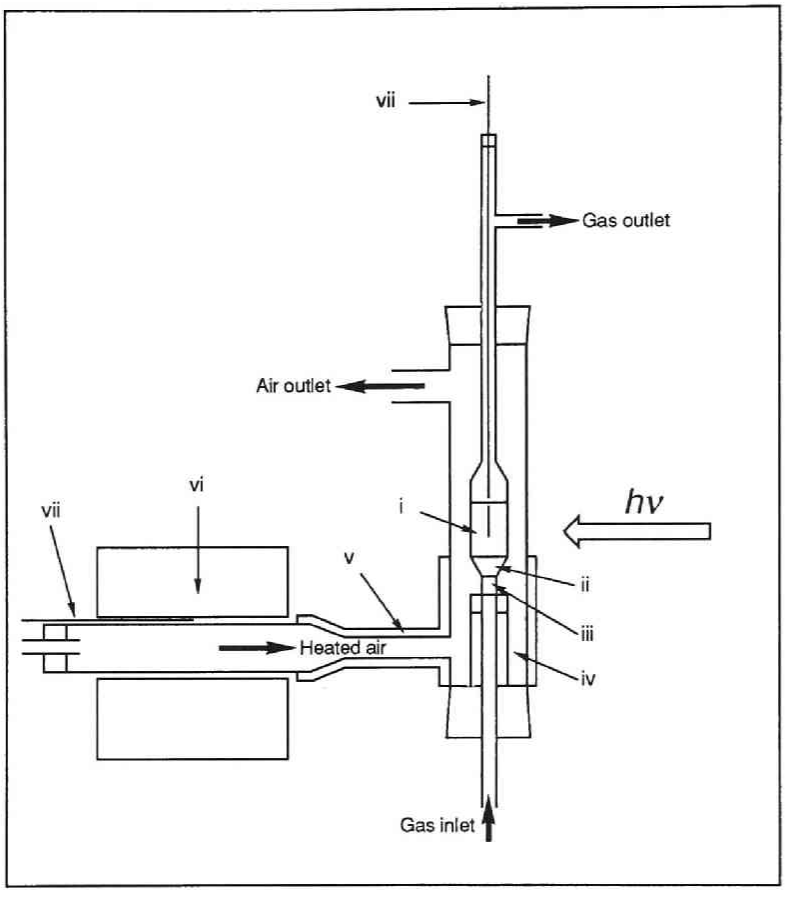

Figure 1. Apparatus for photocatalytic oxidation of gaseous alkanes at elevated temperatures.
(i) catalyst, (ii) silica sand (22 - 42 mesh), (iii) quarz wool plug, (iv) air diffuser, (v) ribbon heater, (vi) electric furnace, (vii) thermocouples.

Results

Yields and selectivities represented in the following text, Tables and Figures were calculated based on the products in the effluent gas. Small amounts of carbon dioxide (less than 1.6 μmol), hydrogen, alkanes and alkenes were evolved by heating the zinc oxide based catalysts to 823 K just after completion of the reaction.

Photocatalytic Oxidation of Methane

Photo-oxidation of methane on various solid oxide catalysts both at an ambient and an elevated temperature was carried out. Table 1 shows the amounts of the products in the effluent gas obtained in the reaction times for the initial 2 h. The reaction at an ambient temperature over ZnO-A (apparent irradiation area; 2.1 cm^2) gave only very small amounts of oxygen-containing chemicals with 3 $\mu mol \cdot h^{-1}$ of carbon dioxide. On the other hand, when the reaction temperature was elevated to 493 K, the catalyst afforded 3.1 $\mu mol \cdot h^{-1}$ of methanal and a large amount of carbon dioxide (27 $\mu mol \cdot h^{-1}$) together with small amounts of methanol, CO and H_2. The selectivity for methanal was *ca.* 9% and that of CO_2 was *ca.* 80%. As shown in run 3, UV irradiation was indispensable for the reaction. The ZnO-B catalyst (irradiation area; 2.4 cm^2) also showed catalytic activity, and afforded methanal in higher yield of 4.7 $\mu mol \cdot h^{-1}$. We examined the activities of ZnO(25 wt.%)/SiO_2 using an apparatus shown in chapter 1, Figure 1. The catalyst bed was fluidized during the reaction. A smaller amount of the catalyst, 0.025 g, was mounted in the reaction cell. However, none of the products was formed with silica supported ZnO.

The catalytic activities of various titanium oxides were examined as shown in runs 6 9. With JRC-TIO-1, only 15 $\mu mol \cdot h^{-1}$ of carbon oxides and none of methanal and methanol were given at an ambient temperature. The reaction at 493 K yielded 2.7 $\mu mol \cdot h^{-1}$ of methanal together with large amounts of carbon monoxide and carbon dioxide. Conversion of methane calculated based on the amounts of the products reached 138 $\mu mol \cdot h^{-1}$. The color of the catalyst remained white after the reaction. The TiO_2 in anatase form showed lower activity than JRC-TIO-1. On the other hand, titanium oxide in rutil form did not show any activity for photo-oxidation of methane. Other metal oxides such as ZrO_2 and CeO_2 did not afford a significant amount of methanal (see runs 10, 11).

Formation of oxygen-containing chemicals from methane has not been reported in the previous studies on photo-oxidation over solid oxide semiconductors.[8-10] The present study would therefore provide the first example of the formation of methanal on ZnO and TiO_2 as far as we know.

Although the selectivity for methanal over the zinc oxide catalyst was lower than that over MoO_3/SiO_2 catalyst (over 90%, see chapter 1),[17] zinc oxide was one of

Table 1 Photo-oxidation of methane on solid oxide catalysts with or without elevation of the catalyst bed temperature[a]

Run	Catalyst	Temp. (K)	Yield (μmol·h^{-1})			
			HCHO	CH_3OH	CO	CO_2
1	ZnO-A	342	trace	0.3	n.d.	3
2		493	3.1	0.4	4	27
3[b]		493	n.d.	n.d.	n.d.	n.d.
4	ZnO-B	493	4.7	0.7	6	33
5[c]	ZnO/SiO2	473	n.d.	n.d.	n.d.	n.d.
6	TiO_2 (JRC-TIO-1)	338	n.d.	n.d.	3	12
7		493	2.7	n.d.	64	71
8	TiO_2 (Anatase)	493	1.5	n.d.	30	20
9	TiO_2 (Rutil)	493	n.d.	n.d.	n.d.	n.d.
10	ZrO_2	493	n.d.	n.d.	n.d.	11
11	CeO_2	493	trace	n.d.	n.d.	25

a Amount of catalyst = 0.25 g, methane feed rate = 7.5 mmol·h^{-1}, $CH_4 : O_2 : He = 3 : 1 : 10$, W/F = 7.1 g·h·mol^{-1}, n.d. = not detected.

b Without UV irradiation.

c Loading level of ZnO = 25 wt.% to the support, amount of catalyst = 0.025 g, W/F = 0.71 g·h·mol^{-1}.

the potentially excellent catalysts for the methanal formation. Then effects of variations in reaction conditions were examined on zinc oxide catalyst.

Figure 2 shows changes in the products yields on ZnO-A against catalyst bed temperatures. The methanal and CO yields reached maximum values of 3.9 $\mu mol \cdot h^{-1}$ at 473 K and 4 $\mu mol \cdot h^{-1}$ at 493 K, respectively. By contrast, the yield of CO_2 increased monotonously with an increase in the temperature.

Figure 3 illustrates effects of contact time on the yields of the products over ZnO-B at 493 K. The yield of methanal increased markedly with increasing the amount of the catalyst up to *ca.* 0.050 g. Then the methanal yield leveled off around 4 $\mu mol \cdot h^{-1}$ with the catalyst level more than 0.10 g (2.8 $g \cdot h \cdot mol^{-1}$). On the other hand, the yields of carbon oxides linearly increased with the amount of the catalyst. Thus the high selectivity for methanal was achieved with a small amount of the catalyst. With 0.027 g (0.77 $g \cdot h \cdot mol^{-1}$) of ZnO-B, methanal and methanol were formed in the yield of 2.6 $\mu mol \cdot h^{-1}$ and 0.3 $\mu mol \cdot h^{-1}$, respectively, while that of carbon oxides were 6 $\mu mol \cdot h^{-1}$.

Photocatalytic Oxidation of Ethane

Table 2 shows the products of photo-oxidation of ethane in the effluent gas at an initial stage of the reaction (~1 h). The products were ethanal, ethanol, methanal, CO_2 and small amounts of ethene, CO and H_2. At 493 K, 84 $\mu mol \cdot h^{-1}$ of ethanal (1.1% of ethane feed) was formed together with 70 $\mu mol \cdot h^{-1}$ of CO_2. The hourly products yields did not change in the prolonged run for 5 h. The selectivity for oxygen-containing chemicals in the effluent gas was more than 70%, and this is fairly higher than that with methane oxidation. The reaction with ZnO-A at an ambient temperature gave only 5.2 $\mu mol \cdot h^{-1}$ of ethanal together with a small amount of CO_2. Without UV irradiation, none of the products was detected. The ZnO-B catalyst showed slightly lower yields. The zinc oxide catalyst of a large particle size, ZnO-C, (see Table 4), did not show any significant catalytic activity for the reaction.

Catalytic activities of several TiO_2 on photo-oxidation of ethane were investigated. At around a room temperature, JRC-TIO-1 gave a large amount of CO_2 (111 $\mu mol \cdot h^{-1}$) with small amounts of ethanal, methanal and CO. The conversion of ethane was 0.8% with lower selectivity for oxygen-containing chemicals of 4% than that in the precedent study of photo-oxidation of ethane on TiO_2 (conversion of ethane; 0.59%, selectivity; 18%).[8] At an elevated temperature, formation of carbon dioxide was suppressed, and the yield of ethanal slightly increased. Conversion of ethane was *ca.* 25 $\mu mol.h^{-1}$ at 493 K whereas that was *ca.* 60 $\mu mol.h^{-1}$ at 338 K. It should be noted that the color of the catalyst turned dark gray to black during the reaction at 493 K, and this coloration disappeared when the

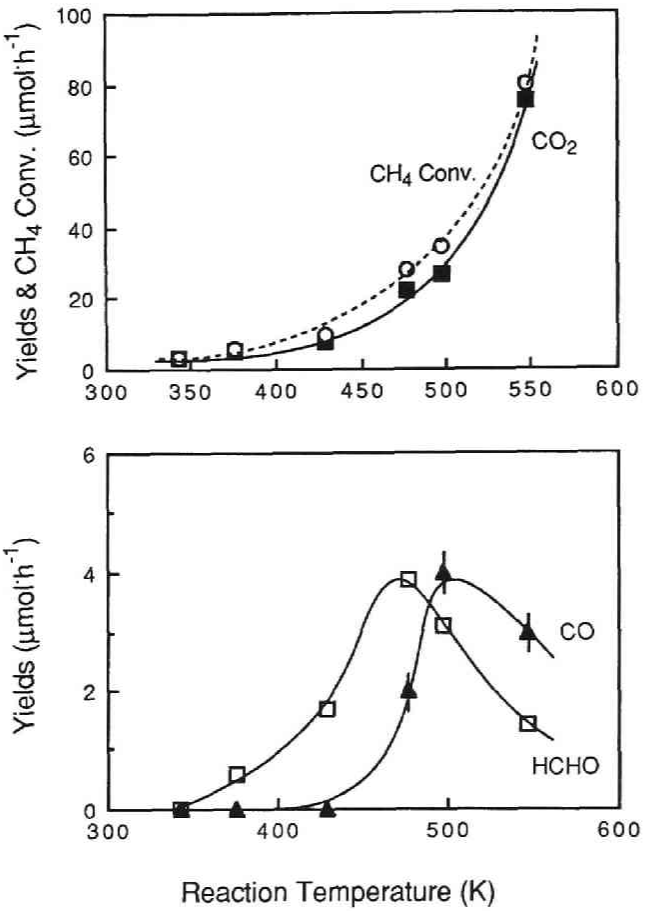

Figure 2. Photo-oxidation of methane at various temperatures over ZnO-A. Yields of (□) HCHO, (▲) CO, (■) CO_2, and (○) CH_4 conversion. Amount of catalyst = 0.25 g, methane feed rate = 7.5 $mmol \cdot h^{-1}$, CH_4: O_2 : He = 3 : 1 : 10, W/F = 7.1 $g \cdot h \cdot mol^{-1}$.

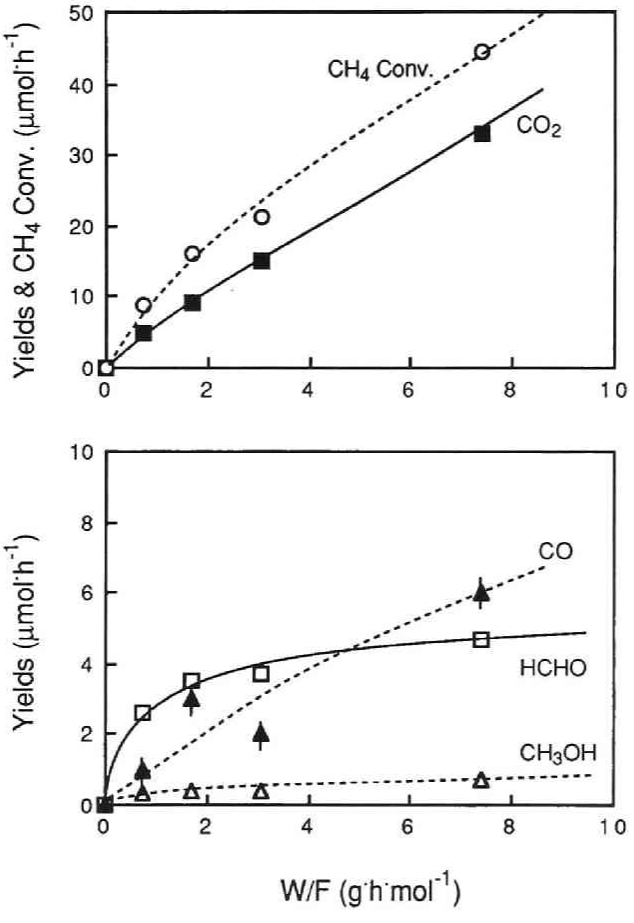

Figure 3. Effects of W/F by changing the amount of the catalyst on photo-oxidation of methane over ZnO-B catalyst. Yields of (□) HCHO, (△) CH_3OH, (▲) CO, (■) CO_2, and (○) CH_4 conversion. Reaction gas composition was the same as shown in Figure 2.

Table 2 Photo-oxidation of ethane on solid oxide catalysts with or without elevation of the catalyst bed temperature[a]

Run	Catalyst	Temp. (K)	Yield (μmol·h^{-1}) CH_3CHO	C_2H_5OH	HCHO	CO	CO_2
12	ZnO-A	340	5.2	n.d.	n.d.	n.d.	7
13		493	84	2.8	5.9	7	70
14[b]		493	n.d.	n.d.	n.d.	n.d.	n.d.
15	ZnO-B	493	77	3.0	4.2	3	54
16	ZnO-C	493	2.7	n.d.	n.d.	n.d.	trace
17	ZnO-D	493	43	1.6	1.1	3	29
18	TiO_2 (JRC-TIO-1)	339	1.5	n.d.	1.7	3	111
19		493	2.3	n.d.	trace	14	29
20[b]		493	n.d.	n.d.	n.d.	n.d.	n.d.
21	TiO_2 (Anatase)	354	1.6	n.d.	trace	trace	58
22		493	5.1	n.d.	4.0	3	24
23[c]	TiO_2 (P-25)	337	0.9	n.d.	n.d.	n.d.	56
24[c]		493	1.0	n.d.	n.d.	n.d.	n.d.
25	V_2O_5	493	trace	n.d.	trace	trace	3
26	ZrO_2	493	trace	n.d.	n.d.	2	37
27	Nb_2O_5	493	1.8	n.d.	n.d.	n.d.	4
28	SnO_2	493	1.9	n.d.	n.d.	n.d.	2
29	CeO_2	493	6.5	n.d.	n.d.	trace	115
30	Nd_2O_3	493	1.1	n.d.	n.d.	n.d.	2
31	Sm_2O_3	493	0.9	n.d.	n.d.	n.d.	trace

a Amount of catalyst = 0.25 g, ethane feed rate = 7.5 mmol·h^{-1}, $C_2H_6 : O_2 : He = 3 : 1 : 10$, W/F = 7.1 g·h·mol^{-1}, n.d. = not detected.

b Without UV irradiation.

c Amount of catalyst = 0.025 g, W/F = 0.71 g·h·mol^{-1}.

catalyst bed was cooled down in a stream of air after the reaction. On the other hand, the catalyst remained white with the reaction at a room temperature. The color of the catalyst in the reaction at 496 K without UV irradiation was kept white. The decrease in the yields and the coloration at an elevated temperature were not observed in the case of methane oxidation. Other TiO_2 catalyst employed showed similar behavior on photo-oxidation of ethane. Titanium oxide P-25 did not gave carbon oxides but ethanal in the yield of only 1.0 $\mu mol \cdot h^{-1}$ at 493 K. Such reversed effect of the reaction temperature on the catalytic activity with TiO_2 has been reported in the case with photo-oxidation of propene.[14] Among other metal oxide catalysts examined, CeO_2 showed a high activity for complete oxidation. The yield of carbon oxide reached 115 $\mu mol \cdot h^{-1}$ with 6.5 $\mu mol \cdot h^{-1}$ of ethanal.

We investigated effects of reaction conditions using the ZnO- A or B, which exhibited the highest activity and selectivity. The yields of the products against various temperatures are shown in Figure 4. The reaction temperature around 500 K was most suitable for ethanal formation. A further increase in the temperature enhanced deep oxidation. The conversion of ethane levelled off above 500 K.

Figure 5 shows effects of W/F on the yields by changing the amount of the ZnO-B catalyst. The yield of ethanal increased with increasing W/F, but not linearly. The conversion of ethane also showed similar behavior. On the other hand, the carbon dioxide yield increased linearly with W/F. Higher selectivity (82%) for ethanal was given with a smaller amount of ZnO-B (0.027 g, W/F; 0.77 $g \cdot h \cdot mol^{-1}$).

Effects of partial pressure of ethane and oxygen on photo-oxidation of ethane were examined. Figure 6 shows that the yield of ethanal and the amount of converted ethane increased with an increase in partial pressure of ethane, P_{ethane}. Similar tendencies were observed for the yields of methanal and ethanol. On the other hand, the yields of CO and CO_2 were constant over the range of ethane partial pressure from 7.3 kPa to 54 kPa. Higher P_{ethane} was preferable to oxygen-containing products.

Effects of partial pressure of oxygen, P_{oxygen}, are shown in Figure 7. Without oxygen in the feed, ethanal, ethanol and carbon dioxide were formed in the yields of 13 $\mu mol \cdot h^{-1}$, 1.3 $\mu mol \cdot h^{-1}$ and 2 $\mu mol \cdot h^{-1}$, respectively, during the reaction of first 1 h. The yields of these products gradually decreased in the course of the reaction, and the reaction after 3 - 4 h gave only 8 $\mu mol \cdot h^{-1}$ of the products. Ethane conversion was markedly enhanced with an increase in P_{oxygen}, and then leveled off at P_{oxygen} above *ca.* 8 kPa. An increase in P_{oxygen} up to 8 kPa enhanced formation of all the products including carbon oxides. A further increase in P_{oxygen} slightly decreased the yields of ethanal, ethanol and methanal, whereas that of carbon oxides slightly increased. The results in Figure 7 suggest that higher selectivities for aldehydes and alcohols are given at lower P_{oxygen}. At P_{oxygen} of 1.4 kPa, the yield of oxygen-containing products was 57 $\mu mol \cdot h^{-1}$, and the selectivity was 83 %.

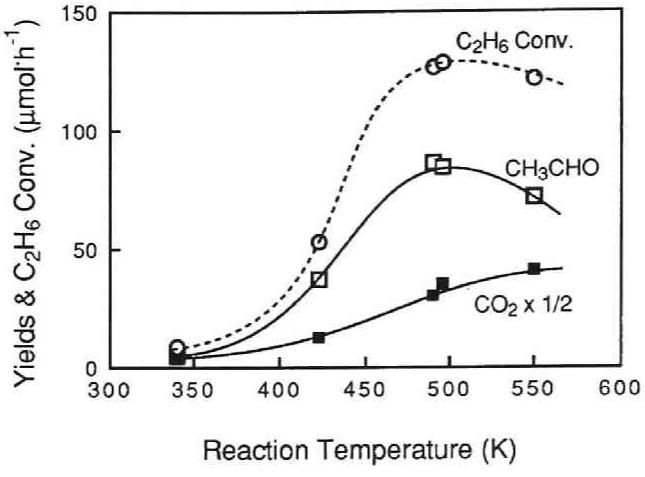

Figure 4. Photo-oxidation of ethane at various temperatures over ZnO-A. Yields of (□) CH_3CHO, (■) CO_2 (x 1/2) and (○) C_2H_6 conversion. Amount of catalyst = 0.25 g, ethane feed rate = 7.5 mmol·h^{-1}, C_2H_6 : O_2 : He = 3 : 1 : 10, W/F = 7.1 g·h·mol^{-1}.

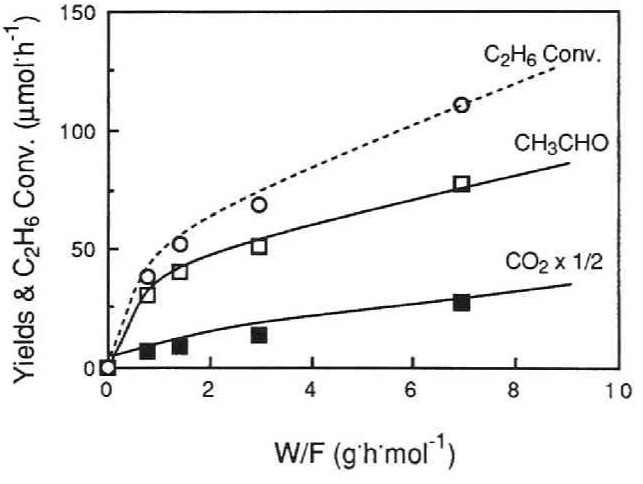

Figure 5. Effects of W/F by changing the amount of the catalyst on photo-oxidation of ethane over the ZnO-B catalyst.
Yields of (□) CH_3CHO, (■) CO_2 (x 1/2) and (○) C_2H_6 conversion. Reaction gas composition was the same as shown in Figure 4.

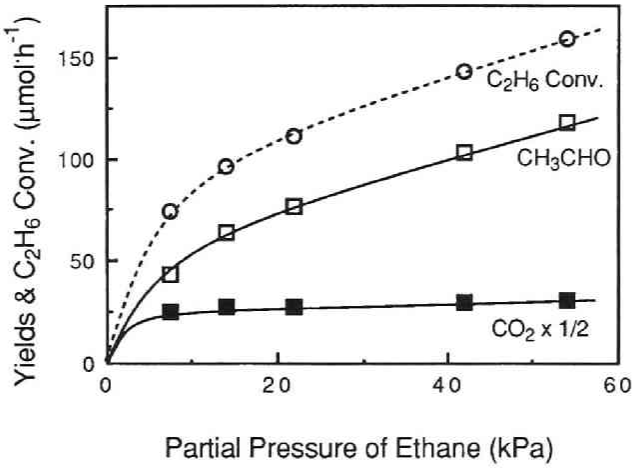

Figure 6. Effects of partial pressure of ethane on photo-oxidation of ethane over ZnO-B. Yields of (□) CH_3CHO, (■) CO_2 (x 1/2), and (○) C_2H_6 conversion. Amount of catalyst = 0.25 g, oxygen feed rate = 2.5 mmol·h^{-1} (7.2 kPa), W/F = 7.1 g·h·mol^{-1}.

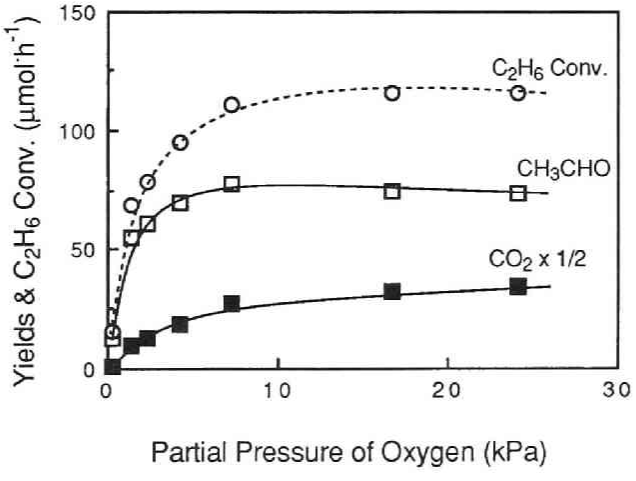

Figure 7. Effects of partial pressure of oxygen on photo-oxidation of ethane over ZnO-B. Yields of (□) CH_3CHO, (■) CO_2 (x 1/2), and (○) C_2H_6 conversion. Amount of catalyst = 0.25 g, ethane feed rate = 7.5 mmol·h^{-1} (22 kPa), W/F = 7.1 g·h·mol^{-1}.

Photo-oxidation of Propane

Table 3 shows results of ZnO-B catalyst for the initial 1 h. At 493 K, about 140 $\mu mol \cdot h^{-1}$ of oxygen-containing products (propanal, acetone, ethanal and methanal) were formed together with carbon oxides. The selectivity for the useful products amounted to 87% on carbon base, indicating the zinc oxide catalyst is one of the excellent catalysts for selective photo-oxidation of propane. On the other hand, the reaction at a room temperature yielded only 4 $\mu mol.h^{-1}$ of CO_2.

Effects of the reaction temperature were shown in Figure 8. The profile of the dependency on the temperature was similar to those in the cases of photo-oxidation of methane (Figure 2) and ethane (Figure 4). The yields of oxygen-containing chemicals reached maxima at 500 K. Formation of carbon dioxide continued to increase with a further increase in the reaction temperature.

Catalytic activity of TiO_2 for propane oxidation has been investigated by Teichner et al.[8] Aldehydes and ketone were reported to be formed in the combined yield of 0.5% with the selectivity of 68%. Our results of photo-oxidation of propane at an ambient or elevated temperatures were shown in Table 3. The predominant product was carbon dioxide, and the selectivity for oxygen-containing chemicals was about 40%. The conversion of propane at an ambient temperature was higher than that at 493 K.

Desorption of Carbon Dioxide from the Catalyst

Because of basic character of ZnO and the higher decomposition temperature of $ZnCO_3$ (573 K) than the reaction temperature, a part of carbon dioxide produced could be adsorbed on the surface of ZnO as carbonate species. The amount of adsorbed carbon dioxide was measured by heating the catalyst in argon atmosphere to 823 K after the oxidation reactions. From the ZnO-B catalyst after the completion of photo-oxidation of methane for 1 h at 493 K, being flushed with argon, a small amount of carbon dioxide (*ca.* 1.3 μmol) was evolved during the heat treatment. After the reaction with ethane and propane, the catalysts also desorbed *ca.* 1.3 μmol of carbon dioxide. Very small amounts of methane and ethene were also desorbed. It should be noted that *ca.* 1.3 μmol of carbon dioxide was evolved from ZnO-B after the reaction at an ambient temperature. The possibility that formation of CO_2 was responsible for the presence of the surface intermediate species leading to aldehydes or ketones, which were oxidized to CO_2 by bulk oxygen of the catalyst, can not be ruled out.

Table 3 Photo-oxidation of propane on zinc and titanium oxide[a]

Run	Catalyst	Temp. (K)	Yield ($\mu mol \cdot h^{-1}$)				
			C_2H_5CHO	$(CH_3)_2CO$	CH_3CHO	CO	CO_2
32	ZnO-B	329	trace	trace	trace	n.d.	4
33		493	57	56	27	9	45
34[b]		493	n.d.	n.d.	n.d.	n.d.	n.d.
35	TiO_2 (Anatase)	347	0.6	9.5	3.1	trace	48
36		493	0.3	2.2	2.0	trace	12

a Amount of catalyst = 0.25 g, propane feed rate = 7.5 $mmol \cdot h^{-1}$, $C_3H_8 : O_2 : He = 3 : 1 : 10$, W/F = 7.1 $g \cdot h \cdot mol^{-1}$, n.d. = not detected.

b Without UV irradiation.

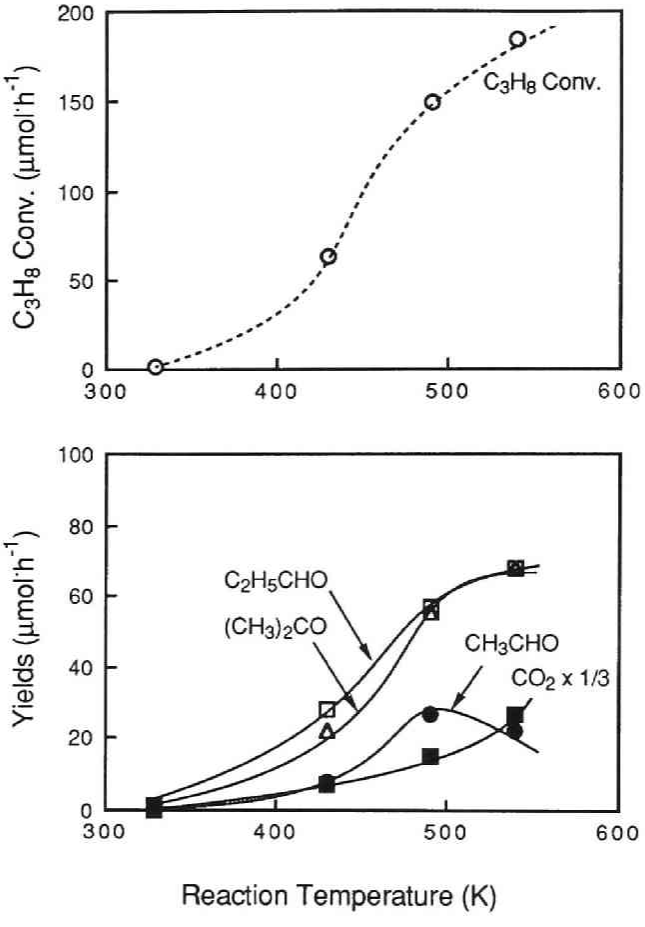

Figure 8. Photo-oxidation of propane at various catalyst bed temperatures over ZnO-B. Yields of (□) C_2H_5CHO, (△) $(CH_3)_2CO$, (●) CH_3CHO, (■) CO_2 (x 1/3), and (○) C_3H_8 conversion. Amount of catalyst = 0.25 g, propane feed rate = 7.5 mmol·h^{-1}, $C_3H_8 : O_2 : He = 3 : 1 : 10$, W/F = 7.1 g·h·mol^{-1}.

Physical Properties of Zinc Oxide Catalysts

Table 4 shows packing densities, BET surface areas and particle sizes of the zinc oxide catalysts used for the reaction. SEM photographs of several zinc oxide catalysts were shown in Plate 1. ZnO-A and ZnO-B showed similar characteristics, whereas ZnO-C exhibited the lower surface area and higher packing density. ZnO-C consisted of larger particles (mean diameter was *ca.* 3 μm) than those of other ZnO samples. It should be noted that ZnO-C colored yellow, and this coloration did not disappear by heating the catalyst in a stream of air at 823 K for 2 h. ZnO-D, less active than ZnO-A or ZnO-B, also consisted of large particles (*ca.* 1 μm), suggesting a smaller particle size is preferred to show higher catalytic activity.

Figure 9 shows UV diffuse reflectance spectra of the ZnO-A and silica supported ZnO(25 wt.%) catalyst. The red limit of absorption spectra of ZnO was 380 nm, whereas that of silica supported ZnO shifted to longer wavelength (410 ~ 430 nm). Any significant peaks attributed to crystalline ZnO were not observed in the XRD spectrum of the ZnO/SiO_2 catalyst, indicating an absence of large crystallite of ZnO on the surface.

Discussion

It is generally accepted that photocatalytic oxidation is initiated by the formation of a pair of electron and positive hole by irradiation on n-type solid semiconductors such as ZnO and TiO_2, requiring the band gap irradiation.[20,21] There are kinds of active oxygen species proposed over n-type solid semiconductors. Teichner et al.[8,22] studied photo-oxidation of several alkanes (>C_2) to ketones and aldehydes over TiO_2. They proposed that neutral atomic oxygen, O^*_{ads}, is the active species to form alcohol which was proposed to be an intermediate compound. The O^*_{ads} species was assumed to be formed through the reaction between adsorbed oxygen species, such as $O_2^-{}_{ads}$, and the positive hole.

The roles of the lattice oxygen species have also been investigated, and the photoactivated lattice oxygen species, O^-, which is formed by trapping the hole with a lattice oxygen, has been proposed to be responsible for the photocatalytic oxidation. The studies on the isotopic exchange reactions between the lattice oxygen of TiO_2 and gaseous oxygen,[23] and the reaction of alcohols with $^{18}O_2$,[24,25] have revealed the participation of the lattice oxygen as the active species.

In the present study, the reaction of ethane in the absence of oxygen primarily gave ethanal in low yield, and the yield gradually decreased during the prolonged run. These results indicate that the lattice oxygen could react with alkanes under irradiation to form aldehydes or ketones. Although alcohols have been often considered to be intermediate compounds for the formation of aldehydes

Table 4 Physical properties of zinc oxide catalysts.

Catalyst	Source	Color	Apparent packing density ($g \cdot cm^{-3}$)	BET S.A. ($m^2 \cdot g^{-1}$)	Particle size[a] (μm)
ZnO-A	Mitsuwa	white	0.8	4.2	0.3
ZnO-B	Wako	white	0.7	4.7	0.3
ZnO-C	Mitsuwa	yellow	2.8	0.5	3
ZnO-D[b]		white	0.8	5.9	1
ZnO/SiO_2[c]		white	0.4	152	(10)

[a] Mean particle size estimated from SEM photography, the value of ZnO/SiO_2 is that of the support.

[b] Prepared by thermal decomposition of zinc oxalate at 1023 K.

[c] Prepared by the impregnation method, loading level of ZnO = 25 wt.%.

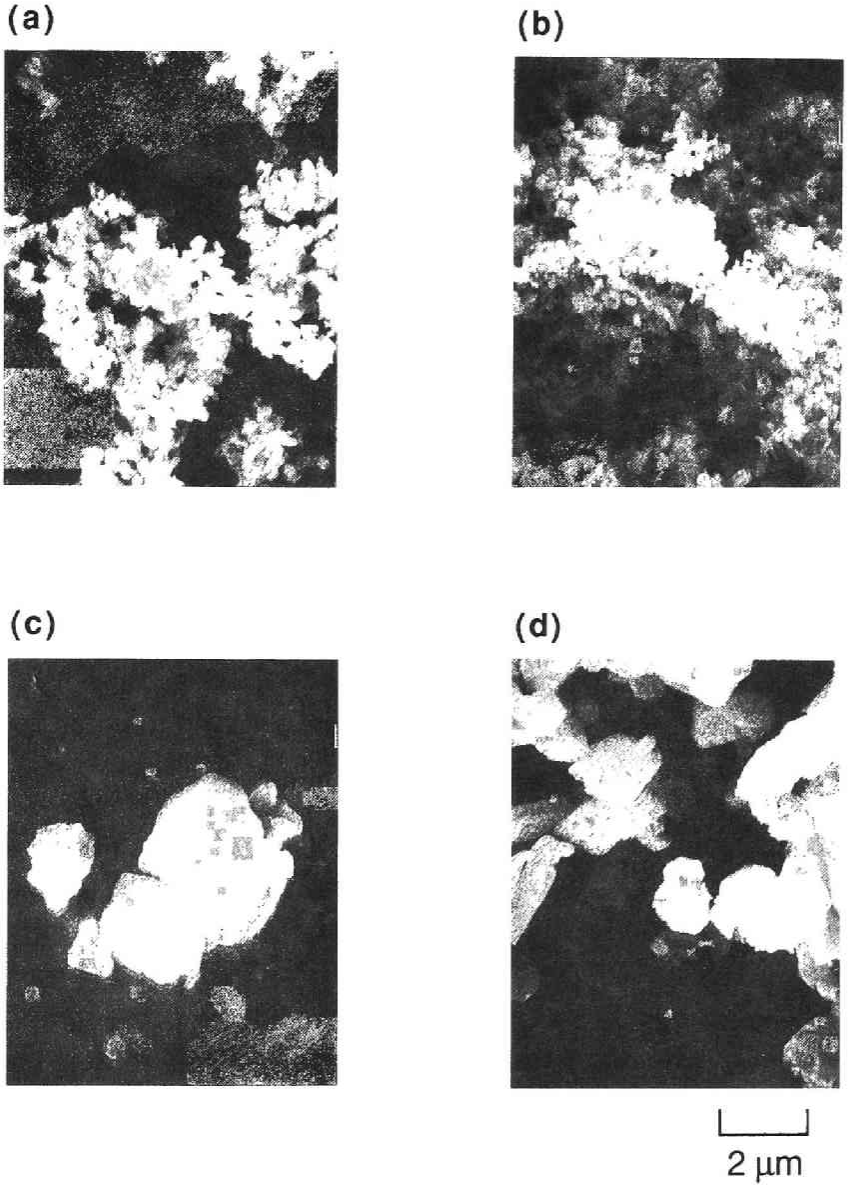

Plate 1. SEM photographs of (a) ZnO-A, (b) ZnO-B, (c) ZnO-C and (d) ZnO-D.

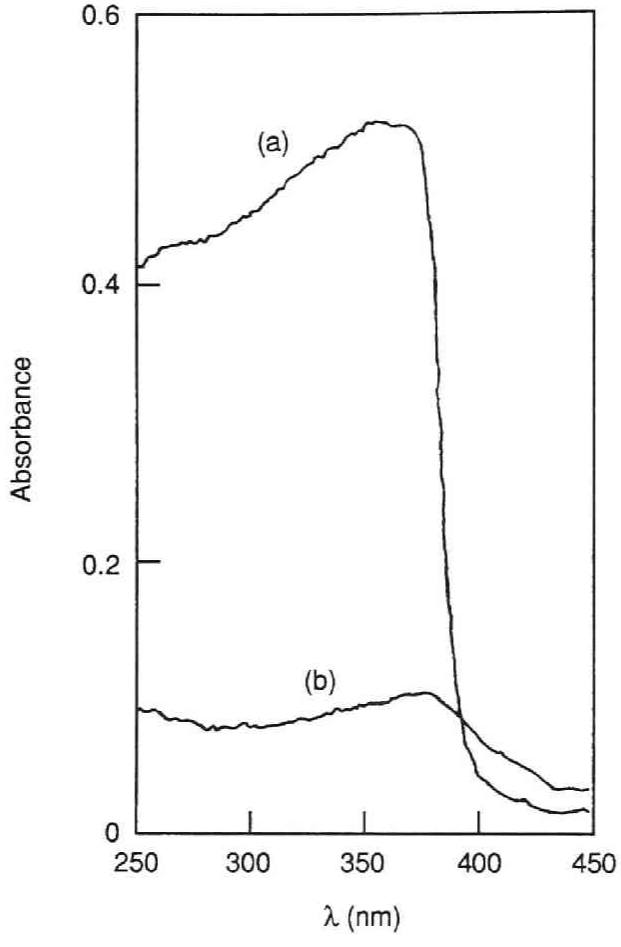

Figure 9. UV diffuse reflectance spectra of (a) ZnO-A and (b) ZnO(25 wt.%)/SiO_2. Samples were diluted with MgO, sample : MgO = 1 : 3.

and ketones, only a small amount of ethanol was produced even in the absence of molecular oxygen. This suggests that aldehydes and ketones were not secondary products formed by the oxidation of alcohols, but directly formed by the reaction of alkanes on the catalyst surface. In addition, the selectivity for oxygen-containing products was very high at an initial stage of the reaction without molecular oxygen, and an only small amount of carbon oxides was formed. This suggests that the active species from the lattice oxygen is selective for the formation of aldehydes or ketones. But the nature of the species,[16,26] e.g. O^- or O^{3-}, is still unclear. The decreases in the yields of aldehydes against the reaction period would be due to the decreases in the amount of the lattice oxygen that could be activated by light.

The most important role of molecular oxygen may be the rapid re-oxidation of reduced surface, resulting in regenerating active species. In addition to lattice oxygen species, several types of adsorbed oxygen species might be formed on the surface. Contribution of them in the reaction could not be negligible. Molecular oxygen might accept an electron generated by UV irradiation, resulting in the formation of negatively charged adsorbed oxygen species, such as superoxide anion or peroxide ion. The results in our study, however, did not clarify the detailed roles of adsorbed oxygen species. The results obtained in the presence of molecular oxygen suggest that these adsorbed species were partly responsible for deep oxidation of alkanes, intermediates or products to carbon oxides, since the selectivity gradually decreased with increasing P_{oxygen} (see Figure 7).

One plausible reason why an increase in the temperature reduced the catalytic activity of TiO_2 on photo-oxidation of ethane and propane may be interpreted as follows: The coloration is probably due to the partial reduction of TiO_2 surface, since the color of reduced titanium oxide, TiO or Ti_2O_3, is black. If the active lattice oxygen may take part in direct attack to alkanes, the lattice oxygen of TiO_2 surface might be transformed to alkane, and then re-oxidized by molecular oxygen. At an elevated temperature, consumption of the lattice oxygen would proceed much faster than re-oxidation of the catalyst, since photo-oxidation of ethane or propane was much enhanced. Methane is more difficult to be activated, thus the reduction of the surface would not occur.

The behavior of ethane conversion versus W/F shown in Figure 5 can be explained as follows. With a larger amount of the catalyst, adsorption of products on the catalyst may occur. The adsorbed species would occupy the active sites on the surface, and therefore decreases the number of accessible sites for photo-oxidation of ethane, resulting in the lower ethane conversions than those expected. The adsorbed species might be readily further oxidized to form carbon oxides. This could be a reason for decreases in the selectivity for ethanal. Such adsorption of the products on the catalyst might be occur in the case of methane oxidation. As shown in Figure 3, the yield of carbon dioxide increased almost linearly with increasing

W/F, whereas the yield of methanal leveled off around 4 $\mu mol \cdot h^{-1}$ irrespective of W/F above *ca.* 3 $g \cdot h \cdot mol^{-1}$. Influence of adsorption of methanal would be more conspicuous for leveling off the yield of methanal, and less for CO_2 formation, since a much smaller amount of oxygen-containing chemicals were formed than those with ethane oxidation. The decreases in the number of accessible sites might be fairly small, although a large part of produced methanal would be adsorbed on the surface.

The results obtained in the reaction with various types of zinc oxide catalysts revealed that smaller particle size is favorable to show significant catalytic activity. Effects of particle size on photocatalytic reactions have been reported with the noble metal catalysts and metal oxide catalysts. The mechanistic aspect has been discussed in detail.[27] To exhibit photocatalytic activity, a pair of electron and positive hole, which is formed in the bulk of the solid by irradiation, is required to reach the surface without re-combination. As a size of the solid particle become larger, it should be more difficult to reach the surface before recombination, resulting in the decreases in the number of active sites. In addition to effects of particle size, other physical properties such as surface areas would greatly affect the reaction as is in the case with thermal process on the solid catalyst. Therefore care must be taken in the discussion of the reasons of differences in their activities. It should be noted that non-active ZnO-C colored yellow, indicating the presence of defects in its structure. As described before, this coloration was maintained during the heat treatment in dried air, thus we may ascribe that this coloration probably due to the deficiency of Zn^{2+} cation. Such defects in the crystalline structure of ZnO would provide the recombination site of the excited hole and electron.

References

1 P. Pitchai and K. Klier, *Catal. Rev.-Sci. Eng., 28 (1),* **1986**, 13.

2 M.D. Ward, J.F. Brazdil, S.P. Mehandru and A.B. Anderson, *J. Phys. Chem., 91,* **1987**, 6515.

3 S.L. Kaliaguine, B.N. Shelimov and V.B. Kazansky, *J. Catal., 55*, **1978**, 384.

4 K. Marcinkowska, S. Kaliaguine and P.C. Roberge, *J. Catal., 90,* **1984**, 49.

5 K. Marcinkowska, S. Kaliaguine and P.C. Roberge, *Proc. 9th. Congr. Catal. Calgary, 4*, **1988**, 521.

6 S.F. Gerasimov, *React. Kinet. Catal. Lett., 32 (1),* **1986**, 57.

7 W. Hill, B.N. Shelimov and V.B. Kazansky, *J. Chem. Soc., Faraday Trans. 1, 83*, **1987**, 2381.

8 N. Djeghri, M. Formenti, F. Juillet and S.J. Teichner, *Faraday Discuss. Chem. Soc., 58*, **1984**, 185.

9 K.R. Thampi, J. Kiwi and M. Grätzel, *Catal. Lett.*, **1989**, 109.

10 M. Grätzel, K.R. Thampi and J. Kiwi, *J. Phys. Chem., 93,* **1989**, 4128.

11 M. Daroux, D. Klvana, M. Duran and M. Bideau, *Can. J. Chem. Eng., 63*, **1985**, 668.

12 J. Lacoste, R. Arnaud, R.P. Singh and J. Lamaire, *Makromol. Chem., 189 (3)*, **1988**, 651.

13 L.V. Lyashenko, Y.B. Gorokhovatskii, V.I. Stepanenko and F.A.Yampol'skaya, *Teor. Eksp. Khim., 13,* **1977**, 35.

14 P. Pichat, J.M. Herrmann, J. Disdier and M.N. Mozzanega, *J. Phys. Chem., 83*, **1979**, 3122.

15 W. Doerffler and K. Hauffe, *J. Catal., 3*, **1964**, 156, 171.

16 K. Tanaka and G. Blyholder, *J. Phys. Chem., 76*, **1972**, 1807.

17 T. Suzuki, K. Wada, M. Shima and Y. Watanabe, *J. Chem. Soc., Chem. Commun.,* **1990**, 1059 (Chapter 1).

18 K. Wada, K. Yoshida, Y. Watanabe and T. Suzuki, *Appl. Catal., 74*, **1991**, L1, (Chapter 1).

19 T. Suzuki, K. Wada and Y. Watnabe, *Appl. Catal., 59*, **1990**, 213 (Chapter 5).

20 V.S. Zakharenko, A.E. Cherkasin, N.P. Keier and S.V. Koshceev, *Kinet. Katal., 16*, **1975**, 74.

21 W.R. Murphy, T.F. Veerbamp and T.W. Leland,
J. Catal., 43, **1976**, 304.
22 M. Formenti and S.J. Teichner,
Catalysis, The Chemical Society, London, *2*, **1978**, 87.
23 H. Courbon, M. Formenti and P. Pichat,
J. Phys. Chem., 81, **1977**, 550.
24 J. Cunningham, B. Doyle and E.M. Leahy,
J. Chem. Soc., Faraday Trans., 1, 75, **1979**, 2000.
25 J. Cunningham, B.K. Hodnett, M. Ilyas and E.M. Leahy,
J. Chem. Soc., Faraday Trans., 1, 78, **1982**, 3297.
26 M. Iwamoto, *Shokubai, 26 (1)*, **1984**, 30.
27 H. Arai, *Hyoumen, 17*, **1979**, 675, 746.

Chapter 3

Selective Photo-oxidation of Methane using Molybdenum Oxide Loaded Zinc Oxide Catalysts

Abstract

Photocatalytic oxidation of methane with the zinc oxide based catalysts was performed using a fixed bed flow reactor at 500 - 550 K. Loading of a small amount of molybdenum oxide onto a zinc oxide catalyst drastically improved the selectivity for methanal. An effluent gas from the reaction on the MoO3(0.1 wt.%) loaded ZnO catalyst at 548 K included 8.0 $\mu mol \cdot h^{-1}$ of methanal together with small amounts of methanol and carbon dioxide, whereas that with a parent ZnO afforded a large amount of carbon dioxide and the selectivity for methanal was less than 10%. UV irradiation and a catalyst bed temperature above 450 K were indispensable for the formation of a significant amount of methanal. On the other hand, for the photocatalytic oxidation of ethane and propane, loading of molybdenum oxide on ZnO did not increase the selectivity for oxygen-containing chemicals, but decreased the yields of all the products.

Introduction

Although photocatalytic oxidation of various alkanes over a solid oxide surface has been reported, surprisingly few attempts for selective photo-oxidation of methane into more valuable compounds were successful.[1-6] Photo-oxidation of methane on solid oxide semiconductors such as TiO_2 was found to give mainly CO_2. None of the studies have reported the formation of oxygen-containing chemicals such as methanal or methanol. Grätzel et al. reported that loading of tungstsilicate on titanium oxide enhanced the formation of carbon monoxide in place of carbon dioxide at an ambient temperature,[4] and the yields of carbon monoxide increased with an increase in the reaction temperature.[5]

As described in chapter 2, selective photo-oxidation of ethane and propane has been achieved on ZnO at around 500 K. Photo-oxidation of

methane on ZnO, however, afforded a large amount of carbon dioxide together with a small amount of methanal. Therefore the selectivity for methanal was low. Selective formation of methanal by the photocatalytic oxidation of methane on silica supported molybdenum oxide has been described in chapter 1.[7] Selective photo-oxidation of ethane and propane was also performed.[8]

This chapter describes selective photo-oxidation of methane to methanal on molybdenum oxide or several metal oxides loaded zinc oxide at an elevated temperature of around 500 K. Loading of molybdenum oxide to the zinc oxide catalyst suppressed formation of carbon oxides, resulting in a drastic increase in the selectivity for oxygen-containing products.[9]

Experimental Section

Materials

Several kinds of zinc oxide were delivered from Mitsuwa Pure Chemicals Co. Ltd. (further designated as ZnO-A) and Wako Pure Chemical Industry Ltd. (ZnO-B), and used as the catalyst. Their physical properties have been shown in chapter 2. One of the ZnO-B catalyst, which was bathed in distilled water and followed by drying and calcination at 823 K, is designated as the 'H_2O treated' ZnO-B catalyst. The molybdenum oxide loaded catalyst was prepared by the usual impregnation method with an aqueous solution of ammonium heptamolybdate. The dried paste was calcined under air at 823 K for 2 h. Other loaded catalysts were prepared in a similar manner. A loss of molybdenum species from the molybdenum oxide loaded zinc oxide catalyst during the calcination in air at 823 K was determined by the atomic absorption analysis. The catalyst was leached out with a dilute NH_4OH aqueous solution. Fairly large part of molybdenum species on the surface was found to be lost during the activation, especially for the catalyst of high loading levels more than 1 wt.% (as MoO_3 calculated for impregnating solution). For other metal oxide loaded catalysts, amounts of the additives in the impregnating solution are given in the Tables. All the catalysts mounted in the reaction cell, typically 0.25 g, were again subjected to the calcination in air at 823 K for 2 h, and followed by UV irradiation at the same temperature to the reaction temperature under air for 0.5 h just before the reaction. Gaseous

reactants used for the reaction in this chapter were delivered and purified in the same manner as described in chapter 2.

Apparatus and Procedures

An upstream flow type fixed bed apparatus equipped with a quartz glass tube to cover the whole reactor was used for the reaction. Details of the apparatus have been described in chapter 2. The temperature of the catalyst bed was maintained uniformly by passing heated air around the reactor. A high-pressure mercury vapor lamp (200 W, arc length = 75 mm) with a water filter was used for UV irradiation. The reaction was carried out typically under the following conditions: feed rate of alkane; 7.5 $mmol \cdot h^{-1}$, the molar ratio alkane : O_2 : He; 3 : 1 : 10, and W/F; 7.1 $g \cdot h \cdot mol^{-1}$. Liquid products from the reaction with methane, ethane and propane were collected into an ice-water trap at 273 K, an acetone trap at 195 K and a methanol trap at 195 K. Gaseous products passed through the traps were collected into gas sampling bags. Procedure of heat treatment after the reaction completed has been described in chapter 2.

Analysis

X-ray photoelectron spectroscopy (XPS) spectra of the MoO_3 loaded zinc oxide catalysts were recorded with a Perkin Elmer 5500 MT system using Al $K\alpha_{1,2}$ radiation (15 kV, 400 W) operated at a room temperature, under the pressure less than 10^{-8} torr. The electron take off angle was set at 45 deg. Spectral accumulation time was approximately 40 min for Mo(3d) and 10 min for Zn(3p3) lines. The binding energies were referenced to the C(1s) level. The extent of the dispersion of supported molybdenum species was estimated on the basis of the measurements in terms of relative peak area intensities of Mo($3d_{5/2}$) (232.7 eV), Mo($3d_{3/2}$) (235.9 eV), Mo(3p3) (398.2 eV), Zn(2p3) (1021 eV), O(1s) (531.1 eV), and C(1s) (285.0 eV), where the atomic sensitivity ratio of Mo(3d)/Zn(2p3); 0.891.[10]

The GC analyses of the products have been described in chapter 2.

Results and Discussion

Photo-oxidation of Methane

The yields and the selectivities represented in the following text, Tables and Figures were calculated from the products in the effluent gas. Heating of the catalyst bed up to 823 K in argon just after the completion of the reaction gave a small amount of carbon dioxide. The amount of desorbed carbon dioxide was not more than 1.5 μmol. Similar desorption of carbon dioxide (*ca.* 1.3 μmol) was also observed on unloaded zinc oxides (see chapter 2). On the other hand, hydrogen, alkanes and alkenes, which were generated from ZnO after the reaction, were not detected with the metal oxide loaded zinc oxide catalysts by GC analysis.

The results of photo-oxidation of methane on various metal oxide loaded zinc oxide catalysts are listed in Table 1. The products were methanal and carbon dioxide with very small amounts of methanol and carbon monoxide. The parent zinc oxide catalyst, ZnO-A, gave 3.1 $\mu mol \cdot h^{-1}$ of methanal with a large amount of carbon dioxide, 27 $\mu mol \cdot h^{-1}$. The selectivity for methanal was therefore very low (*ca.* 9%). Apparent irradiation areas of ZnO-A and ZnO-B were 2.1 cm^2 and 2.4 cm^2, respectively (see chapter 2). ZnO-B also gave mainly carbon dioxide, and a smaller amount of methanal. Packing density of ZnO-B fairly increased by the treatment with H_2O. Mean size of the particles and BET surface area were almost unchanged. The decreases in the yields of the products were probably due to a decrease in the apparent irradiation area of the catalyst from 2.4 cm^2 to 1.5 cm^2. The metal oxide loaded catalysts had similar particle sizes, packing densities and irradiation surface areas to those of a H_2O-treated zinc oxide. Therefore we should compare the activities of the loaded catalysts with that of the H_2O-treated zinc oxide in order to precisely discuss effects of additives. Loading of MoO_3 on both ZnO-A and ZnO-B increased the yield of methanal and suppressed formation of carbon oxides almost completely. The MoO_3 (0.8 wt.% after calcination in air, 1.0 wt.% in the impregnating solution) loaded ZnO-B catalyst gave 5.4 $\mu mol \cdot h^{-1}$ of methanal and 2 $\mu mol \cdot h^{-1}$ of carbon dioxide.

Since our previous study has revealed that selective photo-oxidation of methane with highly dispersed molybdenum oxide loaded on silica required irradiation of wavelength shorter than 300 nm,[7] we tried to cut off this region of irradiation with a Pyrex filter. However, methanal was

Table 1 Photo-oxidation of methane on the various metal oxide-loaded zinc oxide catalysts at 493 K.[a]

Run	Catalyst	BET S.A. ($m^2 \cdot g^{-1}$)	ρ_p[b] ($g \cdot cm^{-3}$)	Yield ($\mu mol \cdot h^{-1}$)[c] HCHO	CH_3OH	CO	CO_2
1[d]	ZnO-A	4.2	0.8	3.1	0.4	4	27
2[e]				2.5	0.5	trace	23
3[d]	ZnO-B	4.7	0.7	4.7	0.7	6	33
4	ZnO-B[f]	4.1	1.3	2.8	0.4	2	24
5	MoO_3(2.0 wt.%)/ZnO-A	2.3	1.1	4.8	0.1	n.d.	1
6[e]				4.0	0.1	n.d.	trace
7[g]				n.d.	n.d.	n.d.	n.d.
8	MoO_3(0.8 wt.%)/ZnO-B			5.4	0.2	trace	2
9	V_2O_5(5.0 wt.%)/ZnO-B			4.0	trace	n.d.	1
10	Na_2O(1.0 wt.%)/ZnO-B			1.0	0.4	1	19
11	CaO(0.5 wt.%)/ZnO-B			0.6	0.2	trace	5

a Amount of catalyst = 0.25 g, methane feed rate = 7.5 $mmol \cdot h^{-1}$, $CH_4 : O_2 : He$ = 3 : 1 : 10, W/F = 7.1 $g \cdot h \cdot mol^{-1}$.

b Apparent packing density.

c n.d. = not detected.

d Data from Chapter 2.

e Irradiated through the Pyrex filter

f H_2O treated catalyst.

g Without UV irradiation.

produced in a slightly smaller yield, 4.0 $\mu mol \cdot h^{-1}$, with irradiation through the Pyrex filter. A decrease in the yields of similar order was observed in the reaction with ZnO-A (see run 2), indicating that the MoO_3/ZnO catalyst is activated by irradiation corresponding to the band gap energy of zinc oxide, < 380 nm.

We examined loading effects of several metal oxide on ZnO-B. Among them, V_2O_5 loaded one showed a significant yield and selectivity for methanal formation.

Figure 1 shows changes in the product yields with variations in the catalyst bed temperature. The yield of methanal increased markedly with the temperature up to 548 K, whereas the combined yield of carbon oxides in the effluent gases did not exceed 1 $\mu mol \cdot h^{-1}$. At 548 K, 8.0 $\mu mol \cdot h^{-1}$ of methanal was selectively formed together with 0.2 $\mu mol \cdot h^{-1}$ of methanol. Without heating the catalyst bed, only a trace amount of methanal was observed.

Figure 2 shows the yields of the products on the MoO_3/ZnO-B catalyst at various loading levels of MoO_3 at 493 K. Although the H_2O-treated ZnO-B catalyst gave mainly carbon dioxide, loading of 0.11 wt.% of MoO_3 drastically increased the methanal yield to 8.8 $\mu mol \cdot h^{-1}$, and suppressed carbon dioxide formation to 10 $\mu mol \cdot h^{-1}$. Further increases in the loading levels of MoO_3, the yields of methanal and carbon dioxide gradually decreased, and then leveled off above 0.5 wt.% of MoO_3 loading. The results clearly show that loading of MoO_3 on ZnO generally increases the selectivity for oxygen-containing chemicals without decreasing the yield of methanal.

Photo-oxidation of Ethane and Propane

Table 2 shows the results of photo-oxidation of ethane at 493 K with the several metal oxide loaded zinc oxide catalysts. Loading of MoO_3 on ZnO-A and ZnO-B decreased not only formation of carbon oxides, but also that of ethanal (see runs 16 and 18). For example, 2.0 wt.% (5.0 wt.% in the impregnating solution) of MoO_3 loaded ZnO-A catalyst yielded 14 $\mu mol \cdot h^{-1}$ of ethanal and 8 $\mu mol \cdot h$-1 of carbon oxides, whereas the parent ZnO-A catalyst produced them in much higher yields. Thus the selectivity for oxygen-containing chemicals was not improved with a loading of MoO_3 (*ca.* 73% for ZnO-A, and *ca.* 68% for MoO_3(2.0 wt.%)/ZnO-A). Again cutting off UV irradiation of a wavelength shorter than 300 nm slightly

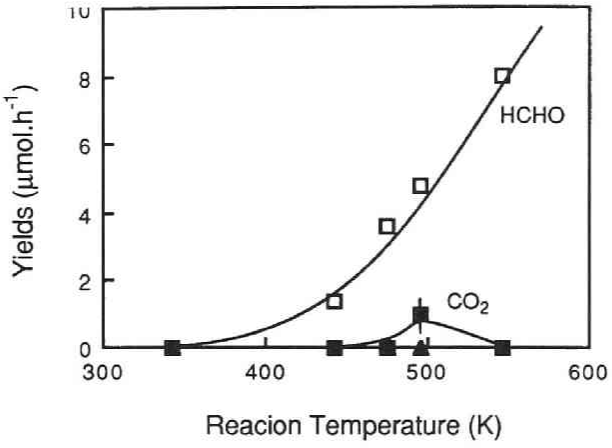

Figure 1. The product yields at various catalyst bed temperatures on MoO_3(2 wt.%) loaded on ZnO-A. The yields of (□) methanal, (▲) CO, and (■) CO_2. Amount of catalyst = 0.25 g, methane feed rate = 7.5 mmol·h^{-1}, $CH_4 : O_2 : He = 3 : 1 : 10$, W/F = 7.1 g·h·mol^{-1}.

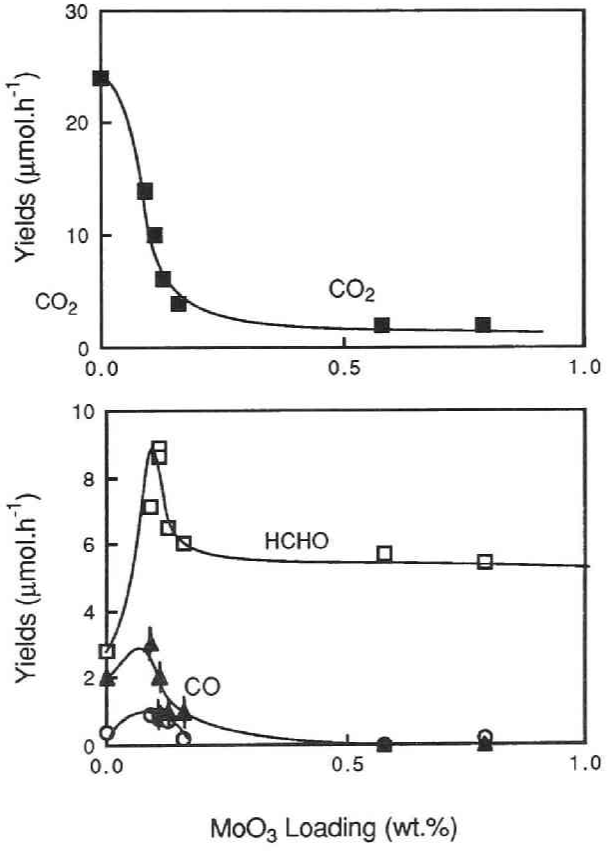

Figure 2. Yields of the products of photo-oxidation of methane over MoO_3/ZnO-B at various loading levels. The yields of (□) methanal, (○) methanol, (▲) CO, and (■) CO_2. Reaction conditions were the same as described in Figure 1.

Table 2 Photo-oxidation of ethane on the various metal oxide-loaded zinc oxide catalysts at 493 K.[a]

Run	Catalyst	Yield (μmol·h^{-1})[b]				
		CH_3CHO	C_2H_5OH	HCHO	CO	CO_2
12[c]	ZnO-A	84	2.8	5.9	7	70
13[d]		64	2.1	6.5	3	38
14[c]	ZnO-B	77	3.0	4.2	3	54
15	ZnO-B[e]	53	0.8	2.1	2	29
16	MoO_3(2.0 wt.%)/ZnO-A	14	n.d.	4.5	n.d.	8
17[d]		11	n.d.	2.6	n.d.	5
18	MoO_3(0.8 wt.%)/ZnO-B	14	n.d.	3.3	n.d.	8
19	V_2O_5(5.0 wt.%)/ZnO-B	14	n.d.	1.0	n.d.	5
20	Fe_2O_3(0.5wt.%)/ZnO-B	5.9	n.d.	trace	trace	4
21	Na_2O(1.0 wt.%)/ZnO-B	38	1.7	0.7	3	43
22	CaO(0.5 wt.%)/ZnO-B	11	n.d.	trace	1	14

a Amount of catalyst = 0.25 g, ethane feed rate = 7.5 mmol·h^{-1}, C_2H_6 : O_2 : He = 3 : 1 : 10, W/F = 7.1 g·h·mol^{-1}.

b n.d. = not detected.

c Data from Chapter 2.

d Irradiated through the Pyrex filter

e H_2O treated catalyst.

Table 3. Photo-oxidation of propane at an elevated reaction temperature.[a]

Run	Catalyst	Temp. (K)	Yield (μmol·h^{-1})					
			propanal	acetone	ethanal	methanal	CO	CO_2
23[a]	ZnO	493	57	56	27	trace	9	45
24	MoO_3(0.8 wt.%)ZnO	493	7.0	7.3	13	trace	1	9

a Amount of catalyst = 0.25 g, propane feed rate = 7.5 mmol·h^{-1}, C_3H_8 : O_2 : He = 3 : 1 : 10, W/F = 7.1 g·h·mol^{-1}.

b Data from Chapter 2.

reduced the yields of the oxygen-containing chemicals with both ZnO-A and MoO_3/ZnO-A. It should be noted that the yield of carbon dioxide with ZnO-A greatly decreased from 70 $\mu mol \cdot h^{-1}$ to 38 $\mu mol \cdot h^{-1}$ with the use of the Pyrex filter, whereas the yield of ethanal decreased to a smaller extent (from 86 $\mu mol \cdot h^{-1}$ to 64 $\mu mol \cdot h^{-1}$). One possible explanation is that the photochemical decomposition of produced ethanal, which requires UV irradiation of a shorter wavelength, would be suppressed with the use of the Pyrex filter.

Loading effects of other metal oxides on zinc oxide were also examined. The decreases in the yields without improvement in the selectivity for oxygen-containing chemicals were observed again with the V_2O_5 loaded zinc oxide catalyst. On the other hand, loading of Na_2O enhanced the formation of CO_2 from 29 $\mu mol \cdot h^{-1}$ to 43 $\mu mol \cdot h^{-1}$.

Figure 3 shows changes in the yields of the products of photo-oxidation of ethane against loading levels of MoO_3 on ZnO-B. The reactions were carried out at 493 K. The yields of ethanal decreased with an increase in the loading level, then leveled off around 14 $\mu mol \cdot h^{-1}$ above 0.5 wt.% of loading. The yield of carbon dioxide in the effluent gas showed the same dependency with MoO_3 loading levels. Therefore the selectivity for oxygen-containing chemicals of *ca.* 70% was not improved irrespective of Mo loading levels.

Table 3 shows photo-oxidation of propane on the MoO_3 loaded zinc oxide catalyst. Loading of MoO_3 markedly suppressed the formation of propanal, acetone and carbon oxides. On the other hand, the yield of ethanal was relatively high, 13 $\mu mol \cdot h^{-1}$. This suggests that loading of MoO_3 not only simply decreased overall catalytic activity, but also modified the nature of the active species.

Roles of Loaded Molybdenum Oxide

Figure 4 plots the XPS intensity ratio $I_{Mo(3d)}/I_{Zn(2p3)}$ as a function of the total atomic ratio N_{Mo}/N_{Zn}, where $I_{Mo(3d)}$ and $I_{Zn(2p3)}$ represent the XPS peak intensities, and N_{Mo} and N_{Zn} are the numbers of atoms. The catalysts with loading levels of MoO_3 higher than 0.2 wt.% showed considerably lower $I_{Mo(3d)}/I_{Zn(2p3)}$ ratios than those expected from the linear extrapolation of the line passing through the origin and the data with the catalyst of the smaller Mo content. This fact indicates that well dispersed species were formed on the catalyst of smaller loading levels

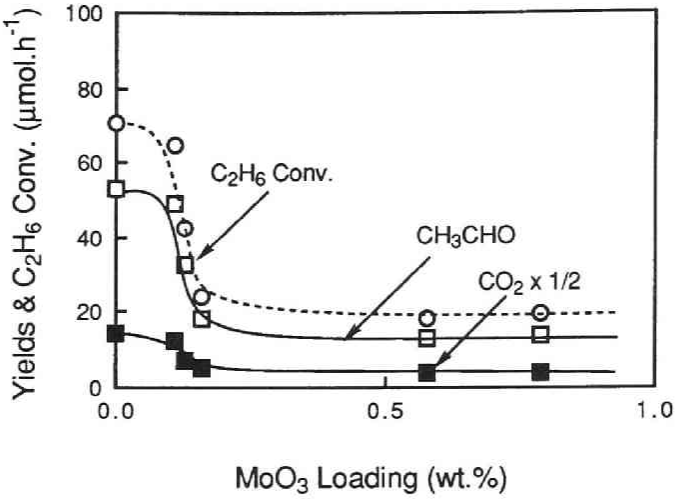

Figure 3. Effects of loading level on the yields of photo-oxidation of ethane over MoO_3/ZnO-B. Amount of catalyst = 0.25 g, ethane feed rate = 7.5 mmol·h^{-1}, C_2H_6 : O_2 : He = 3 : 1 : 10, W/F = 7.1 g·h·mol^{-1}.

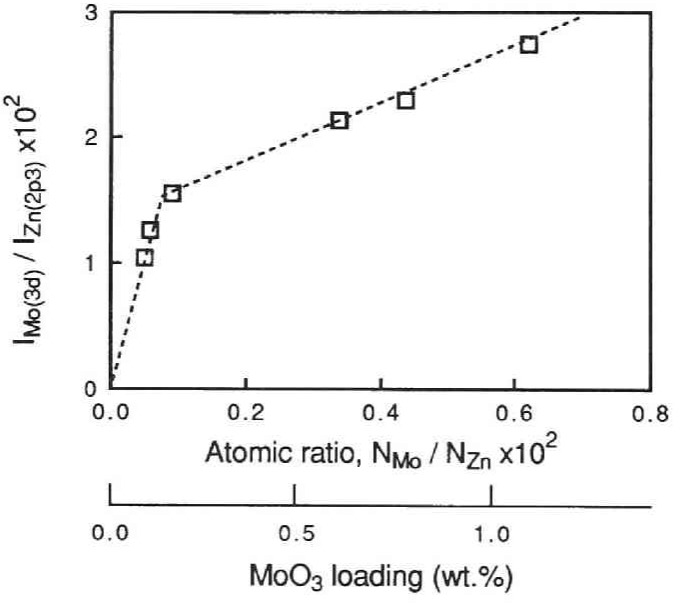

Figure 4. The XPS intensity ratio $I_{Mo(3d)}$ / $I_{Zn(2p3)}$ as a function of overall atomic ratio of Mo and Zn of the MoO_3/ZnO catalysts.

than 0.2 wt.% (as MoO_3), but further increases in the loading level induced formation of multilayers of molybdenum species. In the X-ray diffraction analysis of the MoO3(2.0 wt.%) loaded catalyst, very small peaks that could be attributed to crystalline $ZnMoO_4$ were observed. Although formation of crystalline MoO_3 was not observed by XRD analysis, formation of MoO_3 particles of multilayers smaller than *ca.* 5 nm could not be excluded. These results shown in Figures 2 4 lead to an idea that the surface species modifying the catalytic activities would not be segregated crystalline $ZnMoO_4$ or smaller MoO_3 particles, but well dispersed molybdenum species.

In general, the molybdenum species loaded ZnO catalysts showed lower activities for conversion of alkanes than those of parent ZnO. One of the plausible roles of loaded species would be to totally suppress the activity of the catalyst for oxidation. In the case of the reaction with methane, formation of carbon oxides was reduced, and consequently the selectivity for methanal was improved. Lowered activity would decrease the extent of secondary oxidation of produced methanal. Possibility of secondary oxidation of methanal on ZnO has been discussed in chapter 2. In the case of photo-oxidation of ethane, only a small part of produced ethanal is considered to be suffered from secondary deep oxidation, since the amounts of aldehydes produced from ethane on ZnO were larger than the yield of methanal formed by photo-oxidation of methane. Therefore the decrease in overall catalytic activity would decreased the yields of the products without improving the selectivity for desired products. Physical coverage of the active sites of ZnO by loaded molybdenum species is one of the most plausible reason of the decreasing activity. In addition, promotion of re-combination of hole and electron by loaded Mo species seems to be possible. In addition, the results in Table 3 suggest the modification of the nature of the active sites by loading of Mo species. The possibility that the reaction site is shifted to molybdenum species loaded on the surface, which would be selective for the partial oxidation but low in activity, can not be ruled out. The detailed roles of the additives and the detailed reaction mechanisms on the loaded catalyst are, however, still veiled.

References

1 M.D. Ward, J.F. Brazdil, S.P. Mehandru and A.B. Anderson, *J. Phys. Chem., 91,* **1987**, 6515.

2 S.L. Kaliaguine, B.N. Shelimov and V.B. Kazansky, *J. Catal., 55*, **1978**, 384.

3 W. Hill, B.N. Shelimov and V.B. Kazansky, *J. Chem. Soc., Faraday Trans. 1, 83 (3)*, **1987**, 2381.

4 M. Grätzel, K.R. Thampi and J. Kiwi, *J. Phys. Chem., 93,* **1989**, 4128.

5 K.R. Thampi, J. Kiwi and M. Grätzel, *Catal. Lett.,* **1989**, 109.

6 G.A. Ozin and F. Hugues, *J. Phys. Chem., 86,* **1982**, 5174.

7 T. Suzuki, K. Wada, M. Shima and Y. Watanabe, *J. Chem. Soc., Chem. Commun.,* **1990**, 1059 (Chapter 1).

8 K. Wada, K. Yoshida, Y. Watanabe and T. Suzuki, *Appl. Catal., 74*, **1991**, L1 (Chapter 1).

9 K. Wada, K. Yoshida, Y. Watanabe and T. Suzuki, *J. Chem. Soc., Chem. Commun.*, **1991**, 726.

10 C.D. Wanger, W.M. Riggs, L.E. Davis, J.F. Moulder and G.E. Muilenberg, *Handbook of X-ray Photoelectron Spectroscopy*, Perkin-Elmer Corporation, Physical Electronics Division, **1979**, Minnesota.

Chapter 4

Effects of Reaction Temperatures on Photocatalytic Oxidation of Propene using Various Metal Oxide Catalysts

Abstract

Photocatalytic activities of zinc oxide based catalysts for the oxidation of propene were greatly enhanced when the reaction temperature was raised to 450 - 500 K. The ZnO catalysts gave 21 $\mu mol \cdot h^{-1}$ of ethanal, 16 $\mu mol \cdot h^{-1}$ of propenal and 49 $\mu mol \cdot h^{-1}$ of carbon oxides together with small amounts of propanal and methanal at 493 K under the reaction conditions employed. Loading of MoO_3 (0.8 wt.%) on ZnO suppressed the formation of carbon oxides and propenal, whereas a small amount of propanal was observed in addition to ethanal. Since MoO_3/SiO_2 catalyst showed the similar product distribution in photo-oxidation of propene, surface active centers from Mo species on ZnO surface seem to be responsible for the reaction.

Introduction

Studies on the photocatalytic reaction of alkenes such as propene on the solid oxide catalysts that span the range from those including discrete molecules[1-10] to solid oxide semiconductors[11] have been developed. Many of the studies on the highly dispersed supported oxides focused on the details of the reaction mechanisms. Anpo et al. have investigated photo-isomerization and photoinduced metathesis of alkenes on the highly dispersed supported transition metal oxide catalysts such as V_2O_5/PVG (porous Vycol glass), MoO_3/PVG and MoO_3/SiO_2.[1-5] Formation of the intermediate bridge type π-complex with the reaction between alkene and O^- site on the charge transfer excited triplet species was proposed on the basis of photo-luminescence spectroscopy. Photo-oxidation of alkenes with molecular oxygen on the supported vanadium and niobium oxide catalysts has been investigated extensively by Yoshida et al.[6-9] The selective formation of ethanal from ethene, and the formation of ethanal,

propanal and propenal from propene were reported. Propanal was formed with the reaction of 1-butene, while ethanal was predominantly formed from 2-butene. They proposed the one-to-one intermediate complex comprised of one molecule of alkene and one molecule of oxygen on the basis of the kinetic study[7] and the *ab initio* Hartree-Fock molecular orbital calculation.[10] On the other hand, photo-oxidation of propene on solid oxide semiconductors such as TiO_2 has been investigated by Pichat et al.[10] They found that TiO_2 showed the highest catalytic activity, but most of the products on TiO_2 was, however, carbon dioxide even at a low conversion level. Zinc oxide was reported to show a significantly lower activity than that of TiO_2 at a room temperature. They also reported that raising the temperature to 455 K had a decreasing effect on the photocatalytic activity of TiO_2.

In previous chapters, selective photocatalytic oxidation of light alkanes on the MoO_3/SiO_2[12,13] and the ZnO based catalysts was described.[14] A raise in the reaction temperature to *ca.* 500 K enhanced the catalytic activities of the MoO_3/SiO_2 and ZnO based catalysts.

In this chapter, the study is extended to photocatalytic oxidation of propene over the zinc oxide based catalyst. Effects of the reaction temperature and changes in the product distributions by loading of molybdenum oxide to zinc oxide are described.

Experimental Section

Materials

Zinc oxide (Wako, designated as ZnO-B in chapters 2 and 3) was used as received. A loaded catalyst was prepared by the usual impregnation method from an aqueous solution of ammonium heptamolybdate or ammonium metavanadate. Preparation of the MoO_3/SiO_2 catalyst has been described in chapter 1 in detail. Gaseous reactant, propene, oxygen and helium, were used as received without any further purification.

Apparatus and Procedures

An upstream flow type fixed bed reaction apparatus that can maintain the catalyst bed temperature by passing the heated air around

the reactor was used for the reaction. UV irradiation was carried out using a high-pressure mercury vapor lamp (200 W, arc length = 75 mm) with a water filter. The reaction was carried out typically on the following conditions: propene feed rate; 7.5 $mmol \cdot h^{-1}$, the molar ratio $C_3H_6 : O_2 :$ He; 3 : 1 : 10, W/F; 7.1 $g \cdot h \cdot mol^{-1}$, catalyst bed temperature; 493 K. Liquid products were collected into a trap containing tetrahydrofuran at 195 K, and gaseous products were collected into gas sampling bags. Procedure of the heat treatment after some of the reaction has been described in chapter 2.

Analysis

Products were analyzed by gas chromatography using a Porapak-N column at 433 K with FID for ethanal, propylene oxide and acetone; a Gaskuropak 54 column at 413 K with FID for propenal and propanal; a TSG-1 on Shimarite-F column at 393 K with TCD for methanal. Gaseous products were analyzed using a Porapak-Q column at 353 K with FID for C_1 - C_4 hydrocarbons; a molecular sieves-5A column at 323 K with TCD for oxygen; and an active carbon column at 323 K with TCD for H_2, CO and CO_2 (detection limit; carbon oxides ~20 ppm, aldehydes and alcohols ~0.1μmol).

Results and Discussion

The yields in following Tables and Figures were calculated from the amounts of the products in the effluent gases on unit time base. A small amount of carbon dioxide (~0.5 μmol) was evolved by heating the zinc oxide based catalysts to 823 K under argon just after the completion of the reactions.

Photo-oxidation of propene over the zinc oxide, molybdenum oxide or vanadium oxide loaded zinc oxide, and silica supported molybdenum oxide catalysts was carried out. Table 1 shows the results obtained during the first 1 h at 493 K. UV irradiation of ZnO in the presence of propene and oxygen at 493 K induced the formation of ethanal, propenal and carbon oxides together with small amounts of propanal, acetone and methanal. Formation of carboxylic acids could not be completely excluded, although none of them was detected by GC analysis. One-pass conversion of propene was estimated to be 50 $\mu mol \cdot h^{-1}$ (0.7% of propene feed) with the

selectivity of 67% for the oxygen-containing chemicals, whereas Pichat et al. reported that the reaction at 320 K using ZnO catalysts gave aldehydes and acetone in the lower selectivity of 22 - 53% even at very low conversion levels (0.055%).[11] The reaction with irradiation through a Pyrex filter yielded smaller amounts of the products, but there were no significant changes in the product distribution except for a intense decrease in the yield of methanal. Contribution from thermal oxidation of propene could be excluded, because none of the products was observed in the absence of UV irradiation (run 3). The zinc oxide catalyst bathed in distilled water followed by calcination in air at 823 K had a higher apparent packing density, and gave the products in lower yields than ZnO without the H_2O treatment, probably due to its lower apparent irradiation area (see Table 1 in chapter 3).

As shown in Figure 1, catalytic activity of ZnO for photo-oxidation of propene was more improved as an increase in the reaction temperature to 493 K. Very small amounts of oxidation products were observed at an ambient temperature, 336 K. The oxygen-containing chemicals were given in the highest yields at 493 K. Further increase in the reaction temperature decreased the yields of aldehydes as well as the conversion of propene, whereas formation of carbon oxides was more enhanced. Secondary oxidation of the products or intermediates to carbon oxides might be enhanced at such a higher temperature.

The impregnation of MoO3 on ZnO changed the product distribution significantly (run 5 in Table 1). The yield of ethanal slightly decreased, and a small amount of propanal (2.5 $\mu mol \cdot h^{-1}$) was formed, which was detected only in a trace amount with the ZnO catalyst. The yields of propenal markedly decreased from 16 $\mu mol.h^{-1}$ to 2.3 $\mu mol.h^{-1}$ with loading of MoO3. Formation of carbon oxides was also suppressed. UV irradiation and elevated reaction temperatures were indispensable for the reaction with the MoO3/ZnO catalyst (runs 6 and 8). Cutting off UV irradiation of a wavelength shorter than 300 nm by the use of the Pyrex filter slightly decreased yields of all the products except for propanal, but did not significantly change the selectivities of them. The V_2O_5 loaded ZnO catalyst, prepared by the usual impregnation method, showed similar activity for the photo-oxidation of propene to that of MoO3/ZnO.

We examined photo-oxidation of propene over the silica supported MoO3 catalyst, which has been found to show excellent catalytic activities for the photo-oxidation of light alkanes at elevated temperatures, as

Table 1. Photo-oxidation of propene on the various solid oxide catalysts[a]

Run	Catalyst	Temp. (K)	Yields(μmol·h^{-1})						
			propanal	acetone	propenal	ethanal	methanal	CO	CO_2
1	ZnO	493	trace	1.4	16	21	5.4	10	39
2[b]		493	0.4	0.6	8.6	12	0.8	7	23
3[c]		493	n.d.	n.d.	n.d.	n.d.	n.d.	n.d.	n.d.
4	ZnO(H_2O treated)	493	0.7	0.3	7.2	10	0.7	4	18
5	MoO_3(0.8 wt.%)/ZnO	493	2.5	0.6	2.3	15	3.3	1	8
6		339	n.d.	n.d.	n.d.	1.1	n.d.	n.d.	trace
7[b]		493	2.6	0.5	1.5	9.2	2.4	trace	5
8[c]		493	n.d.	n.d.	n.d.	n.d.	n.d.	n.d.	n.d.
9	MoO_3(0.1 wt.%)/ZnO	493	0.5	0.4	6.7	12	1.8	3	12
10	V_2O_5(5 wt.%)/ZnO	493	1.1	0.7	2.1	9.3	2.5	1	8
11[d]	MoO_3(2.5 wt.%)/SiO_2	493	2.3	0.9	7.1	5.3	1.8	1	4
12[d]		335	n.d.	n.d.	n.d.	1.8	n.d.	n.d.	trace
13[c,d]		493	n.d.	n.d.	n.d.	n.d.	n.d.	n.d.	n.d.

[a] Amount of catalyst = 0.25 g, propene feed rate = 7.5 mmol·h^{-1}, C_3H_6 : O_2 : He = 3 : 1 : 10, W/F = 7.1 g·h·mol^{-1}, n.d. = not detected.

[b] Irradiated through the Pyrex filter

[c] Without UV irradiation.

[d] Amount of catalyst = 0.025 g, W/F = 0.71 g·h·mol^{-1}, fluidized catalyst bed.

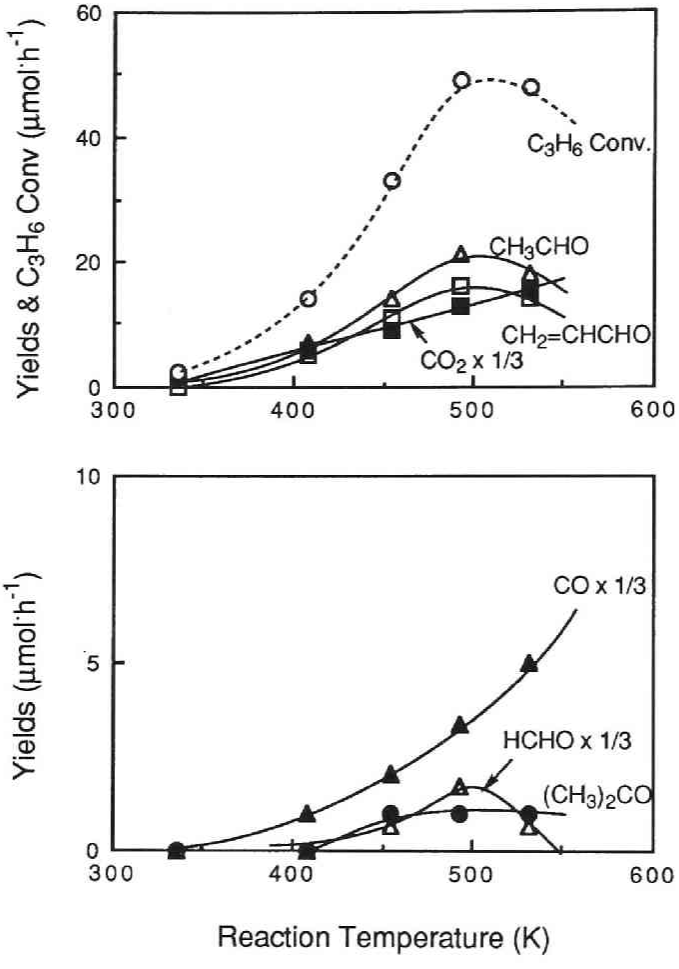

Figure 1. Photo-oxidation of propene on the zinc oxide catalyst at various reaction temperatures. Amount of catalyst = 0.25 g, propene feed rate = 7.5 $mmol \cdot h^{-1}$, $C_3H_6 : O_2 : He = 3 : 1 : 10$, $W/F = 7.1\ g \cdot h \cdot mol^{-1}$.

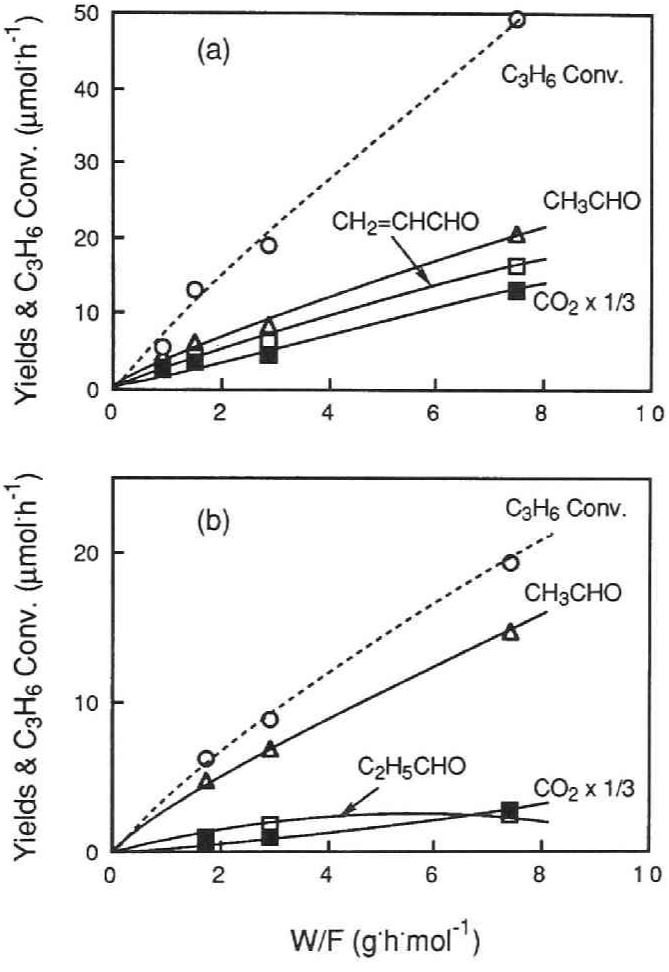

Figure 2. Effects of W/F by changing the amount of the (a) ZnO and (b) MoO_3(0.8 wt.%)/ZnO catalyst. Reaction gas composition was the same as shown in Figure 1.

described in previous chapters.[12,13] It should be noted that the product distribution over MoO_3/SiO_2 was quite similar to those over the MoO_3(0.8 wt.%)/ZnO catalyst. A considerable amount of propanal (2.3 $\mu mol.h^{-1}$) was formed in addition to ethanal and propenal, suggesting that the formation of propanal is characteristic feature of the Mo or V loaded catalysts.

Figure 2 shows effects of W/F on the yields of the products by changing the amount of the ZnO and MoO_3(0.8 wt.%)/ZnO catalysts. Conversion of propene and all the product yields increased linearly with an increase in W/F. On the other hand, the selectivities were not affected by changing W/F. These results suggest that most of the products including carbon oxides were not formed with the secondary oxidation of the primary products on the catalyst.

Studies of the photo-oxidation of propene over the highly dispersed supported vanadium oxide catalysts have mainly focused on the elucidation of the reaction mechanisms.[6-8,10] In addition to simple allylic oxidation pathway to form propenal, the route via formation of the epoxide species to produce propanal, and double-bond fission to ethanal have been proposed. The results in the present study revealed that predominant formation of ethanal and propanal rather than simple allylic oxidation was characteristic feature for the Mo or V loaded ZnO catalysts. Since similar product distribution was observed on photo-oxidation of propene over the silica supported MoO_3 catalyst, we may estimate that the reaction via both double-bond fission and epoxide-like intermediates mainly proceeded at the active centers on ZnO surface provided from loaded Mo or V species. It is also possible that the similar types of active oxygen species formed on the surfaces of MoO_3/ZnO and MoO_3/SiO_2. These ideas are supported by the results of photo-oxidation of propane on ZnO and MoO_3 loaded ZnO (see Table 3 in chapter 3). The reaction of propane over the parent ZnO catalyst mainly gave propanal, acetone and carbon oxides together with a smaller amount of ethanal. With the MoO_3/ZnO catalyst, formation of propanal, acetone and carbon oxides was greatly suppressed, while ethanal was formed as the principal product.

The photo-oxidation of propene on MoO_3/ZnO was not essentially suppressed by cutting off UV irradiation of a wavelength shorter than 300 nm, whereas photo-oxidation of alkanes on the MoO_3/SiO_2 required irradiation in this range.[12] UV diffuse reflectance studies have revealed that MoO_3(2.5 wt.%)/SiO_2 shows no significant absorption bands above 300

nm, as shown in chapter 1. Therefore the reaction seems hardly to be initiated with the direct photo-activation of Mo species on the surface.

References

1 M. Anpo, I. Tanahashi and Y. Kubokawa,
J. Chem. Soc., Faraday Trans. 1, 78, **1982**, 2121.

2 M. Anpo and Y. Kubokawa, *J. Catal., 75*, **1982**, 204.

3 M. Anpo, T. Suzuki, Y. Kubokawa, F. Tanaka and S. Yamashita,
J. Phys. Chem., 88, **1984**, 5778.

4 M. Anpo, M. Kondo, Y. Kubokawa, C. Louis and M. Che,
J. Chem. Soc., Faraday Trans. 1, 84, **1988**, 2771.

5 M. Anpo, M. Kondo, S. Coluccia, C. Louis and M. Che,
J. Am. Chem. Soc., 111, **1989**, 8791.

6 S. Yoshida, Y. Magatani, S. Noda and T. Funabiki,
J. Chem. Soc., Chem. Commun., **1982**, 601.

7 S. Yoshida, T. Tanaka, M. Okada and T. Funabiki,
J. Chem. Soc., Faraday Trans. 1, 80, **1984**, 119.

8 T. Tanaka, M. Ooe, T. Funabiki and S. Yoshida,
J. Chem. Soc , Faraday Trans. 1, 82, **1986**, 35.

9 S. Yoshida, Y. Nishimura, T. Tanaka, H. Kawai and T. Funabiki,
Catal. Today, 8(1), **1990**, 67.

10 H. Kobayashi, M. Yamaguchi, T. Tanaka and S. Yoshida,
J. Chem. Soc., Faraday Trans. 1, 81, **1985**, 1513.

11 P. Pichat, J.M. Herrmann, J. Disdier and M.N. Mozzanega,
J. Phys. Chem., 83, **1984**, 3122.

12 T. Suzuki, K. Wada, M. Shima and Y. Watanabe,
J. Chem. Soc., Chem. Commun., **1990**, 1059 (Chapter 1).

13 K. Wada, K. Yoshida, Y. Watanabe and T. Suzuki,
Appl. Catal., 74, **1991**, L1 (Chapter 1).

14 K. Wada, K. Yoshida, Y. Watanabe and T. Suzuki,
J. Chem. Soc., Chem. Commun., **1991**, 726 (Chapters 2 and 3).

Part II

Selective Conversion of Methane into Higher Hydrocarbons via Oxidative Coupling Reactions using Basic Metal Oxide Catalysts

Chapter 5

Effects of Carbon Dioxide and Catalyst Preparation on Oxidative Dimerization of Methane

Abstract

The use of carbon dioxide as a reactive diluent for oxidative coupling of methane increased the combined yield of ethane and ethene (C_2 compounds) from 13.4% to 18.3% with an increase in the C_2 selectivity from 42.3% to 49.4% over a MgO catalyst at 1073 K, a CH_4-to-O_2 ratio of 2 and W/F of 6.07 $g \cdot h \cdot mol^{-1}$. Alkaline earth metal oxide catalysts prepared by thermal decomposition of their oxalates at 1023 K gave a high C_2 space time yield (e.g., 8.6 $mmol \cdot (g \cdot h)^{-1}$). A Sm_2O_3(15 wt.%) loaded porous MgO catalyst prepared at 1173 K showed the high selectivity (47.9% with a C_2 yield of 13.3%). The selectivity for C_2 compounds was further improved to 57.4% in a stream of CH_4-O_2-CO_2 without reducing the C_2 yield (13.6%). Addition of carbon dioxide suppressed deactivation of the catalyst and decreased the amount of coke deposited on the catalyst surface in a prolonged run. Partial adsorption of carbon dioxide on the catalyst surface inhibited deep oxidation of methane or the C_2 products, resulting in increased C_2 selectivities on dilution of the feed stream with carbon dioxide.

Introduction

Oxidative coupling of methane to ethane and ethene has been carried out by a number of research groups since Keller and Bhasin[1] demonstrated the possibility of this reaction. Various metal oxide catalysts have been reported to be effective.[2-18] Ito et al.[2] reported that a lithium-promoted magnesium oxide catalyst exhibited high catalytic activity and the selectivity for C_2 compounds. They proposed that Li^+ - O^- species was active and selective for methane activation. Otsuka[3] and Otsuka et al.[4] reported that rare earth metal oxides doped with sodium, potassium and lithium exhibited high catalytic activities and the

selectivities for this reaction. They claimed that the oxygen species responsible for abstraction of hydrogen from methane over Sm_2O_3 would be O_2^{2-}. Iwamatsu and Aika[19] reported that a catalyst having a lower surface area showed higher activity for C_2 formation. Throughout these studies, inert gas such as helium or nitrogen was used as a diluent of methane and oxygen in order to avert the risk of explosion. Little attention has been paid to effects of diluents on oxidative coupling of methane.

Effects of the inclusion of carbon dioxide in the feed gas, CH_4-O_2-CO_2-N_2, were recently reported by Korf et al.[20] Deactivation of the Li/MgO catalyst during a prolonged run could be avoided by addition of a small amount of carbon dioxide. Aika and Nishiyama[21] reported that oxidative coupling of methane with oxygen was promoted by combination with the reaction of methane with carbon dioxide to form carbon monoxide at 1073 K over the PbO/MgO and PbO/CaO catalysts. However, no studies employed a large amount of carbon dioxide compared with the reactant gases.

This chapter describes effects of carbon dioxide as a reactive diluent of the feed gas on oxidative coupling of methane into ethane and ethene over the alkaline earth metal oxide based catalysts. The possibilities of obtaining the higher C_2 yields and C_2 selectivities were studied by controlling the surface areas of the catalysts by changing the method of preparation of these oxides.

Experimental Section

Materials

Commercial magnesium oxide (Wako, >99% purity) and strontium oxide (Mitsuwa, >95% purity) were used as received. BET (Brunauer-Emmet-Teller) surface area of magnesium oxide after the reaction was 3.4 $m^2 \cdot g^{-1}$. Loaded catalysts such as Na_2CO_3 (4 wt.% as Na)/MgO and PbO(5 wt.%)/MgO were prepared by the usual impregnation method from their aqueous solutions.

A calcium oxide catalyst was prepared by thermal decomposition of calcium carbonate (Nacalai Tesque, >98% purity) at 1173 K for 2 h under argon (BET surface area; 5.4 $m^2 \cdot g^{-1}$).

A porous magnesium oxide catalyst (further designated as MgO-OX) was prepared as follows. An aqueous solution (*ca.* 50 cm^3) of oxalic acid (6.27 g) was placed in a simple distillation apparatus fitted with a dropping funnel. Into this, with gentle boiling, *ca.* 20 cm^3 of an aqueous solution of magnesium acetate (10.72 g) was added dropwise. During this period, liberated acetic acid was constantly distilled off, resulting in formation of a white precipitate. After evaporating excess water, the resulting white precipitate was dried at 400 K for 2 h under argon and calcined at 1023 K in an air stream for 1 h and then under argon for 1 h. The X-ray diffraction pattern of this MgO-OX showed broad peaks with width at half-hight about twice that of commercial MgO. The MgO-OX catalyst has a larger surface area of 56 $m^2 \cdot g^{-1}$. In a similar manner, Sm_2O_3/ MgO-OX (BET surface area; 53 $m^2 \cdot g^{-1}$), Sm_2O_3-OX (4.9 $m^2 \cdot g^{-1}$), CaO-OX (2.5 $m^2 \cdot g^{-1}$) and SrO-OX (1.3 $m^2 \cdot g^{-1}$) were prepared.

Apparatus and Procedure

A conventional fixed bed flow type reaction system was used with a quartz reactor (9 mm i.d.). A 0.010 - 0.50 g of the catalyst was placed at the center of the reactor and activated in a flow of air (20 $cm^3 \cdot min^{-1}$) at 1023 K for 2 h just before the reaction. From the outlet of the reactor, an inner tube (5 mm o.d.) was inserted into the end zone of the catalyst bed, and air was introduced into the inner tube to cool the products immediately.

The reaction was conducted at 1023 K or 1073 K by passing a gas mixture of methane, oxygen and helium or carbon dioxide: Typical flow rate of the gases was 3.0 $cm^3 \cdot min^{-1}$ (7.5 $mmol \cdot h^{-1}$), 1.5 $cm^3 \cdot min^{-1}$ and 28.5 $cm^3 \cdot min^{-1}$, respectively. The products were collected in a gas burette for 20 min after reaching steady state. For prolonged runs, effluent gases were collected for 20 min at regular intervals (every one hour).

Analysis

Products were analyzed by gas chromatography using a Porapak-Q column with flame ionization detection for C_2 compounds; an active carbon column with thermal conductivity detection (TCD) for hydrogen and carbon oxides; a molecular sieves-5A column with TCD for oxygen.

The amount of carbon dioxide produced from methane was calculated from the balance between methane feed, the amount of products, carbon monoxide and recovered methane.

The BET surface area of the catalysts was measured with nitrogen at 77 K by using a micro processor-controlled BELSORP 28, an automatic instrument (BEL Japan Inc.). The X-ray powder diffraction study was carried out using a Geigerflex (Rigaku Inc.) by means of copper Kα radiation (λ = 1.5405 Å).

Results and Discussion

Effects of Carbon Dioxide as a Diluent over the Commercial Metal Oxide Catalysts

Effects of carbon dioxide as a diluent on oxidative coupling of methane were examined with various alkaline earth metal oxides which were known to be the active catalysts in CH_4-O_2-He system. The products were ethane and ethene (C_2 compounds), CO, CO_2, H_2 and H_2O together with very small amounts of C_3 and C_4 hydrocarbons. The results using a constant weight of the catalysts (0.50 g) are summarized in Table 1. These catalysts have similar packing densities (0.76 $g \cdot cm^{-3}$ for MgO, 0.81 $g \cdot cm^{-3}$ for SrO and 0.83 $g \cdot cm^{-3}$ for Sm_2O_3-OX).

With MgO, the C_2 yield and selectivity increased with inclusion of carbon dioxide to the feed gas at 1073 K (runs 3 and 4). At 1023 K, as shown in runs 1 and 2, the C_2 yields decreased to less than half those at 1073 K. Again the higher C_2 yield and selectivity were achieved under CO_2 than those under He.

Use of carbon dioxide as a diluent suppressed catalytic activities of CaO and SrO (runs 5 - 8). These changes in the activity were due to the reaction between the oxide catalyst and carbon dioxide. This was confirmed by an immediate change in the temperature of the catalyst bed when the feed gas containing carbon dioxide was introduced into the reactor. The X-ray diffraction analyses of the used catalysts showed the patterns of correspond carbonates (see below).

Effects of carbon dioxide were examined over alkali metal or PbO loaded MgO, which have been reported to be one of the most active catalysts.[5,8,15] With Na_2CO_3(4 wt.% as Na)-doped MgO, almost no changes in the C_2 yield and selectivity at a methane-to-oxygen ratio of 2

Table 1. Effects of CO_2 as reactive diluent on the reaction using the commercial alkaline earth metal oxide-based catalysts[a]

Run	Catalyst	Diluent	Temp. (K)	Conv.(%) CH_4	Conv.(%) O_2	Yield(%) C_2	Selectivity(%) C_2	Selectivity(%) (C_2H_4)	Selectivity(%) (C_2H_6)	Selectivity(%) CO	Selectivity(%) CO_2[b]	C_2 STY $(mmol \cdot (g.h)^{-1})$
1	MgO	He	1023	22.3	60.5	6.5	29.2	11.9	17.3	25.6	45.0	0.9
2		CO_2		17.5	44.5	7.3	41.8	17.0	24.7	34.7	(24)	1.1
3		He	1073	31.7	74.0	13.4	42.3	23.3	19.0	18.5	32.9	1.9
4		CO_2		37.1	100	18.3	49.4	30.1	19.3	5.6	(45)	2.8
5	CaO[c]	He		37.6	100	8.0	21.3	11.9	9.4	5.2	73.5	1.2
6		CO_2		13.0	30.9	4.5	34.3	12.0	22.3	41.6	(24)	0.3
7	SrO	He		23.5	38.7	11.4	48.4	25.4	23.0	8.1	43.5	1.5
8		CO_2		6.6	23.2	1.1	16.1	3.0	13.1	8.3	(76)	0.2
9	Na(4 wt.%)/MgO	He		39.6	97.6	15.2	38.5	23.5	15.0	3.9	57.6	2.3
10		CO_2		41.9	86.1	16.4	39.1	23.3	15.8	23.1	(38)	2.4
11[d]		He		32.0	100	15.3	47.8	27.9	19.9	2.3	49.9	2.3
12[d]		CO_2		24.0	52.5	16.9	70.3	38.6	31.7	12.4	(17)	2.4
13	PbO(5 wt.%)/MgO	He		39.4	100	18.5	47.1	26.0	21.1	0.6	52.3	2.6
14		CO_2		34.5	100	17.2	50.0	26.4	23.5	0.8	(49)	2.4
15	Sm_2O_3(15 wt.%)/MgO	He		36.6	100	12.6	34.7	20.1	14.5	11.3	54.1	1.6
16		CO_2		40.0	100	13.8	34.5	20.8	13.8	45.2	(20)	1.7
17[e]		He		38.6	92.9	14.0	36.2	20.6	15.6	14.3	49.5	7.8
18[e]		CO_2		37.8	97.0	15.5	41.1	23.7	17.4	38.2	(21)	9.3

[a] Amount of catalyst = 0.50 g, methane feed rate = 7.5 $mmol \cdot h^{-1}$, $CH_4 : O_2$: diluent = 2 : 1 : 19, W/F = 6.1 $g \cdot h \cdot mol^{-1}$.

[b] Values in parentheses are calculated CO_2 selectivities.

[c] Prepared from $CaCO_3$

[d] $CH_4 : O_2 = 3.3 : 1$.

[e] Amount of catalyst = 0.10 g.

were observed. With increase in the methane-to-oxygen ratio in the feed to 3.3, addition of carbon dioxide dramatically increased the C_2 selectivity from 47.3% to 70.3% (run 11 and 12). On the other hand, carbon dioxide did not affect the C_2 yield and the product distribution with the PbO loaded MgO catalyst. The presence of a small amount of carbon dioxide (CH_4 : CO_2; 1 : 100) in the reactant gas was reported to increase C_2 formation over the PbO-MgO catalyst.[21] Differences in the reported result and ours may partly be accounted for by differences in the reaction conditions where higher oxygen concentration were employed in our study (CH_4 : O_2; 2 : 1).

A Sm_2O_3 loaded MgO was a fairly active catalyst and achieved nearly 100% oxygen consumption with 0.10 g of the catalyst

Figure 1 shows effects of W/F on the C_2 yield and selectivity by changing the amount of the MgO catalyst at a constant feed rate. The yield of C_2 compounds decreased in proportion to the amount of catalyst. Under helium, the C_2 selectivity decreased markedly with a decrease in the amount of the catalyst from 0.30 to 0.10 g. Under carbon dioxide, the C_2 selectivity did not change even with a smaller amount of the catalyst. These results suggest the possibility that certain amounts of carbon monoxide and dioxide were formed via a non-catalytic pathway, for example, oxidation of methane on the quartz wool plug, or on the wall of the reactor and in the gas phase. When the feed gas was diluted with carbon dioxide, oxidation via these routes might be suppressed.

Metal Oxide Catalysts Derived from Thermal Decomposition of Oxalate Salts

In order to find a catalyst which gives a higher C_2 space time yield (STY), we tried to prepare magnesium oxide by several methods, and examined their catalytic activity under carbon dioxide at 1073 K. The catalysts designated as MgO-CA and MgO-ET were prepared by thermal decomposition of magnesium carbonate and magnesium ethoxide, respectively. The MgO-OX catalyst was prepared from magnesium oxalate. As magnesium oxides thus prepared showed large specific volumes (MgO-OX; 0.25 $g \cdot cm^{-3}$), the reaction was carried out at a W/F of 1.21 $g \cdot h \cdot mol^{-1}$ (0.10 g of the catalyst). As shown in Table 2, although less selective, MgO-OX and MgO-CA were more active catalysts than commercial MgO, on the basis of either the amount of the catalyst or its

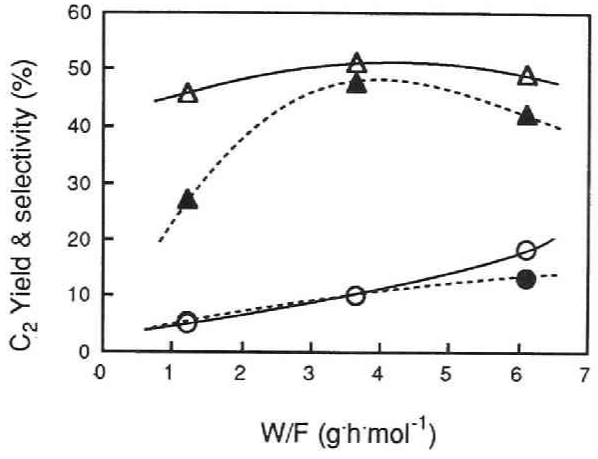

Figure 1. Effects of W/F by changing the amount of the MgO catalyst. Reaction temperature = 1073 K, methane feed rate = 7.5 $mmol \cdot h^{-1}$, $CH_4 : O_2$: diluent = 2 : 1 : 19. The C_2 yields under (●) He and (○) CO_2, and the C_2 selectivities under (▲) He and (△) CO_2.

Table 2. Effects of preparation method of the magnesium oxide catalysts on oxidative coupling of methane[a]

Run	Catalyst	Conv.(%)		Yield(%)	Selectivity(%)					C_2 STY
		CH_4	O_2	C_2	C_2	(C_2H_4)	(C_2H_6)	CO	CO_2[b]	($mmol \cdot (g \cdot h)^{-1}$)
19	MgO	11.1	22.7	5.1	45.8	18.9	26.8	44.8	(9)	3.8
20	MgO-OX	31.0	77.6	11.2	36.1	21.0	15.1	35.5	(28)	7.6
21	MgO-CA	39.7	81.5	11.6	29.3	17.3	12.0	32.5	(38)	7.6
22	MgO-ET	25.1	61.9	7.7	30.8	16.9	13.8	49.4	(20)	5.4

[a] Reaction temperature = 1073 K, amount of catalyst = 0.10 g, methane feed rate = 7.5 $mmol.h^{-1}$, $CH_4 : O_2 : CO_2$ = 2 : 1 : 19, W/F = 1.2 $g \cdot h \cdot mol^{-1}$.

[b] Values in parentheses are calculated CO_2 selectivities.

volume (see Fig. 1). Then we tried to examine the catalytic activities of the oxides prepared by thermal decomposition of their oxalates.

Table 3 summarizes the results obtained by using the several catalysts prepared from alkaline earth metal oxalates. Packing densities of CaO-OX and SrO-OX were 0.60 $g \cdot cm^{-3}$ and 0.46 $g \cdot cm^{-3}$, respectively. Whereas the MgO catalyst showed poor C_2 STY (maximum 3.8 $mmol \cdot (g \cdot h)^{-1}$ at W/F of 1.21 $g \cdot h \cdot mol^{-1}$), the MgO-OX catalyst exhibited a higher catalytic activity for C_2 formation. The C_2 STY reached 8.6 $mmol \cdot (g \cdot h)^{-1}$ at 1073 K in a stream of helium, but the selectivity for C_2 compounds was lower than that of commercial MgO. The amount of carbon monoxide produced using MgO-OX in a flow of carbon dioxide was larger than that under helium. When the decomposition temperature of magnesium oxalate was raised to 1173 K, the surface area increased from 56 to 75 $m^2 \cdot g^{-1}$, but the catalytic activity decreased (runs 24 and 25).

We prepared the CaO-OX and SrO-OX catalysts, and examined their catalytic activities. In a stream of helium, the CaO-OX catalyst showed the high C_2 selectivity (61.1%) with the C_2 yield of 7.9%. When the reaction temperature was raised to 1073 K, the C_2 yield increased to 11.6% (selectivity; 38.6%). Higher activity of CaO-OX per unit surface area than that of CaO from $CaCO_3$ (see runs 5, 26 and 27) indicates that CaO-OX was more active for C_2 formation, and an increase in surface areas was not essential to increase the C_2 yield (CaO from $CaCO_3$; 5.4 $m^2 \cdot g^{-1}$, CaO-OX; 2.5 $m^2 \cdot g^{-1}$). CaO-OX prepared at 1173 K showed a very small surface area (< 1.0 $m^2 \cdot g^{-1}$) and low catalytic activity (run 28). The highest C_2 selectivity was obtained with the SrO-OX catalyst (run 29).

As mentioned above, use of excess carbon dioxide as a diluent for the calcium oxide and strontium oxide catalysts dramatically decreased their catalytic activities. Effects of partial pressure of carbon dioxide in the reaction gas on CaO-OX and SrO-OX were examined, and the results are given in Figure 2. With CaO-OX, the yield and selectivity of C_2 compounds had maximum values at partial pressure of carbon dioxide of *ca.* 1 kPa. When the ratio of CH_4 to O_2 was increased to 3.3, the C_2 selectivity further increased to 72.7% at P_{CO_2} = 1 kPa (C_2 yield = 17.0%). Excess carbon dioxide, however, suppressed not only the activity but also the C_2 selectivity. Over SrO-OX, there were no significant maxima in the C_2 yield and selectivity with variations in partial pressure of carbon dioxide. Inclusion of carbon dioxide in the feed only decreased the

Table 3. Effects of CO_2 on activities of the catalysts prepared from their oxalates[a]

Run	Catalyst	Diluent	Temp. (K)	Conv.(%) CH_4	Conv.(%) O_2	Yield(%) C_2	Selectivity(%) C_2	Selectivity(%) (C_2H_4)	Selectivity(%) (C_2H_6)	Selectivity(%) CO	Selectivity(%) CO_2[b]	C_2 STY $(mmol \cdot (g \cdot h)^{-1})$
23	MgO-OX	He	1073	34.2	91.8	11.5	33.7	20.5	13.3	17.3	49.0	8.6
20		CO_2		31.0	77.6	11.2	36.1	21.0	15.1	35.5	(28)	7.6
24	MgO-OX[c]	He		24.4	51.3	7.3	30.0	15.2	14.8	36.1	33.9	4.6
25		CO_2		15.8	36.3	4.4	28.2	10.9	17.3	71.8	(0)	2.9
26	CaO-OX	He	1023	13.0	21.8	7.9	61.1	32.0	29.1	15.3	23.6	5.5
27		He	1073	31.6	84.1	11.6	36.8	28.4	8.4	39.5	23.7	8.1
28	CaO-OX[c]	He		13.1	58.8	2.8	21.0	6.2	14.8	30.2	48.8	1.5
29	SrO-OX	He		11.5	20.6	7.6	66.4	27.8	38.6	18.5	15.1	5.2
30	Sm_2O_3-OX	He		37.5	100	11.2	29.7	18.3	11.5	11.2	59.0	7.6
31		CO_2		38.8	100	14.0	36.0	22.7	13.2	31.5	(33)	10.4
32	Sm_2O_3(15 wt.%)/MgO-OX	He		36.3	100	10.5	29.0	17.7	11.3	13.8	57.2	7.7
33		CO_2		38.5	94.9	11.3	29.4	20.3	9.1	45.6	(28)	7.3
34	Sm_2O_3(15 wt.%)/MgO-OX[c]	He		27.8	80.2	13.3	47.9	26.7	21.2	27.4	24.7	8.5
35		CO_2		23.6	90.1	13.6	57.4	30.8	26.6	42.6	(0)	9.8

[a] Amount of catalyst = 0.10 g, $CH_4 : O_2$: diluent = 2 : 1 : 19, W/F = 1.2 $g \cdot h \cdot mol^{-1}$.

[b] Values in parentheses are calculated CO_2 selectivities.

[c] Catalysts prepared by thermal decomposition of their oxalates at 1173 K.

catalytic activity of SrO-OX. The X-ray diffraction pattern of the catalyst after the reaction with a small amount of carbon dioxide suggested formation of $SrCO_3$.

Samarium oxide has been known to be active for this reaction.[1,14] With the Sm_2O_3-OX catalyst prepared by thermal decomposition of samarium oxalate, both the C_2 yield and C_2 selectivity obtained under carbon dioxide were higher than those under helium, indicating that use of carbon dioxide was effective for this catalyst (runs 30 and 31 in Table 3).

We tried to prepare Sm_2O_3 on MgO by coprecipitation with oxalic acid followed by calcination at 1023 K or 1173 K. The Sm_2O_3(15 wt %)/MgO-OX catalyst prepared at 1023 K had a large BET surface area (53 $m^2 \cdot g^{-1}$), and gave a high C_2 STY, but the C_2 selectivity was inferior to that obtained with Sm_2O_3/MgO prepared by the usual impregnation method (see runs 15, 16, 32, and 33). However, Sm_2O_3/MgO-OX prepared at 1173 K (BET surface area; 81 $m^2 \cdot g^{-1}$) gave a very high C_2 selectivity without a decrease in the C_2 STY. With this catalyst, use of carbon dioxide further increased the C_2 selectivity to 57.4% (runs 34 and 35).

Roles of Carbon Dioxide

Effects of carbon dioxide described above can be partly explained as follows. On the surface of the catalyst, metal carbonate might be formed:

$$MO + CO_2 \rightleftharpoons MCO_3 \qquad (1)$$

M = Mg, Ca, Sr

The decomposition temperature (T_d) of $SrCO_3$ is 1613 K, much higher than the reaction temperature.[22] Even if a very small amount of carbon dioxide was present in the feed gas, SrO would immediately react with carbon dioxide to give inactive carbonate species. Hence catalytic activity would be lost.

On the other hand, T_d of $CaCO_3$ is 1171 K, and ΔG for eq. (1) at 1073 K is -13.7 $kJ \cdot mol^{-1}$.[22] From these thermochemical data, addition of a small amount of carbon dioxide migh cause competitive adsorption of carbon dioxide, methane and molecular oxygen on the catalyst surface. Consequently, any secondary oxidation of the C_2 products or

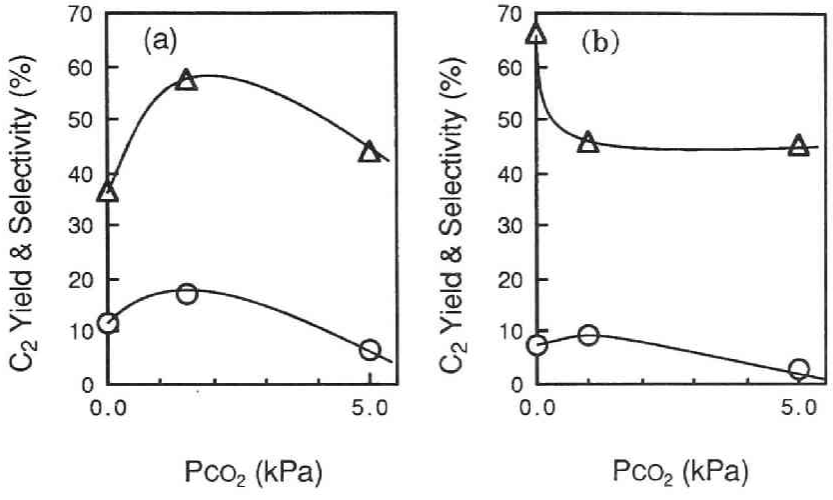

Figure 2. Effects of partial pressure of CO_2 in the reaction gas over the (a) CaO-OX and (b) SrO-OX catalysts. Amount of catalyst = 0.10 g, reaction temperature = 1073 K, methane feed rate = 7.5 mmol·h^{-1}, CH_4 : O_2 = 2 : 1. (○) The C_2 yields and (△) the C_2 selectivities.

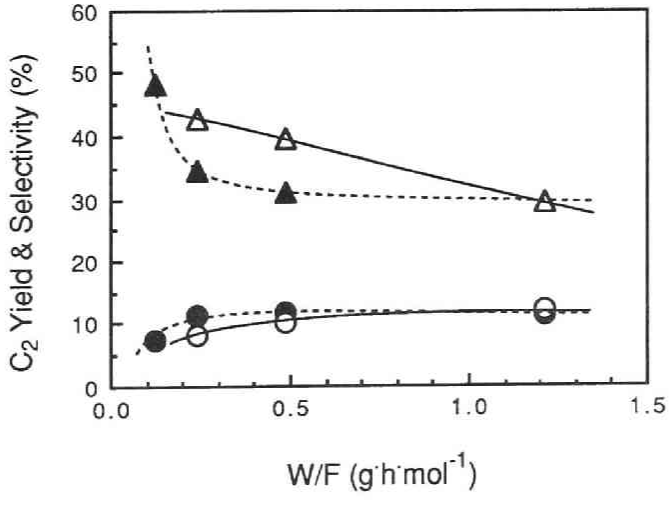

Figure 3. Effects of W/F by changing the amount of the Sm_2O_3(15 wt.%)/MgO-OX catalyst at 1073 K. Reaction gas composition was the same as shown in Figure 1. The C_2 yields under (●) He and (○) CO_2, and the C_2 selectivities under (▲) He and (△) CO_2.

intermediates could be partly suppressed, resulting in increases in the C_2 yield and selectivity. Excess carbon dioxide would give carbonates over the entire surface of the oxide catalyst, and would reduce its catalytic activity.

The surface of the MgO catalyst seemed not to be covered with inactive carbonate species owing to low T_d of $MgCO_3$ (813 K).[22]

Oxidation of methane with carbon dioxide is an alternative possibility.[21] C_2 compounds and carbon monoxide can be produced from methane and carbon dioxides via the following two reactions, respectively;

$$CH_4 + CO_2 \longrightarrow 1/2C_2H_4 + CO + H_2O \qquad (2)$$
$$\Delta G = 34.7 \text{ kJ/mol (at 1073 K)}$$

$$CH_4 + 3CO_2 \longrightarrow 4CO + 2\,H_2O \qquad (3)$$
$$\Delta G = -44.8 \text{ kJ/mol (at 1073 K)}$$

From these thermochemical data, it is possible to increase the C_2 yield via eq. (2) to *ca.* 2%. At the same time, carbon monoxide production via eq. (3) is thermochemically more favoured. This has been experimentally confirmed by the result of the reaction of methane with carbon dioxide without oxygen over Sm_2O_3/MgO, in which carbon monoxide was given as the major product. As a general trend, an increase in the carbon monoxide yield was observed over various catalysts on changing diluent from helium to carbon dioxide. This seemed to be responsible for the reaction (3) and also the suppression of deep oxidation of carbon monoxide to carbon dioxide by modifying the characteristics of metal oxide surface.

Effects of Reaction Conditions

With the Sm_2O_3(15 wt %)/MgO-OX catalyst (prepared at 1023 K), effects of W/F on the C_2 yield and C_2 selectivity by changing the amount of the catalyst were examined, and results are shown in Figure 3.

In a stream of helium, there was little change in the C_2 yield and C_2 selectivity over the range of W/F between 0.24 $g \cdot h \cdot mol^{-1}$ (amount of the catalyst; 0.020 g) and 1.21 $g \cdot h \cdot mol^{-1}$ (0.10 g) at 1073 K. Under carbon

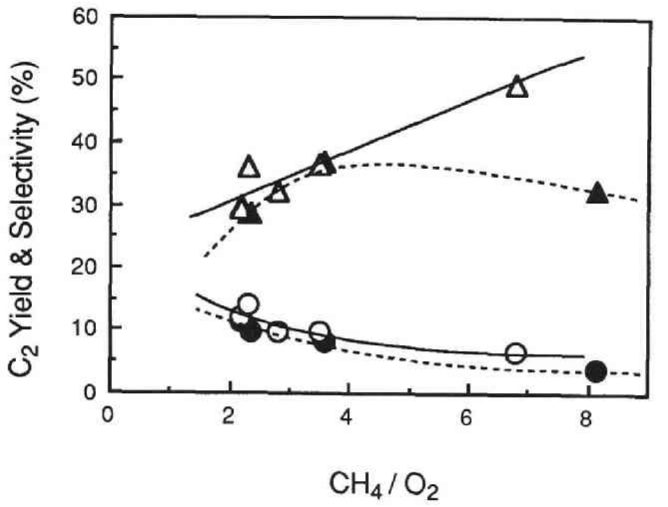

Figure 4. Effects of CH_4/O_2 over the Sm_2O_3-OX(15 wt.%)/MgO catalyst at 1073 K. Amount of catalyst = 0.10 g, methane feed rate = 7.5 $mmol \cdot h^{-1}$. The C_2 yields under (●) He and (○) CO_2, and the C_2 selectivities under (▲) He and (△) CO_2.

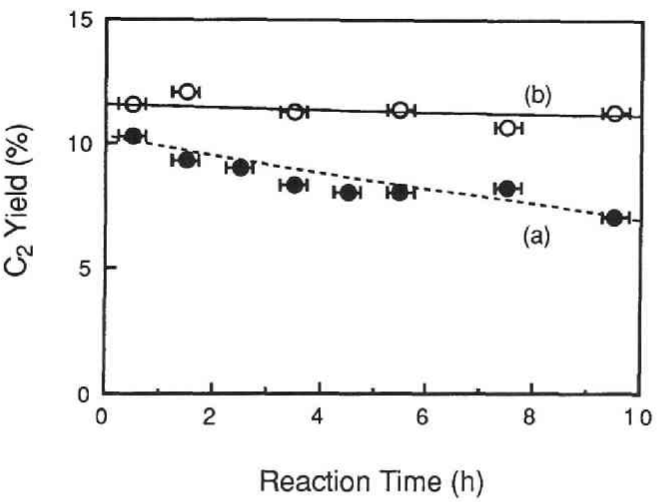

Figure 5. Changes in the C_2 yield with reaction time over the Sm_2O_3(15 wt.%)/MgO-OX catalyst under (a) He and (b) CO_2 at 1073 K. Amount of catalyst = 0.10 g, reaction gas composition was the same as shown in Figure 1.

dioxide, the C_2 selectivity increased markedly, but the C_2 yield gradually decreased with a decrease in the amount of the catalyst used. This suggests that an increase in the C_2 selectivity by using carbon dioxide without a decrease in the C_2 yield could be achieved only when a suitable W/F (in this instance 0.24 - 0.48 $g \cdot h \cdot mol^{-1}$) is employed.

Figure 4 shows effects of the methane-to-oxygen ratio, varied by changing concentration of oxygen, on the C_2 yield and selectivity with Sm_2O_3(15 wt %)/MgO-OX. In a series of experiments, the methane concentration was fixed at 9 vol %. Under both helium and carbon dioxide, the C_2 yields gradually decreased with an increasing methane-to-oxygen ratio. The C_2 selectivity under helium increased from 25% at CH_4/O_2; 2 to 40% at CH_4/O_2; 4. It did not increase with a further increase in the methane-to-oxygen ratio. This suggests that different types of active centers existed for complete oxidation and C_2 formation. The tendency would be enhanced with the catalysts having larger surface areas. Under carbon dioxide, the C_2 selectivity increased up to about 50% with increasing CH_4/O_2 to 6.8. Thus addition of carbon dioxide increased the C_2 selectivity at lower concentrations of oxygen, probably owing to the suppression of deep oxidation of methane and C_2 compounds by preferential adsorption of carbon dioxide on the active centers for complete oxidation.

Changes in the catalytic activity of Sm_2O_3(15 wt %)/MgO-OX against the reaction period are shown in Figure 5. Activity for C_2 formation under helium gradually decreased with an increase in the reaction time. After 10 h, the C_2 yield decreased to *ca.* 70% of the initial value and the catalyst surface became dark grey to black. This color was eliminated by calcination of the catalyst at 873 K in an air stream, and the catalytic activity was almost restored. The deactivation seemed to be a direct result of deposition of carbon. Under carbon dioxide, the C_2 yield was constant over the reaction for 10 h, and the catalyst remained white. Use of carbon dioxide as a diluent improved the stability of the catalyst and suppressed deactivation.[20]

With Li-doped MgO catalyst, a loss of Li was suggested to be responsible for the deactivation of the catalyst.[20] A small amount of carbon dioxide was reported to fix Li as Li_2CO_3 to suppress such deactivation. With the Sm_2O_3/MgO-OX catalyst, the deactivation of the catalyst under helium seemed to be responsible for deposition of coke

(see above). Carbon dioxide could immediately oxidize deposited coke on the surface to carbon monoxide at an elevated temperature:[23]

$$C + CO_2 \xrightarrow{Sm} 2CO \qquad (4)$$

$$\Delta G = -17.7\ kJ \cdot mol^{-1}\ (at\ 1073\ K)$$

It seems to be also possible that carbon dioxide poisoned strongly interaction sites, resulting in prevention of coke formation.

References

1 G.E. Keller and M.M Bhasin, *J. Catal., 73,* **1982**, 9.

2 T. Ito, J.X. Wang, G.H. Lin and J.H. Lunsford, *J. Am. Chem. Soc., 107,* **1985**, 5062.

3 K. Otsuka, *Sekiyu Gakkaishi, 30,* **1987**, 385.

4 K. Otsuka, K. Jinno and A. Morikawa, *Chem. Lett.,* **1985**, 499.

5 W. Hinsen, W. Bytyn and M. Baerns, *Proc. 8th. Cong. Catal. Weinheim, 3,* **1984**, 581.

6 T. Imai and T. Tagawa, *J. Chem. Soc., Chem. Commun.,* **1986**, 52.

7 K. Aika, T. Moriyama, N. Takasaki and E. Iwamatsu, *J. Chem. Soc., Chem. Commun.,* **1986**, 1210.

8 K. Asami, S. Hashimoto, T. Shikada, K. Fujimoto and H. Tominaga, *Chem. Lett.,* **1986**, 1233.

9 I. Matsuura, Y. Utsumi, M. Nakai and T. Doi, *Chem. Lett.,* **1986**, 1981.

10 N. Yamagata, K. Tanaka, S. Sasaki and S. Okazaki, *Chem. Lett.,* **1987**, 81.

11 K. Otsuka and T. Komatsu, *J. Chem. Soc., Chem. Commun.,* **1987**, 388.

12 K. Otsuka, Y. Shimizu and T. Komatsu, *Chem. Lett,* **1987**, 1835.

13 K. Machida and M. Enyo, *J. Chem. Soc., Chem. Commun.,* **1987**, 1639.

14 K. Fujimoto, S. Hashimoto, K. Asami and H. Tominaga, *Chem. Lett.,* **1987**, 2157.

15 C.H. Lin, T. Ito, J.X. Wang and J.H. Lunsford, *J. Am. Chem. Soc., 109,* **1987**, 4808.

16 J.M. Thomas, X. Kuan and J. Stachurski, *J. Chem. Soc., Chem. Commun.,* **1988**, 162.

17 J.E. France, A. Shamsi and M.Q. Ahsan, *Energy & Fuels, 2,* **1988**, 235.

18 A. Morikawa, N. Takasaki, E. Iwamatsu and K. Aika, *Chem. Lett.,* **1986**, 1165.

19 E. Iwamatsu, T. Moriyama, N. Takasaki and K. Aika, *J. Chem. Soc., Chem. Commun.,* **1987**, 19.

20 S.J. Korf, J.A. Roose, N.A. de Bruijn, J.G. van Ommen and J.H.R. Ross, *J. Chem. Soc., Chem. Commun.,* **1987**, 1433.

21 K. Aika and T. Nishiyama,
J. Chem. Soc., Chem. Commun., **1987**, 19.
22 M.W. Chase, C.A. Davies, J.R. Downey, D.J. Frurip, R.A. McDonard and A.N. Syverud, *JANAF Thermochemical Tables*, American Chemical Society, Washington, DC, **1985**.
23 T. Suzuki, S. Nakajima and Y. Watanabe,
Energy & Fuels, 2, **1988**, 848.

Chapter 6

Oxidative Methylation of Toluene with Methane using Metal Oxide Catalysts Promoted with Alkali and Alkaline Earth Metal Halides

Abstract

Oxidative methylation of toluene with methane was performed over various basic oxide catalysts at around 1023 K. Lanthanum oxide prepared by thermal decomposition of lanthanum oxalate, La_2O_3-OX, afforded the high yield (6.2 %) and selectivity (21.2 %) of styrene and ethylbenzene. Addition of alkali metal halides to the parent oxides increased their catalytic activities. The NaBr loaded La_2O_3-OX catalyst gave the highest C_8 yield of 11.6 % with the selectivity of 31.4 %. With NaBr loaded La_2O_3-OX, higher CH_4 / toluene ratio in the feed gas increased the yield of C_8 compounds. At toluene partial pressure of 1.7 kPa, the highest C_8 yield (23.9 %) and C_8 selectivity (40.2 %) were obtained. An isotope study using toluene-d_8 and light methane (d_0) proved that most of styrene and ethylbenzene were formed by the cross-coupling reaction between toluene and methane.

Introduction

Direct conversion of methane into chemical feedstock or transportational liquid fuel is an attractive process. Recently, oxidative dimerization of methane into ethane and ethene has been developed, and a large number of effective catalysts involving basic metal oxides were reported by Keller and Bhasin,[1] Ito et al.,[2] Otsuka et al.,[3] Aika et al.,[4] Asami et al.,[5] and Moriyama et al.[6]

Kcheyan et al.[7] have investigated oxidative methylation of compounds with a methyl group at an α-position to the electron-withdrawing functional groups, such as toluene and acetonitrile. Oxides of Bi, Mo, and Zn promoted with alkali and alkaline metal earth oxides were reported to be effective. Yakovich et al.[8] reported that a silica supported KBr catalyst gave the highest selectivity for oxidative

methylation of toluene. Oxidative methylation of propene to form C_4 compounds (butane and butenes) over the Na_2O/La_2O_3 catalyst was reported by Sodesawa et al.[9] Osada et al.[10-12] reported that the alkali-promoted Y_2O_3-CaO catalysts and the PbO loaded MgO catalysts, which were active for oxidative coupling of methane, showed excellent catalytic activities for oxidative methylation of toluene.

In this chapter, investigations on oxidative methylation of toluene are described. The basic oxide catalysts including rare earth oxides, other group IIA and IIIB metal oxides and Bi_2O_3 were found to be excellent. Promotional effects of alkali metal and alkaline earth metal halides are described. Effects of reaction conditions, plausible reaction paths, and roles of metal halide promoters are also described in detail.[13]

Experimental Section

Materials

Commercial La_2O_3 (Wako, >99.5% purity), MgO (Wako, >99.0%), Bi_2O_3 (Nacalai Tesque, >99.9%), and silica gel (Alfa, surface area = 300 $m^2.g^{-1}$) were used as received. A porous La_2O_3 catalyst (further designated as La_2O_3-OX) was prepared by thermal decomposition of lanthanum oxalate at 1023 K for 1 h in a flow of air and then for 1 h in a flow of argon. Other oxide-OX catalysts were prepared similarly. The alkali or alkaline earth metal halide loaded catalysts were prepared by the usual impregnation method from aqueous solutions of the respective halides followed by evaporating, and drying at 393 K for more than 2 h in an argon atmosphere.

Apparatus and Procedures

The reaction was carried out with the use of a conventional fixed bed flow type quartz glass reactor (9 mm i.d.). From the outlet of the reactor, an inner quartz glass tube (5 mm o.d.) was inserted, and air was introduced into it to quench the products immediately. The catalyst (typically 40 mg) was activated *in situ* in a flow of air (20 $cm^3 \cdot min^{-1}$) at the reaction temperature (typically at 1023 K) for 2 h just before the reaction. The typical experimental conditions were as follows: Reaction temperature; 1023 K, CH_4 flow rate; 25 $mmol \cdot h^{-1}$, toluene flow rate; 1.5

mmol·h^{-1}, W/F; 0.80 g·h·mol^{-1}. the molar ratio CH_4 : O_2 : CO_2 (diluent) : toluene; 50 : 5 : 45 : 3, $P_{methane}$; 49 kPa, $P_{toluene}$; 3 kPa, P_{oxygen}; 5 kPa. Toluene was introduced by passing the reactant gas mixture into a toluene vapor saturator equipped just before the inlet of the reactor. Liquid products were trapped in a condenser containing heptane at 273 K. Highly volatile products and gaseous products were collected into a dry ice-methanol trap connected to the heptane trap, and gas sampling bags, respectively.

Analysis

Both liquid and gaseous products were analyzed by gas chromatography using a Porapak-Q column (3 mm i.d. x 3.0 m) at 353 K for C_1-C_4 hydrocarbons, an SE-30 column (3 mm i.d. x 3.0 m, temperature programmed mode from 333 to 473 K at the heating rate of 2 K·min^{-1}) for >C_5 hydrocarbons, an active carbon column (3 mm i.d. x 3.0 m) at 323 K for H_2, CO, and CO_2, and a molecular sieves-5A column (3 mm i.d. x 3.0 m) at 323 K for O_2. The yield of produced carbon dioxide was calculated from the balance between molecular oxygen feed and the amounts of oxygen containing products and recovered molecular oxygen.

BET (Brunauer-Emmet-Teller) surface area of the catalyst was measured with nitrogen at 77 K by using a BELSORP-28 (BEL Japan Inc.), a microprocessor controlled automatic instrument. For the powder X-ray diffraction (XRD) study, a RIGAKU Geigerflex with Kα-ray of copper (λ = 1.5405 Å) was used. The amount of residual sodium in the catalyst after the reaction or pretreatment was measured by the atomic absorption analysis (Nippon Jarrell Ash Inc., AA-8200 atomic absorption spectrometer), in which the solid La_2O_3 based catalyst was dissolved in a concentrated hydrochloric acid solution. The TGA (thermo-gravimetric analysis) study was performed by a Shimadzu TGC-31 thermal balance in order to measure the loss of additives from the catalyst. Although NaBr content decreased during the activation of the catalysts, the amounts of alkali metal halides loaded in the preparation of the catalysts are given in the Tables and Figures.

Isotope study

Toluene-*d*8 (Aldrich, >99%) was used as received. Liquid products were analyzed by the use of a gas-chromatography / mass-spectrometer (Shimadzu Inc., QP-2000) equipped with a chemically bonded cyanopropylsilicon capillary column (0.2 mm i.d. x 25 m, Shimadzu HiCap-CPB10), and gaseous products were analyzed by an on-line quadrupole mass-spectrometer (MSQ-150A, ULVAC Inc.).

Results and Discussion

Since the use of carbon dioxide as a diluent increased the yields of ethane and ethene in oxidative coupling of methane as described in chapter 5,[14] throughout this study we employed carbon dioxide as a reactive diluent. Products were benzene, ethylbenzene, and styrene (C_8 compounds), 1,2-diphenylethane and 1,2-diphenylethene (C_{14} compounds), ethane and ethene (C_2 compounds), CO, CO_2, H_2O, H_2, and very small amounts of unidentified hydrocarbons. Trace amounts of xylenes were also detected. The yields and selectivities were calculated on the basis of toluene feed. Duplicate runs showed variations in the C_8 yield and selectivity within the range of 1% and 3%, respectively. Such deviations seem to be responsible for the reaction on a small scale resulting in difficulties in controlling the amount of toluene feed. The reaction with a quartz wool plug used for fixing the catalyst bed afforded a small amount of C_8 compounds (yield = 2.7%), indicating contribution of the thermal process on a small scale.

Oxidative Methylation of Toluene over Group IIA and IIIB Metal Oxides

Table I shows results at an initial stage (20 - 80 min) of the reaction on various group IIIB metal oxide catalysts, some of which were known to be active for oxidative dimerization of methane.[3] Under the conditions employed, scarcely any deep oxidation of methane to carbon oxides was calculated to occur based on the balance of toluene conversion.

Among commercially available rare earth oxides, lanthanum oxide exhibited the highest catalytic activity. The highest C_8 yield was

Table I. Oxidative Methylation of Toluene over Rare-Earth Oxides and Group IIIB Oxides[a]

			conversion		yield			selectivity					
run	catalyst	catal wt, mg	toluene, %	O_2, %	C_8,[b] %	C_2,[c] mmol/h	H_2, mmol/h	C_8, %	(EB,[d] %	ST,[e] %)	benzene, %	CO, %	CO_2, %
1	quartz wool		9.0	22	2.7	0.04	trace	29.8	(23.2	6.6)	22.5	33.8	10
2	La_2O_3	100	34.6	95	5.6	0.19	0.23	16.3	(8.5	7.8)	25.1	44.5	13
3	La_2O_3-OX	40	29.2	79	6.2	0.13	0.26	21.2	(14.6	6.6)	20.8	43.8	13
4	La_2O_3-OX	100	30.0	100	5.9	0.26	0.17	19.6	(12.0	7.6)	20.8	30.2	26[f]
5	Yb_2O_3-OX	40	27.4	84	4.7	0.11	0.28	17.1	(11.6	5.5)	14.2	48.0	20
6	Dy_2O_3-OX	40	31.2	86	4.3	0.11	0.30	13.7	(9.1	4.6)	19.6	46.1	20
7	Ce_2O_3-OX	40	19.3	100	0.8	0.04	0.16	4.4	(3.1	1.3)	13.3	28.0	54
8[g]	Pr_6O_{11}-OX	40	13.4	100	1.4	0.04	0.10	10.0	(7.0	3.0)	14.1	19.9	45[f]
9[g]	Nd_2O_3-OX	40	15.4	100	1.2	0.01	0.28	7.7	(4.9	2.8)	12.9	46.5	25[f]
10[h]	Sc_2O_3	40	27.5	95	2.7	0.12	0.25	9.9	(5.9	4.0)	22.8	48.4	19
11	Y_2O_3-OX	40	25.9	95	3.2	0.11	0.23	12.5	(8.4	4.1)	17.4	42.5	27

[a] Reaction temperature = 1023 K; CH_4:O_2:CO_2:toluene = 50:5:45:3. [b] Ethylbenzene + styrene. [c] Ethane + ethene. [d] Ethylbenzene. [e] Styrene. [f] Coke deposition was observed. [g] CH_4:O_2:CO_2:toluene = 100:5:95:6. [h] CH_4:O_2:CO_2:toluene = 100:7:93:6.

Table II. Oxidative Methylation of Toluene over Alkaline-Earth Oxides[a]

			conversion		yield			selectivity					
run	catalyst	catal wt, mg	toluene, %	O_2, %	C_8, %	C_2, mmol/h	H_2, mmol/h	C_8, %	(EB, %	ST, %)	benzene, %	CO, %	CO_2, %
12	MgO	100	22.5	100	1.0	0.03	0.08	4.5	(2.7	1.8)	12.0	26.9	52[b]
13[c]	CaO-OX	40	22.4	77	4.5	0.12	0.27	20.0	(13.3	6.7)	15.1	32.7	32
14[c,d]	SrO-OX	40	21.4	77	2.5	0.10	nm	11.7	(8.6	3.2)	30.5	24.2	33
15[c]	BaO-OX	40	20.7	65	3.0	0.09	0.25	14.6	(10.6	4.0)	26.9	25.3	31

[a] Reaction temperature = 1023 K; diluent = CO_2; CH_4:O_2:diluent:toluene = 50:5:45:3; nm = not measured. [b] Coke deposition was observed. [c] Diluent = He. [d] CH_4:O_2:diluent:toluene = 100:7:93:6.

5.6% with 100 mg of commercial low surface area La_2O_3 (BET surface area; 2.0 $m^2 \cdot g^{-1}$). Almost all of oxygen in the feed was consumed to convert 34.6% of toluene feed. Large amounts of benzene, CO and CO_2 were produced as byproducts, thus the selectivity for C_8 compounds was low (16.9%). Homo-coupling products of methane, C_2 compounds, and hydrogen were also formed in the yields of 0.19 $mmol \cdot h^{-1}$ and 0.23 $mmol \cdot h^{-1}$, respectively.

On the other hand, a smaller amount (40 mg) of La_2O_3-OX (BET surface area; 4.1 $m^2 \cdot g^{-1}$), prepared by thermal decomposition of lanthanum oxalate, showed the higher C_8 yield (6.2%) and C_8 selectivity (21.2%) (run 3). The space time yield (STY) of C_8 compounds on La_2O_3-OX (2.3 $mmol \cdot (g \cdot h)^{-1}$) increased to 2.5 times that using commercial La_2O_3 (0.9 $mmol \cdot (g \cdot h)^{-1}$). When the amount of the catalyst increased to 100 mg (run 4), both the C_8 yield and selectivity slightly decreased, and formation of coke on the catalyst surface was observed. The yields of CO_2 and C_2 compounds also increased, whereas those of H_2 and CO decreased. This indicates that a longer residence time induced secondary oxidation of cross-coupling products, H_2 and CO. Formation of C_2 compounds from methane has been reported to proceed via coupling of two methyl radicals that were formed on the catalyst surface.[1] Abstraction of hydrogen from methane to form methyl radical might be promoted with increasing the amount of the catalyst, resulting in an increase in the C_2 yield. Coke formation was probably due to the strong adsorption and dehydrogenation of toluene, methane, cross-coupling products, or intermediates that could not be eliminated by further oxidation because of the deficiency of molecular oxygen (O_2 conversion; 100%).

Among other rare earth oxides, Yb_2O_3-OX and Dy_2O_3-OX showed the relatively high C_8 yields (4.7% and 4.3%, respectively). But oxides of Ce and Pr showed poor catalytic activities, suggesting that oxides of rare earth metals having more than one stable oxidation state are not active and selective for the cross-coupling reaction. Nd_2O_3 gave a lower yield of C_8 compounds as well as C_2 compounds, but produced a larger amount of hydrogen comparable to oxides of La, Yb, and Dy.

Other group IIIB oxides, Sc_2O_3-OX and Y_2O_3-OX, showed lower C_8 yields and the selectivities than La_2O_3-OX (runs 10 and 11), but the yields of C_2 compounds and hydrogen were similar to those with the La_2O_3-OX catalyst.

Results with the alkaline earth oxide catalysts are summarized in Table II. With CaO-OX, SrO-OX, and BaO-OX, helium was employed as a diluent of the reactant gas, because use of carbon dioxide as a diluent with these catalysts completely suppressed their catalytic activities of oxidative coupling of methane (see chapter 5).[14] The yield of C_8 compounds decreased in following order, CaO-OX > BaO-OX ~ SrO-OX > MgO-OX (MgO). The C_8 yield with CaO-OX, however, was lower than those with rare earth oxides. Magnesium oxide did not show significant catalytic activity under the conditions employed, and only deep oxidation of toluene proceeded. Lower catalytic activities of more basic BaO-OX and SrO-OX relative to that of CaO-OX were probably responsible for the formation of inactive carbonate species by the reaction between the basic oxide surfaces and CO_2 which was formed by deep oxidation of the reactant. This corresponds to the result that catalytic activity of strontium oxide markedly decreased with addition of a very small amount of carbon dioxide in oxidative coupling of methane.[14]

Activities of Alkali and Alkaline Earth Metal Bromide Loaded Catalysts

Table III summarizes promoter effects of alkali metal bromides on the La_2O_3-OX catalyst. The loading level of the bromide was 5 wt.% as the weight of the alkali metal. For all of the alkali metal bromide loaded catalysts, after activation for 2 h at 1023 K in a stream of air, a small amount of needlelike crystal was observed around the inner wall of the outlet of the reactor, suggesting a loss of alkali metal bromide from the catalyst bed. At 1023 K the yield and selectivity for C_8 compounds increased markedly with an addition of alkali metal bromide to the rare earth oxide catalyst. The NaBr/La_2O_3-OX catalyst marked the highest C_8 yield (11.6%), C_8 selectivity (31.4%), and C_8 STY (5.6 mmol·(g·h)$^{-1}$) at 1023 K (run 16). In general, the proportion of styrene in C_8 compounds was high with these bromide promoted catalysts. No decreases in the C_8 yield and selectivity were observed during the prolonged run for 4 h. At lower temperature, 973 K, the NaBr/La_2O_3-OX catalyst afforded C_8 compounds, C_2 compounds, and H_2 in lower yields than those at 1023 K. With KBr loaded La_2O_3-OX, however, the C_8 yield showed a relatively high C_8 yield of 7.0% at 973 K. It should be noted that the C_8 selectivity of 28.5% and the C_2 yield of 0.32 mmol·h^{-1} obtained at 973 K were higher

than those at 1023 K. This is mainly due to the fact that formation of benzene was suppressed at 973 K and the selectivity for benzene decreased to 8.9% (run 19). No decreases in the C_8 yield and the selectivity were also observed during the prolonged run for 4 h with KBr/La_2O_3-OX even at 1023 K. We examined promotional effects of LiBr, NaBr and KBr at a lower loading level of 10 mol% (0.5 wt.% as Li, 1.6 wt.% as Na, and 2.7 wt.% as K, respectively). Promotional effects of these additives at 1023 K decreased in the following order: NaBr > LiBr ~ KBr (runs 20-22).

Halides of alkaline earth metals such as $MgCl_2$ or $CaCl_2$ loaded on CaO or MgO have been reported to be the good catalysts for oxidative coupling of methane by Fujimoto et al.[15] We examined effects of these bromides on La_2O_3-OX in oxidative methylation of toluene. A slight increase in the C_8 yield was observed with $MgBr_2$ from 6.2% to 7.9%. The C_8 yield decreased to 4.3% with $CaBr_2$.

The catalytic activities of La_2O_3-OX promoted with alkali metal carbonates were examined. With Na_2CO_3(4 wt.% as Na) loaded La_2O_3-OX, the yield of C_8 compounds slightly increased from 6.2% to 7.0%, whereas addition of Li_2CO_3 to La_2O_3-OX resulted in a considerable decrease in the C_8 yield to 3.5%.

Table III also shows effects of loading of NaBr on several oxides. Loading of NaBr on CaO-OX afforded a higher C_8 yield (6.8%) than parent CaO-OX (4.5%) in an helium stream. Magnesium oxide essentially gave a very low C_8 yield (run 12 in Table II). Addition of NaBr to MgO did not increase the yield of C_8 compounds, but did increase the formation of benzene, CO, and CO_2. The reaction with NaBr dispersed on silica gel was examined to test the activity of NaBr itself, and C_8 compounds were obtained in the yield of 3.1% (run 29). These results suggest that addition of NaBr is only effective for C_8 formation when the parent oxide shows catalytic activity. The C_8 yield with NaBr loaded La_2O_3-OX (11.6%) was higher than the simple sum of the C_8 yields with parent La_2O_3-OX (6.2%) and NaBr/SiO_2 (3.1%), indicating the presence of a synergistic effect of NaBr loading on La_2O_3-OX.

Figure 1 shows the C_8 yields and the C_8 selectivities at 1023 K with variation in the amount of NaBr in the impregnating solution for the NaBr/La_2O_3(commercial) catalysts. The catalyst containing 22 wt.% of NaBr (5 wt.% as Na to the support) in preparation exhibited the maximum yield (8.9%) of C_8 compounds with C_8 selectivity of 31.0%. The

Table III. Oxidative Methylation of Toluene over Loaded Catalysts[a]

			conversion		yield			selectivity					
run	catalyst	temp, K	toluene, %	O_2, %	C_8, %	C_2, mmol/h	H_2, mmol/h	C_8, %	(EB, %	ST, %)	benzene, %	CO, %	CO_2, %
16	$NaBr/La_2O_3$-OX	1023	33.2	84	11.6	0.17	0.27	31.4	(11.0	20.4)	23.6	20.4	22
17	$NaBr/La_2O_3$-OX	973	18.6	67	3.0	0.06	0.13	16.3	(8.4	7.9)	16.6	21.5	40
18	KBr/La_2O_3-OX	1023	31.1	96	7.5	0.21	0.21	24.2	(15.7	8.6)	17.3	33.6	25
19	KBr/La_2O_3-OX	973	24.9	83	7.0	0.32	0.24	28.5	(18.5	10.0)	8.9	28.7	28
20	$LiBr/La_2O_3$-OX[b]	1023	45.4	87	9.5	0.12	0.44	20.9	(8.7	12.2)	25.6	29.9	21
21	$NaBr/La_2O_3$-OX[b]	1023	41.6	79	10.7	0.12	0.44	25.6	(10.3	15.3)	25.9	18.4	27
22	KBr/La_2O_3-OX[b]	1023	42.2	88	9.3	0.13	0.39	22.5	(12.7	9.8)	14.7	42.1	19
23	$MgBr_2/La_2O_3$-OX[c]	1023	34.5	90	7.9	0.17	0.34	22.9	(8.6	14.3)	25.3	22.8	26
24	$CaBr_2/La_2O_3$-OX[c]	1023	27.6	94	4.3	0.10	0.23	15.7	(7.7	8.0)	24.5	24.6	32
25	Li_2CO_3/La_2O_3-OX	1023	16.6	54	3.5	0.06	0.13	21.0	(16.5	4.5)	15.0	36.5	27
26	Na_2CO_3/La_2O_3-OX	1023	31.3	92	7.0	0.18	0.22	22.3	(15.2	7.1)	18.5	35.2	23
27[d]	NaBr/MgO-OX	1023	20.3	100	1.0	0.04	0.09	5.0	(2.5	2.5)	14.4	27.3	46
28[d,e]	NaBr/CaO-OX	1023	28.1	88	6.8	0.26	0.20	24.1	(11.9	12.3)	26.1	25.5	21
29	$NaBr/SiO_2$	1023	11.7	26	3.1	0.07	0.09	26.8	(19.9	6.8)	27.1	24.9	18

[a] Amount of catalyst = 40 mg; W/F = 0.80 g·h/mol; CH_4:O_2:CO_2:toluene = 50:5:45:3. For the loaded catalysts without any remarks, amount of alkali-metal bromide loaded = 5 wt % as alkali metal. [b] Amount of LiBr, NaBr, and KBr = 10 mol %; CH_4:O_2:CO_2:toluene = 50:6:44:3. [c] Amount of $MgBr_2$ and $CaBr_2$ = 5 wt % as metal bromide. [d] CH_4:O_2:diluent:toluene = 100:7:93:6. [e] Diluent = He.

Table IV. Oxidative Methylation of Toluene over Bi_2O_3-Based Catalysts[a]

			conversion		yield			selectivity					
run	catalyst[b]	catal wt, mg	toluene, %	O_2, %	C_8, %	C_2, mmol/h	H_2, mmol/h	C_8, %	(EB, %	ST, %)	benzene, %	CO, %	CO_2, %
30	Bi_2O_3	300	19.1	69	3.1	0.05	nm	16.5	(13.4	3.1)	8.0	11.8	64[c]
31[d]	Bi_2O_3	300	23.7	97	4.0	0.04	nm	16.9	(13.5	3.3)	5.2	3.1	74[c]
32	KBr/Bi_2O_3	100	33.5	88	11.2	0.11	0.01	33.3	(16.5	16.9)	16.8	13.5	30[c]

[a] Reaction temperature = 1023 K; diluent = CO_2; CH_4:O_2:diluent:toluene = 50:5:45:3; nm = not measured. [b] Amount of KBr loaded = 5 wt % as alkali metal. [c] Sintering on the surface of the catalyst was observed after the reaction of 80 min. [d] Reaction temperature = 973 K.

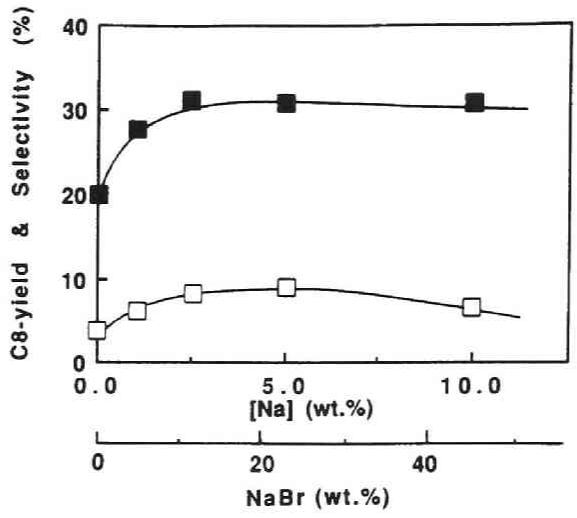

Figure 1. Effects of NaBr level to La_2O_3 on yield (□) and selectivity (■) of C_8 compounds: reaction temperature = 1023 K; amount of catalyst = 40 mg; W/F = 0.80 g·h/mol.

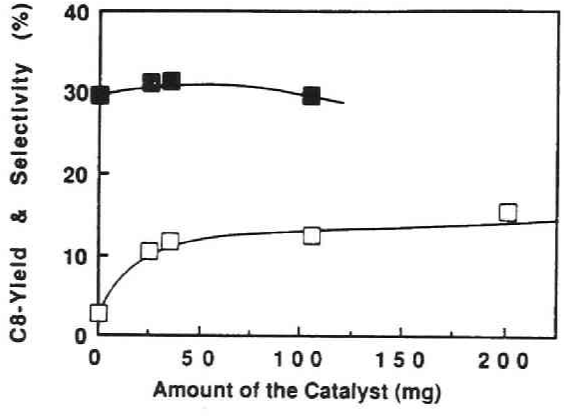

Figure 2. Effects of W/F by changing amount of NaBr (5 wt % as Na)/La_2O_3-OX catalyst on yield (□) and selectivity (■) of C_8 compounds: reaction temperature = 1023 K.

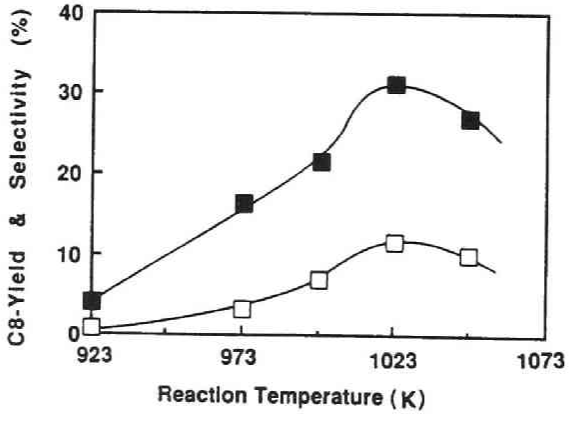

Figure 3. Effects of reaction temperature on yield (□) and selectivity (■) of C_8 compounds: amount of catalyst = 40 mg; W/F = 0.80 g·h/mol.

C_8 yield slightly decreased with a further increase in the loading amount of NaBr in preparation, while the C_8 selectivity leveled off above 11 wt.% of NaBr loading.

Bismuth Oxide Based Catalysts

In addition to group IIA and IIIB metal oxides, catalytic activities of various metal oxides were tested. Among them, Bi_2O_3 gave a considerable C_8 yield of 4.0% at 973 K (Table IV). However, the C_8 selectivity and the C_8 STY (0.2 $mmol \cdot (g.h)^{-1}$) were low. This was mainly due to complete oxidation of CH_4 and lower activity for oxidative methylation, which requires a larger amount of the catalyst. At a higher reaction temperature, 1023 K, Bi_2O_3 (melting point; 1097 K) sintered and exhibited lower catalytic activity, as shown in run 31. A KBr loaded Bi_2O_3 catalyst (100 mg) afforded the high initial C_8 yield (11.2%) and the highest selectivity (33.3%) at 1023 K, but rapid sintering of the catalyst surface was observed during the reaction of 1.5 h.

Effects of Reaction Conditions

Effects of W/F, the reaction temperature, and composition of the reaction gas mixture on the C_8 yield and selectivity were examined over the NaBr(5 wt.% as Na) loaded La_2O_3-OX catalyst, which showed the highest activity on the standard conditions.

We examined effects of W/F by changing the amount of the catalyst and results are shown in Figure 2 (the C_8 selectivity with 200 mg of the catalyst was not determined). With increasing amount of the catalyst, the C_8 yield slightly increased. With 200 mg of the catalyst (W/F; 4.0 $g \cdot h \cdot mol^{-1}$), the C_8 yield reached 15.7%. Coke formation was observed when more than 100 mg of the catalyst was used, but changes in the C_8 yield during the prolonged run for 4 h were not observed. On the other hand, the C_8 selectivity showed maximum around the catalyst amount of 40 mg (W/F; 0.80 $g \cdot h \cdot mol^{-1}$). A further increase in W/F slightly decreased the C_8 selectivity.

Figure 3 shows effects of the reaction temperature. Formation of C_8 compounds proceeded above 923 K. Both the C_8 yield and the C_8 selectivity showed maxima at 1023 K. At a higher reaction temperature, 1048 K, the yield and the selectivity for C_8 compounds decreased, and the

catalyst surface turned dark gray to black after reaction for 80 min. This coloration was eliminated by heating the catalyst at 873 K in an air stream, indicating coke formation on the surface.

Effects of methane partial pressure on the C_8 yield and selectivity are shown in Figure 4. With increasing partial pressure of methane, both the C_8 yield and selectivity increased up to 13.8% and 35.2%, respectively. At high partial pressure of methane (75 kPa), however, after a prolonged run for 5 h the C_8 yield decreased to 10.4%. In this case, no coke formation was observed on the catalyst surface, and the C_8 yield and selectivity were not restored (10.2% and 30.3%, respectively) by heating the catalyst at 1023 K in an air stream for 0.5 h.

Figure 5 shows effects of partial pressure of toluene in the feed. At methane partial pressure of 4 9kPa, the absolute amount of produced C_8 compounds exhibited the maximum value at partial pressure of toluene around 1.7 ~ 3.1 kPa. Thus the apparent C_8 yield based on toluene conversion increased in inverse proportion to toluene partial pressure. At partial pressure of toluene of 1.7 kPa, the highest C_8 yield (0.195 $mmol \cdot h^{-1}$, 23.9%) and the C_8 selectivity (40.2%) were obtained. With further decrease in partial pressure of toluene in the feed to 1.1 kPa, the amount of C_8 compounds and the C_8 selectivity decreased. On the other hand, at higher partial pressure of toluene of 9.3 kPa, the absolute amount of C_8 compounds, the apparent C_8 yield and the selectivity were low. In addition, formation of a large amount of coke was observed on the catalyst bed and even on the wall of the reactor. In general, the C_2 yield decreased with an increase in partial pressure of toluene, suggesting that activation of toluene and methane proceeded competitively. Small changes in partial pressure of toluene around 1.7-3.1 kPa greatly affect the C_8 yield and selectivity based on toluene conversion. Thus a small deviation in the amount of toluene feed caused considerable scatter in the formation of C_8 compounds.

The yields of C_8 compounds at various partial pressure of oxygen, P_{oxygen}, in the reaction gas are shown in Figure 6. The highest C_8 selectivity was obtained at P_{oxygen} of 5 kPa. At higher P_{oxygen}, the C_8 selectivity decreased due to an increase in formation of carbon oxides from toluene, whereas the C_8 yield leveled off at 10 ~ 11 %.

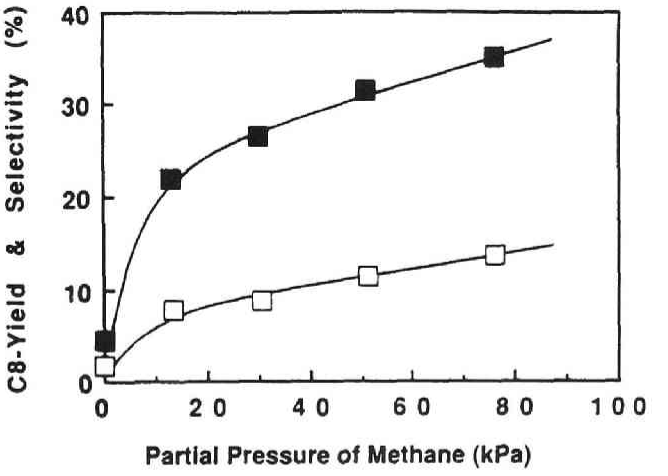

Figure 4. Effects of partial pressure of methane in feed gas on yield (□) and selectivity (■) of C_8 compounds: reaction temperature = 1023 K; partial pressure of toluene = 3 kPa; partial pressure of oxygen = 5 kPa.

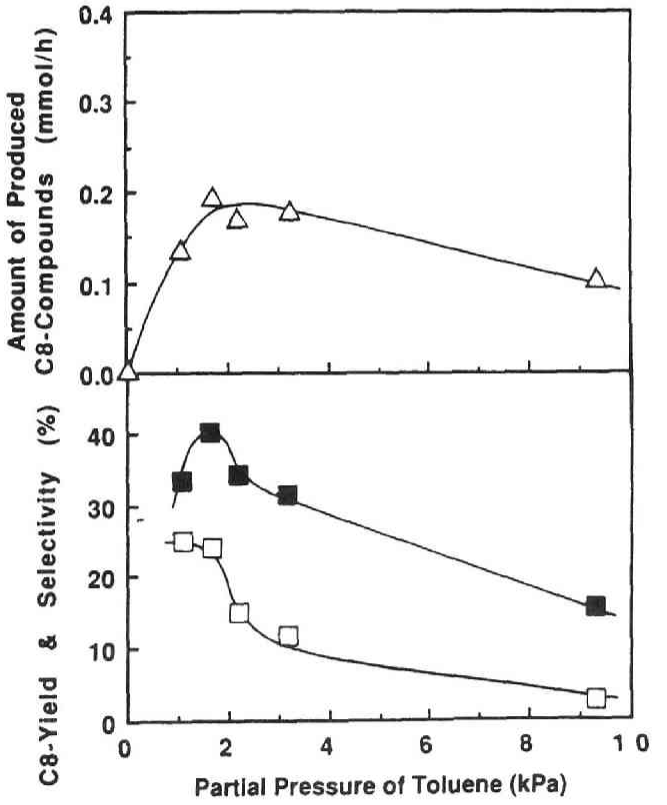

Figure 5. Effects of partial pressure of toluene on yield (□), selectivity (■) of C_8 compounds, and amounts of the C_8 products (△): partial pressure of methane = 49 kPa.

Isotope Studies

Table V shows the distribution of deuterated products obtained in the reaction using toluene-*d8* (carrier gas; CO_2). The predominant component of styrene was the *d6* one (m/Z; 110), probably $C_6D_5CD{=}CH_2$. Highly deuterated products of m/Z of 111 and 112 were also formed. The *d7* isomer was the most abundant one for ethylbenzene, and small amounts of *d8*, *d6*, and *d5* isomers were also obtained. No perdeuterated ethylbenzene was formed. Similar results were reported by Osada et al.[12] On the other hand, the gas phase mass analysis revealed that hydrogen was formed in the following isotope ratio: H_2 : HD : D_2; 6 : 20 : 7. A small amount of CH_3D was observed, and its relative intensity was 1.4% compared to that of CH_4 (after correction of ^{13}C isomers). This corresponds to a rate of CH_3D formation of *ca.* 0.35 mmol·h^{-1}.

Loss of Alkali Metal Bromides from the Catalyst

We examined the loss of alkali metal bromides from the catalyst by TGA method. NaBr or KBr(5 wt.% as Na or K) loaded La_2O_3-OX (*ca.* 40 mg) was heated in an air stream (20 cm^3·min^{-1}) at a heating rate of 100 K·min^{-1} up to 1023 or 973 K and then held at the temperature for 2 h, assuming the activation of the catalyst before the reaction. The weight of the NaBr/La_2O_3-OX catalyst decreased gradually as soon as the temperature reached 1023 K and stopped decreasing after *ca.* 70 min. The average loss of the catalyst weight of duplicate experiments was 14.0%. This catalyst initially contained 18.3% of NaBr, thus 64% of loaded NaBr was lost and one-third of NaBr would remain on the catalyst. The atomic absorption analysis of this catalyst revealed that about half of the Na remained on the catalyst after the heat treatment in air for 2 h at 1023 K.

On the other hand, with KBr loaded La_2O_3-OX a decrease in the weight of the catalyst was more pronounced. Most of KBr loaded on the catalyst amounting to 13.6% was lost within 40 ~ 50 min after the temperature reached 1023 K. At 973 K a decrease in the catalyst weight (14.4%) indicates that KBr on the catalyst was almost completely lost during the treatment for 2 h, but the rate of an weight loss was smaller than that at 1023 K.

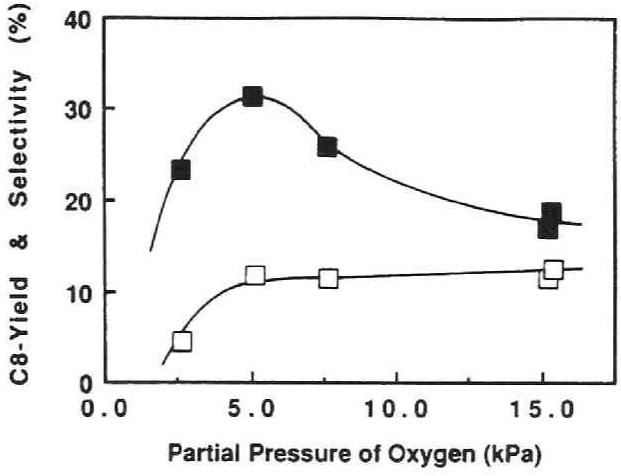

Figure 6. Effects of partial pressure of oxygen in feed gas on yield (□) and selectivity (■) of C_8 compounds: partial pressure of toluene = 3 kPa.

Table V. Deuterium Distribution of the Products from Toluene-d_8 and Methane[a]

compounds	m/z	isotopes[b]	rel intensity
styrene	112	d_8	12
	111	d_7	32
	110	d_6	100
	109	d_5	9
ethylbenzene	116	d_{10}	0
	115	d_9	0
	114	d_8	2
	113	d_7	100
	112	d_6	12
	111	d_5	4
hydrogen	4	d_2	30
	3	d_1	100
	2	d_0	35
methane[c]	17	d_1	1.4
	16	d_0	100

[a] Catalyst = NaBr (5 wt % as Na)/La_2O_3-OX. Styrene and ethylbenzene were analyzed by GC–MS. Hydrogen and methane were analyzed by quadrupole mass spectrography. [b] Styrene-d_6, probably $C_6D_5CD{=}CH_2$; ethylbenzene-d_7, probably $C_6D_5CD_2CH_3$. [c] Methane-d_2–d_4 cannot be analyzed due to H_2O.

The heat-treated catalysts were subjected to an XRD analysis. Since the samples had been exposed to air prior to the analysis, no useful information could be made on the oxidation state of the surface. The samples gave no significant peaks those could be attributed to alkali metal bromides. Instead, oxides of alkali metals, Na_2O or K_2O, seemed to exist on the catalyst surface.

General Discussion

The results shown in Table V make it possible for us to estimate the reaction mechanism of oxidative methylation of toluene. Scheme I illustrates plausible reaction paths. Although we should take into account the hydrogen deuterium exchange reaction which may occur at such a high temperature, the principal isotopic isomer of ethylbenzene-*d*7 firmly indicates that it was formed through the cross-coupling reaction between toluene-*d*8 and CH_4 (path A). The main component of styrene was the *d*6 isomer, indicating that most of styrene was produced through dehydrogenation of ethylbenzene-*d*7. A portion of styrene-*d*8, the perdeuterated product, and styrene-*d*7 should be formed by H/D exchange. Styrene-*d*8 could be produced via perdeuterated 1,2-diphenylethane, a homocoupling product of toluene-*d*8, followed by dissociation to benzene and styrene (path B). The reaction with unlabeled toluene without methane afforded a small amount of styrene and only a trace amount of ethylbenzene. Therefore a very small amount of styrene could be formed via path B, and most of the styrene and nearly all of the ethylbenzene were produced via path A, the cross-coupling process. On the other hand, formation of CH_3D suggests that a considerable amount of methyl radical recombined with H or D to form CH_4 or CH_3D. There is another possible path to form CH_3D, the reaction between methyl radical and toluene (Scheme II).

In general, the alkali metal bromide containing catalysts afforded the higher C_8 yields and selectivities than the unpromoted oxide catalysts in oxidative methylation of toluene, as shown in Table III. For oxidative coupling of methane, excellent catalytic activities with higher selectivities for ethene were reported for the catalysts containing alkali and alkaline earth metal halide, such as $MgCl_2/CaO$[15] and $LiCl/Sm_2O_3$.[16] Chlorine radical was reported to promote coupling of methane to ethene at a higher temperature in the gas phase.[17] On the

Scheme 1.

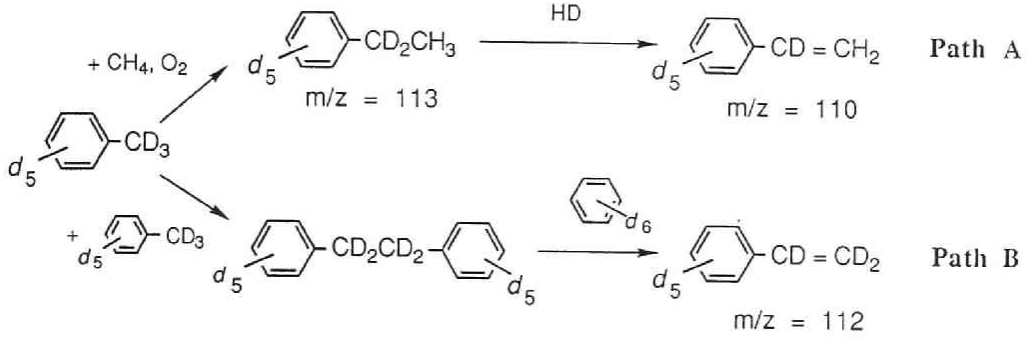

Scheme 2.

other hand, Otsuka and Komatsu[18] reported that with the alkali metal chloride loaded metal oxide catalysts the role of alkali metal is to create compounded oxide which is active for the formation of ethane, and the role of chlorine is to promote the formation of ethene from ethane in the postcatalyst zone. Burch et al.[19] reported that for oxidative coupling of methane an injection of a single pulse of dichloromethane greatly enhanced the selectivity for C_2 products with the potassium-promoted manganese oxide catalysts, and that the high selectivity was maintained after chlorine on the catalyst had been lost. They interpreted their results in terms of the modification of the surface of the catalyst by added chlorine.

In our study, the results obtained by the TGA study suggest that only a small portion of alkali metal bromide was retained on the catalyst surface. Activities of these loaded catalysts, however, were higher than those of unpromoted parent oxides, and maintained for a long period. Then we may estimate that alkali metals supplied from alkali metal bromides were present on the surface in the form of oxides during the reaction, and bromine played the role of modifying the surface state, as proposed by Burch et al.[19] The XRD study also supported such an idea.

References

1 G. Keller and M. Bhasin, *J. Catal.*, *73*, **1982**, 9.

2 T. Ito, J.X. Wang, G.H. Lin and J.H. Lunsford, *J. Am. Chem. Soc.*, *107*, **1985**, 5062.

3 K. Otsuka, K. Jinno and A. Morikawa, *Chem. Lett.*, **1985**, 499.

4 K. Aika, T. Moriyama, N. Takasaki and E. Iwamatsu, *J. Chem. Soc., Chem. Commun.*, **1986**, 1210.

5 K. Asami, S. Hoshimoto, T. Shikada, K. Fujimoto and H. Tominaga, *Chem. Lett.*, **1986**, 1233.

6 T. Moriyama, N. Takasaki, E. Iwamatsu and K. Aika, *Chem. Lett.*, **1986**, 1165.

7 Kh.E. Kcheyan, O.M. Revenko, A.V. Borisoglebskaya and D.L. Fishman, *Zh. Org. Khim.*, *12 (2)*, **1976**, 467 in *Chem. Abstr.*, **1976**, *84*, 164293h: Kh.E. Kcheyan, A.N. Shatalova, O.M. Revenko and L.I. Agrinskaya, *Neftekhimiya*, *20 (6)*, **1980**, 876: Kh.E. Kcheyan, O.M. Revenko, M.P. Tikhonova, and A.V. Borisoglebskaya, *Otkrytiya, Izobret., Prom. Obraztsy, Tovarnye Znaki*, *38*, **1980**, 113 in *Chem. Abstr.*, *94*, **1981**, 191871h: Kh.E. Kcheyan, O.M. Revenko, A.V. Borisoglebskaya and Yu.Z. Faradkov, *Neftekhimiya*, *21 (2)*, **1981**, 83: Kh.E. Kcheyan, A.N. Shatalova, O.N. Temkin and O.M. Revenko, *Neftekhimiya*, *21 (2)*, **1981**, 303: Kh.E. Kcheyan, O.M. Revenko, and Yu.Z. Faradkov, *Otkrytiya, Izobret., Prom. Obraztsy, Tovarnye Znaki*, *47*, **1981**, 101 in *Chem. Abstr.*, *96*, **1982**, 142426z: Kh.E. Kcheyan, N.I. Yakovich, L.P. Bakareva, S.P. Komarova and A.G. Kostiuk, *Otkrytiya, Izobret., Prom. Obraztsy, Tovarnye Znaki*, *47*, **1981**, 101 in *Chem. Abstr.*, *96*, **1982**, 180928x: Kh.E. Kcheyan, F.D. Klevanova, G.L. Bitman, O.B. Sobolev and G.A. Sokolova, *Neftekhimiya*, *22 (3)*, **1982**, 323: Kh.E. Kcheyan, O.M. Revenko, Yu.Z. Faradkov and I.G. Nikolaeva, *Nov. Metody Sint. Org. Soedin. Osn. Neftekhim. Syr'ya*, **1982**, 3 in *Chem. Abstr.*, *101*, **1984**, 74734t.

8 N.I. Yakovich, L.P. Bokareva and A.G. Kostyuk, *Pr-va Krupnotonnazhn, Prouktov Neftekhimii, M.*, **1979**, 37 in *Chem. Abstr.*, *93*, **1980**, 7755d.

9 T. Sodesawa, M. Matsubara, S. Satoh and F. Nozaki, *Chem. Lett.*, **1987**, 1513.

10 Y. Osada, K. Enomoto, T. Fukushima, S. Ogasawara, T. Shikada and T. Ikariya, *J. Chem. Soc., Chem. Commun.*, **1989**, 1156.
11 Y. Osada, N. Okino S. Ogasawara, T. Fukushima, T. Shikada and T. Ikariya, *Chem. Lett.*, **1990**, 281.
12 Y. Osada, S. Ogasawara, T. Fukushima, T.Shikada and T. Ikariya, *J. Chem. Soc., Chem. Commun.*, **1990**, 1434.
13 T. Suzuki, K. Wada and Y. Watanabe, *Appl. Catal.*, *53*, **1989**, L19: T. Suzuki, K. Wada and Y. Watanabe, *Ind. Eng. Chem. Res., 30,* **1991**, 1719.
14 T. Suzuki, K. Wada and Y. Watanabe, *Appl. Catal.*, *59*, **1990**, 213 (Chapter 5).
15 K. Fujimoto, S. Hashimoto, K. Asami and H. Tominaga, *Chem. Lett.*, **1987**, 2157.
16 K. Otsuka, K. Jinno and A. Morikawa, *J. Catal.*, *100*, **1986**, 353.
17 M. Weissman and S.W. Benson, *Int. J. Chem. Kinet.*, *16*, **1984**, 307.
18 K. Otsuka and T. Komatsu, *J. Chem. Soc., Chem. Commun.*, **1987**, 388.
19 R. Burch, G.D. Squire and S.C. Tsang, *Appl. Catal.*, *46*, **1989**, 69: R. Burch, E.M. Crabb, G.D. Squire and S.C. Tsang, *Catal. Lett.*, **1989**, 249: R. Burch, S. Chalker, G.D. Squire and S.C. Tsang, *J. Chem. Soc., Faraday Trans.*, *86 (9)*, **1990**, 1607.

Chapter 7

Oxidative Methylation of Ethane to Propane and Propene using Rare Earth Oxide Based Catalysts

Abstract

Oxidative methylation of ethane with methane on rare earth oxide based catalysts afforded propane and propene (C_3 compounds) together with ethene and carbon oxides at above 773 K. An europium oxide catalyst prepared from europium oxalate (Eu_2O_3-OX) gave C_3 compounds in the highest yield of 7.7% at 923 K when methane feed rate was 45 mmol·h^{-1}, and a molar ratio methane : ethane : oxygen was 18 : 1 : 1. Loading of alkali and alkaline earth metal halides on lanthanum oxide greatly enhanced its catalytic activity. The C_3 yield on La_2O_3-OX increased by loading of 5 mol% of $CaCl_2$ from 1.5 to 2.6% at 923 K. Loading of these halides on europium oxide and samarium oxide decreased their abilities to form C_3 compounds. The C_3 compounds were assumed to be formed mainly via oxidative cross-coupling reaction between methane and ethane.

Introduction

Direct partial oxidation of methane to higher alkanes and alkenes or oxygen-containing chemicals is an attractive reaction for utilizing natural gas as a chemical resource.[1] Recently, oxidative dimerization of methane has been received a great deal of attention, and a variety of metal oxide-based catalysts, including rare earth oxides, have been reported to exhibit significant activities and selectivities.[2-7] In addition to homo-coupling of methane, oxidative methylation of nitriles, alkenes, and alkyl-substituted aromatics in the presence of oxygen has been studied. Kcheyan et al.[8] reported that oxides of bismuth, molybdenum, and zinc together with alkali and alkaline earth metals were active and selective for the oxidative methylation of toluene with methane to form C_8 hydrocarbons (styrene and ethylbenzene). They also reported the

formation of acrylonitrile from methane and acetonitrile. A silica supported potassium bromide catalyst was found to show the high selectivity for oxidative methylation of toluene by Yakovich et al.[9] Osada et al. reported that a lithium-promoted Y_2O_3-CaO catalyst[10, 11] and a lead oxide catalyst supported on magnesium oxide[12] showed high catalytic activities. It has been described in previous chapter that the basic oxide catalysts including rare earth oxides promoted with alkali or alkaline earth metal halides were active and selective for the formation of styrene and ethylbenzene from toluene and methane.[13,14] Sodesawa et al.[15] reported oxidative methylation of propene to form C_4 compounds over a lanthanum oxide modified with Na_2O. Oxidative methylation with methane has been successful only with substrates having a methyl group flanking to an electron withdrawing group.

In this chapter, studies on oxidative methylation of ethane,[16] a simple light alkane, with methane over rare earth oxide based catalysts are described. In this reaction, propane and propene were formed along with a large amount of ethene at 773 - 998 K. Promotional effects of alkali or alkaline earth metal halide additives are also described.

Experimental Section

Materials

Commercial rare earth oxides (delivered from Wako Pure Chemicals Inc.) and silica gel (Alfa, surface area; 300 $m^2.g^{-1}$) were used as received. A porous oxide catalyst (designated as M_xO_y-OX) was prepared by thermal decomposition of corresponding oxalate salts at 1023 K. Details of the preparation method have been described in chapter 5.[14] An alkali or alkaline earth metal halide loaded catalyst was prepared by the usual pore volume impregnation method from an aqueous solution of the respective halide. Although alkali or alkaline earth metal halide content decreased during the activation of the catalysts, the amount of halides used for preparation of the catalysts are given in Tables and captions to Figures.

Highly purified methane gas was used as received. Ethane containing small amounts of carbon dioxide and H_2O was passed through the columns filled with granules of potassium hydroxide and molecular

sieves-5A, and then fed to the reactor. Helium and oxygen were used without any further purifications.

Apparatus and Procedures

A conventional fixed bed flow type reaction system equipped with a quartz glass reactor (9 mm i.d.) was employed for the reaction. An inner quartz tube (5 mm o.d.) was inserted from the outlet of the reactor and air was passed through it to quench the products immediately. The catalyst bed temperature was controlled and measured with seathed CA thermocouples inserted into the catalyst bed. Typically, 0.10 g of the powdered catalyst was mounted at the center of the reactor, and then activated in a flow of air (20 $cm^3.min^{-1}$) at the reaction temperature for 120 min just before the reaction. The mixture of 45 $mmol{\cdot}h^{-1}$ of methane, 7.5 $mmol{\cdot}h^{-1}$ of ethane, 2.5 $mmol{\cdot}h^{-1}$ of oxygen and 25 $mmol{\cdot}h^{-1}$ of helium was fed to the catalyst bed maintained at 773 - 998 K under atmospheric pressure. Flow rates of respective gases were regulated by means of thermal mass flow controllers. Gaseous products were collected into gas sampling bags. In some of the experiments, a cold trap at 197 K was placed just after the outlet of the reactor. However, none of liquid products was observed in the cold trap.

Analysis

Gaseous products were analyzed by gas chromatography using a Porapak-Q column (3 mm i.d. x 3.0 m) at 353 K for C_1-C_4 hydrocarbons with an FID, an active carbon column (3 mm i.d. x 3.0 m) at 323 K for H_2, CO and CO_2 with a TCD, and a molecular sieves-5A column (3 mm i.d. x 3.0 m) at 323 K for O_2 with a TCD. BET (Brunauer-Emmet-Teller) surface area of the catalysts was measured with nitrogen at 77 K by using a BELSORP-28 (BEL Japan Inc.), a micro processor controlled automatic instrument. For the powder X-ray diffraction study, a RIGAKU Geigerflex with Kα-ray of copper (λ = 1.5405 Å) was used.

Results and Discussion

Screening of Rare Earth Oxide Catalysts

Results obtained for various rare earth oxides at 923 K are shown in Figure 1. The oxides prepared from thermal decomposition of corresponding oxalate salts (Ln_xO_y-OX) were used for the reactions. The oxides marked with asterisk were commercial ones. The products were propane, propene, ethene, CO, CO_2, H_2, butane, butenes, and unidentified higher hydrocarbons. Yields of the products were calculated based on the ethane feed. If all of C_3 compounds were produced by cross-coupling between methane and ethane, and other products were formed entirely from ethane, the sum of the products yields was calculated to exceed an amount of converted ethane (*ca.* 140% of ethane conversion). This indicates that a considerable large amount of methane was activated together with ethane. Ethane, ethene and carbon oxides could be formed by oxidative homo-coupling of methane, and apparent conversion of ethane decreased by the formation of ethane from methane. The amounts of produced butane and butenes were less than 0.2% of an ethane feed under the selected reaction conditions. Inspection of Figure 1 reveals that all rare earth oxides except for CeO_2-OX, Nd_2O_3-OX, and Lu_2O_3-OX exhibited activities to form C_3 compounds. The yields of C_3 compounds were relatively low, and amounted less than 5% under the selected conditions, probably due to the co-production of a large amount of ethene. In general, the selective catalysts for C_3 formation produced substantial amounts of ethene. The highest C_3 selectivity was obtained with Eu_2O_3-OX. On Eu_2O_3-OX, C_3 hydrocarbons were formed in the combined yield of 4.3% based on ethane feed, together with ethene in the yield of 16.1%. The yield of carbon oxides produced on Eu_2O_3-OX was 8.1%, then the selectivity of *ca.* 70% for usable products based on the sum of converted methane and ethane was achieved.

We examined catalytic activities of rare earth oxides, La_2O_3, Sm_2O_3, and Eu_2O_3, from different sources to investigate whether their performances were thereby affected. Results are summarized in Table 1. The catalysts prepared from oxalates had larger BET surface areas than commercial ones. The -OX catalysts showed higher activities, though sometime less selective, as reported previously in the study of oxidative coupling of methane on the alkaline earth oxide based catalysts.[17] The

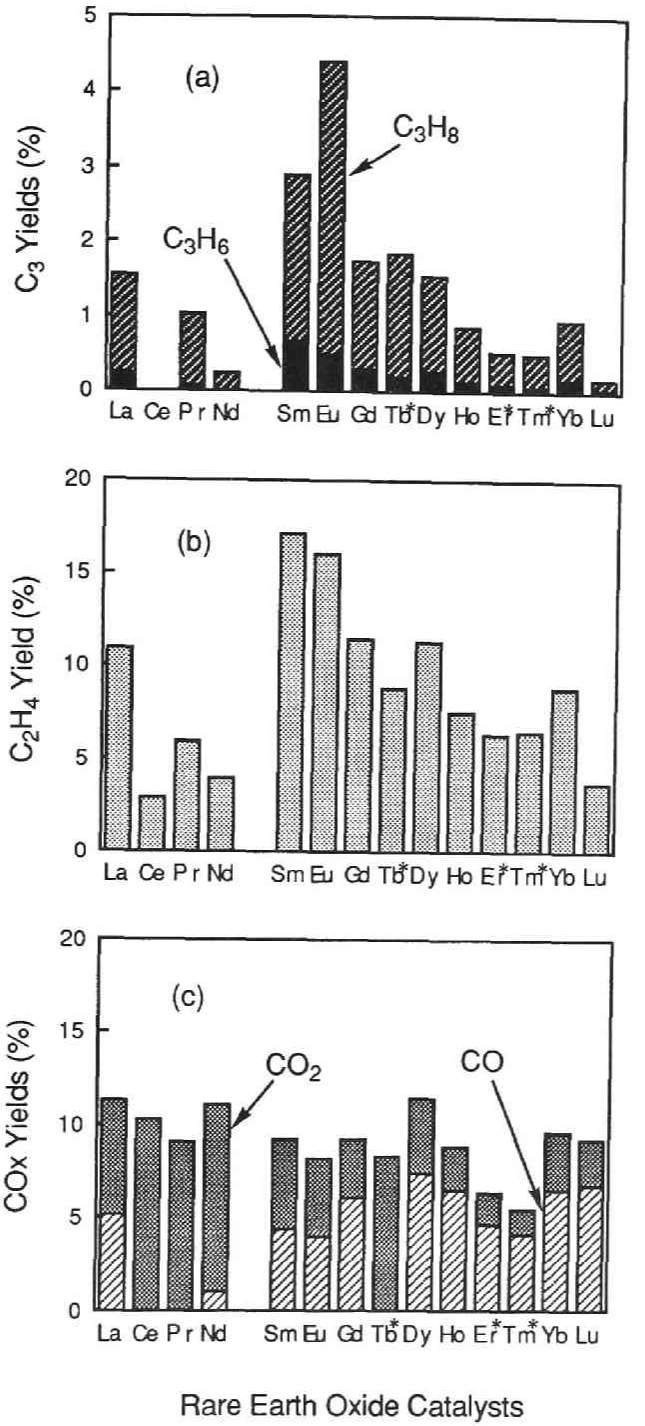

Figure 1. Oxidative methylation of ethane with methane on various rare earth oxides prepared from the oxalate salts at 923 K. Amount of catalyst = 0.10 g, W/F = 1.2 $g \cdot h \cdot mol^{-1}$, C_2H_6 feed rate = 7.5 $mmol \cdot h^{-1}$, $CH_4 : C_2H_6 : O_2 : He = 18 : 3 : 1 : 10$. (a) = C_3, (b) = C_2H_4, and (c) = CO_x yields, Ln* = commercial oxide.

Sm_2O_3-OX and Eu_2O_3-OX catalysts showed higher yields of C_3 compound than those with commercial ones. On the other hand, La_2O_3-OX gave the C_3 products in lower yield and carbon oxides in higher yield than La_2O_3. Higher activity of La_2O_3-OX for oxidation would lead further oxidation of the C_3 products and/or intermediates into CO and CO_2, since C_3 compounds would be oxidized more easily than the reactants and rest of the products. It should be noted that the surface of commercial Eu_2O_3 turned black after the reaction for 40 min, while the Eu_2O_3-OX catalyst remained white even after the reaction for longer period.

Figure 2 shows the yields of the products at variety of reaction temperatures on La_2O_3-OX, Sm_2O_3-OX and Eu_2O_3-OX. On all the catalysts tested, the yields of ethene increased exponentially with an increase in the reaction temperature, while CO_x (CO + CO_2) yield on Eu_2O_3-OX and Sm_2O_3-OX slightly decreased, or kept constant on La_2O_3-OX. The yield of C_3 compounds on La_2O_3-OX catalyst was only 0.2% at 823 K, and gradually increased to 2.0% with an increase in the reaction temperature at 973 K. The yields of C_3 compounds on Eu_2O_3-OX and Sm_2O_3-OX at 823 K were 2.7% and 1.8%, respectively. At 923 K the maximum yields of C_3 hydrocarbons were obtained on the Sm_2O_3-OX (2.9%) and on Eu_2O_3-OX (4.3%) catalysts. Further increases in the reaction temperature decreased the C3 yields on both Sm_2O_3-OX and Eu_2O_3-OX.

We investigated changes in catalytic activities of La2O3-OX and commercial Eu2O3 with time on stream at 923 K or 948 K. No changes in the C3 yield and product distribution were observed in the prolonged run for 300 min with both La2O3-OX at 923 K and Eu2O3 at 948 K. The surface of La2O3-OX remained white after the prolonged reaction. On the other hand, the surface of the Eu2O3 catalyst turned to black as described above. After the reaction for 5 h, the colored Eu2O3 catalyst was treated in a stream of air at 873 K, then the coloration was eliminated within 5 min with evolution of carbon dioxide. Carbon dioxide evolved was amounted to *ca.* 0.06 mmol with 0.040 g of the catalyst. Therefore formation of carbon dioxide seems to indicate carbon deposited on the surface of Eu2O3. Such amount of coke deposition seems not to cause deactivation of the catalyst. We could not rule out the possibility of the coloration due to partial reduction of the surface oxide. Carbon dioxide might possibly be released from the surface carbonate species, which could be formed during the course of oxidative methylation of ethane, since we have found that a

Table 1. Effects of Catalyst Preparation on the Oxidative Methylation of Ethane at 923 K[a]

Run	Catalyst	BET S.A. ($m^2 \cdot g^{-1}$)	Conv.[b](%)		Yield[b](%)					($mmol \cdot h^{-1}$)
			C_2H_6	O_2	C_2H_4	C_3H_6	C_3H_8	CO	CO_2	H_2
1	La_2O_3	2.0	13.1	78	6.9	0.2	1.7	4.9	4.0	0.6
2	La_2O_3-OX	4.1	17.0	~100	10.9	0.2	1.3	5.1	6.3	1.5
3	Sm_2O_3	2.3	14.8	83	8.4	0.2	1.4	6.2	4.0	1.1
4	Sm_2O_3-OX	4.9	21.2	91	17.1	0.7	2.2	4.4	4.9	1.4
5	Eu_2O_3	8.9	23.2	96	17.4	0.7	3.2	5.6	3.3	1.0
6	Eu_2O_3-OX	11	22.3	99	16.1	0.5	3.9	3.9	4.3	0.9

[a] Amount of catalyst = 0.10 g, C_2H_6 feed rate = 7.5 $mmol \cdot h^{-1}$, W/F = 1.2 $g \cdot h \cdot mol^{-1}$, $CH_4 : C_2H_6 : O_2 : He = 18 : 3 : 1 : 10$ (molar ratio).

[b] Based on ethane feed and oxygen feed.

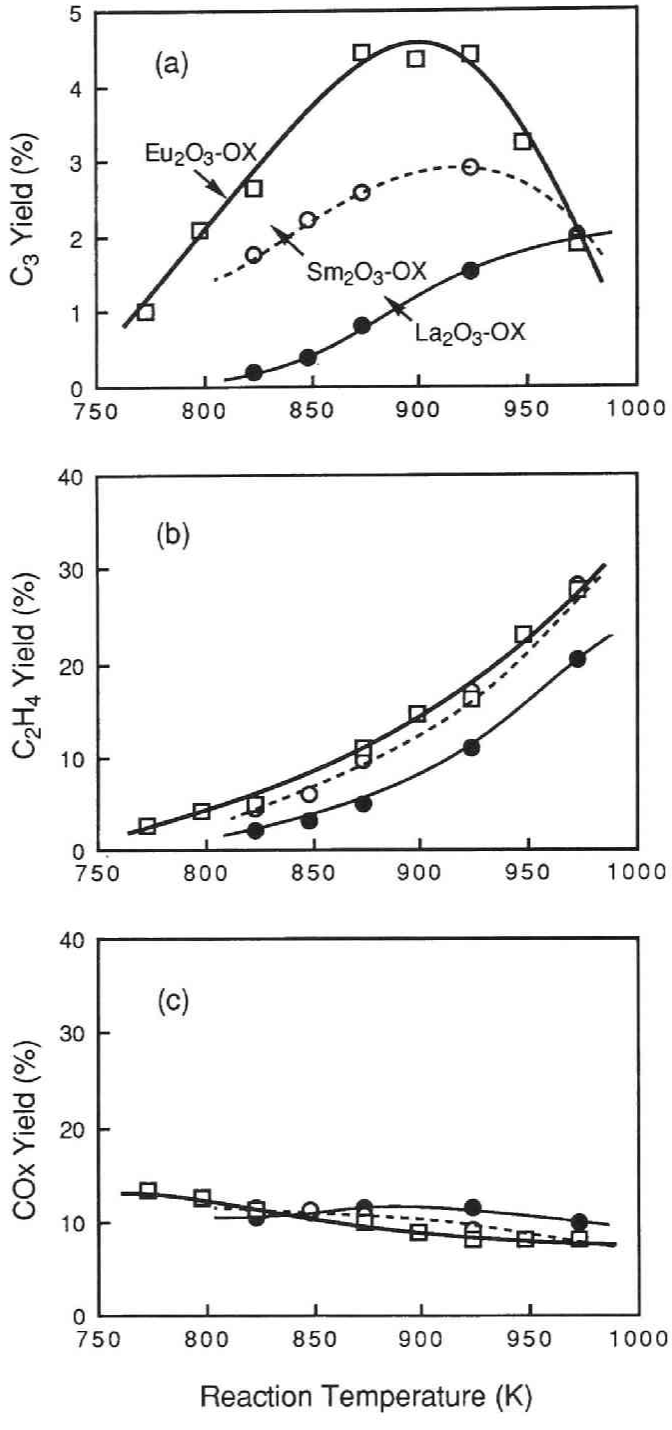

Figure 2. Effects of reaction temperature over rare earth oxide catalysts on (a) C_3 yields, (b) C_2H_4 yield and (c) CO_x yields. W/F, C_2H_6 feed rate, reaction gas composition were the same as shown in Figure 1. (●) = La_2O_3-OX, (○) = Sm_2O_3-OX and (□) = Eu_2O_3-OX.

Table 2. Oxidative Methylation of Ethane with Methane on Alkali and Alkaline Earth Metal Halide Loaded La_2O_3-OX at 923 K[a]

Run	Additive[c]	Conv.[b](%)		Yield[b](%)					(mmol·h^{-1})
		C_2H_6	O_2	C_2H_4	C_3H_6	C_3H_8	CO	CO_2	H_2
2	none	17.0	100	10.9	0.2	1.3	5.1	6.3	1.5
7	NaF (10)	10.6	68	9.9	0.3	1.3	1.9	4.3	0.9
8	KF (10)	12.8	60	8.5	0.1	1.0	1.6	5.1	0.7
9	LiCl (10)	17.0	94	11.4	0.3	2.0	5.6	4.4	1.5
10	NaCl (10)	15.9	78	12.1	0.3	1.8	4.9	4.6	1.5
11	KCl (10)	16.0	73	13.4	0.3	1.6	4.6	4.2	1.4
12	$MgCl_2$ (5)	14.3	85	9.2	0.1	0.7	4.7	5.9	1.0
13	$CaCl_2$ (5)	18.7	89	13.0	0.5	2.1	4.6	6.0	1.9
14	LiBr (10)	18.6	94	14.6	0.5	1.6	7.0	4.3	1.6
15	NaBr (10)	18.1	94	12.4	0.4	1.6	5.3	4.0	1.4
16	KBr (10)	19.5	80	14.0	0.5	1.7	5.4	4.1	1.4
17	$MgBr_2$ (5)	18.0	100	12.7	0.4	1.5	6.8	5.5	1.6
18	$CaBr_2$ (5)	14.3	91	12.0	0.3	1.3	4.5	5.1	1.5

[a] Amount of catalyst = 0.10 g, C_2H_6 feed rate = 7.5 mmol·h^{-1}, W/F = 1.2 g·h·mol^{-1}, CH_4 : C_2H_6 : O_2 : He = 18 : 3 : 1 : 10 (molar ratio).

[b] Based on ethane feed and oxygen feed.

[c] Numerals in the parentheses indicate the amount of halides loaded to La_2O_3-OX in mol%.

surface of the basic oxide catalysts after oxidative coupling of methane was covered with carbon dioxide in the form of metal carbonates.[17]

Activities of Alkali and Alkaline Earth Metal Halide Loaded Catalysts

Our previous study[13,14] revealed that addition of alkali metal halides to some of the alkaline earth metal oxide and rare earth oxide catalysts increased their catalytic activities for oxidative methylation of toluene with methane. Promoting effects of alkaline earth metal halides with alkaline earth oxides on oxidative dimerization of methane have been studied by Fujimoto et al.[18] Addition of these halides was reported to increase selectivity for ethene. In the present study, we examined oxidative methylation of ethane with the rare earth oxide catalysts modified with alkali and alkaline earth metal halides. Table 2 summarizes results on the La_2O_3-OX based catalysts at 923 K. The loading levels of alkali metal halides and alkaline earth metal halides were 10 mol% and 5 mol%, respectively. In chapter 6,[13,14] with the NaBr or KBr (5 wt.% as Na or K) loaded La_2O_3-OX catalysts, a small amount of needle like crystal was deposited on the outlet of the reactor tube after the activation for 120 min in a stream of air at above 973 K. However, in the present study, deposition of such crystals was not observed, probably because of smaller amounts of additives.

Addition of halides except for NaF, KF, and $MgCl_2$ increased the yields of C_3 compounds and ethene. Calcium chloride loaded La_2O_3-OX gave the highest yield of C_3 compounds, 2.6%, among the catalysts listed in Table 2. It should be noted that the loading of fluoride greatly decreased formation of carbon monoxide.

Figure 3 shows the product yields at various catalyst bed temperatures on the KF, KCl, and KBr loaded La_2O_3-OX catalysts. In general, formation of ethene was enhanced and that of carbon oxides was suppressed by addition of potassium halides. The KBr or KCl loaded catalysts showed the enhanced yields of C_3 compounds at relatively low temperatures (823 - 923 K). With KBr loaded La_2O_3-OX, the C_3 yield reached 2.4% at 898 K. An increase in the reaction temperature above 923 K decreased the yields of C_3 compounds. The yields of carbon oxides on La_2O_3-OX or KCl and KBr loaded La_2O_3-OX were almost unchanged from 823 K to 973 K. On the other hand, a KF loaded catalyst suppressed the

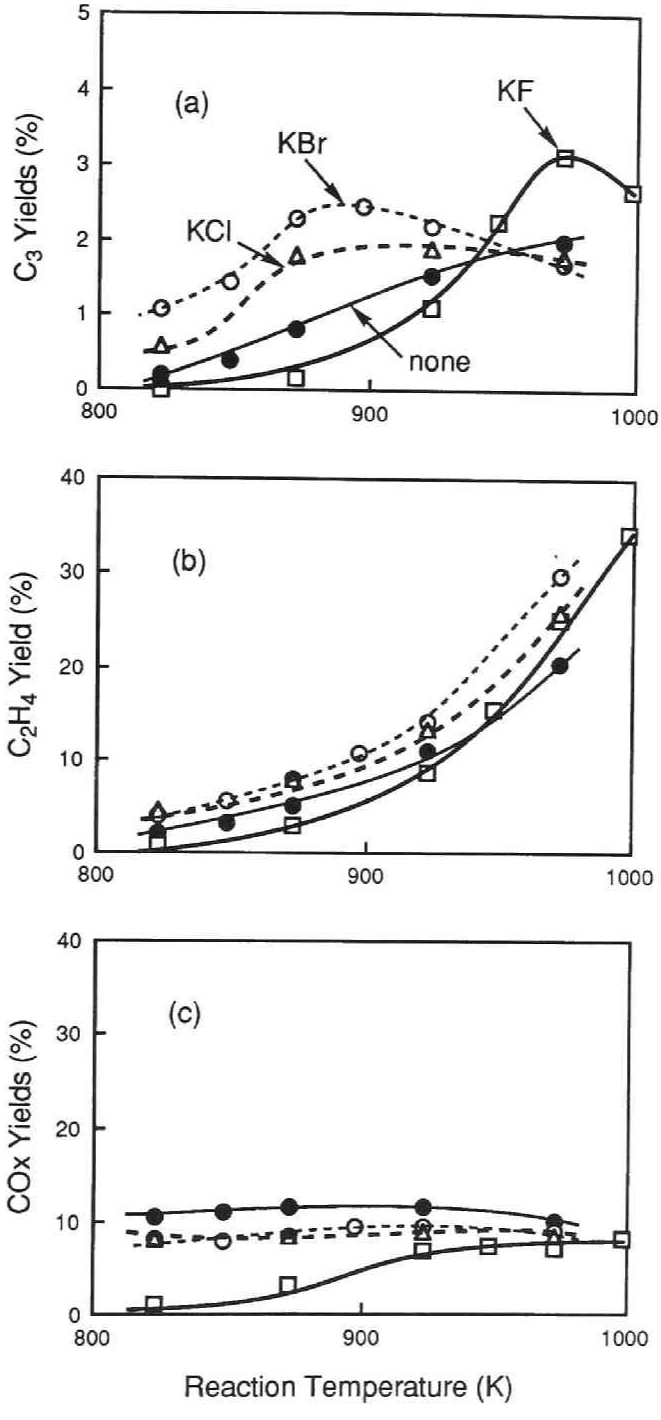

Figure 3. Effects of reaction temperature over potassium halide (10 mol%) loaded La_2O_3-OX catalysts. W/F, C_2H_6 feed rate, reaction gas composition were the same as shown in Figure 1.
(a) C_3, (b) C_2H_4, and (c) COx yields, (●) = La_2O_3-OX, and (□) = KF, (△) = KCl, (○) = KBr loaded La_2O_3-OX.

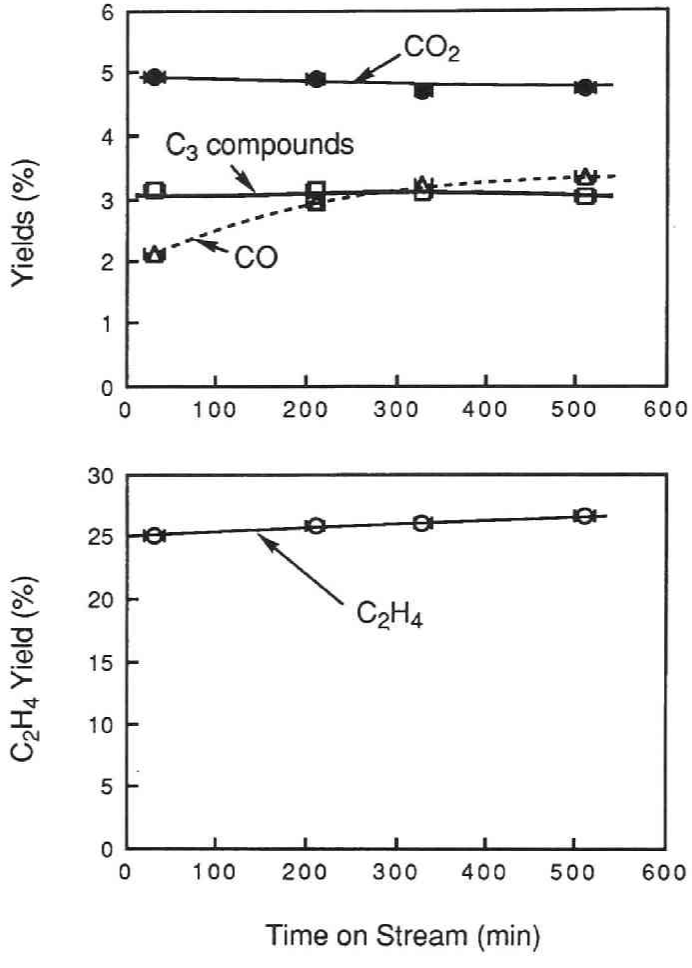

Figure 4. Changes in the yields of the products in the prolonged run at 973 K on KF (10 mol%) loaded La_2O_3-OX catalysts.W/F, C_2H_6 feed rate, reaction gas composition were the same as shown in Figure 1. (□) = C_3, (○) = C_2H_4, (△) = CO and (●) = CO_2 yield.

formation of C_3 compounds below 873 K. Above 923 K, the C_3 yield markedly increased with an increase in the reaction temperature and showed the maximum value of 3.1% at 973 K, indicating that loading of KF promotes C_3 formation at a higher temperature than that of KBr or KCl. Formation of carbon oxides on the KF loaded catalyst was suppressed at the temperature of 823 - 873 K, and gradually increased with an increase in the temperature, then levelled off above 923 K.

We investigated changes in catalytic activities of the KBr and KF loaded La_2O_3-OX catalysts with time on stream. No changes in the product yields and distribution were observed on the KBr (10 mol%) loaded La_2O_3-OX catalyst during the reaction for 180 min at 923 K. As shown in Figure 4, with the KF (10 mol%) loaded catalyst at 973 K, the yield of carbon monoxide increased from 2.1% with an increase in the reaction time and reached 3.4% after 500 - 520 min. The yield of ethene slightly increased in the course of the reaction, whereas those of C_3 compounds and carbon dioxide were unchanged. One of the probable reason for such changes is that KF might remain on the catalyst surface after the pretreatment at 973 K for 2 h. Fluoride would suppress formation of carbon monoxide by its strong electron negativity leading a considerable decrease in the polarization potential located on the surface oxide. During the course of the reaction, fluoride would be gradually lost, resulting in increasing the yields of carbon oxides.

Addition of alkali and alkaline earth halides to the oxides of samarium and europium, however, brought decreases in the yields of C_3 compounds, as shown in Table 3. The yields of carbon oxides were unchanged or slightly decreased, indicating that addition of these halides suppresses cross-coupling reaction rather than deep oxidation. Only the reaction with the KF loaded Eu_2O_3 catalyst at 973 K gave the higher C_3 yield of 3.5% than that with the parent oxide (2.8%). This increase in the yield of C_3 compounds at higher temperature might be due to suppression of ethene formation which would be competitive with cross-coupling reaction. Actually, the yield of ethene decreased with addition of KF from 27.4% to 23.3%.

In all the experiments described above, the catalysts were calcined in air for 120 min at the same temperature to the reaction temperature prior to the coupling reaction. Effects of pretreatment of the loaded catalyst were examined. As shown in Table 4, the C_3 yield of 1.2% on the KBr loaded La_2O_3-OX catalyst without pretreatment was lower than that

Table 3. Oxidative Methylation of Toluene on Alkali Metal Halide Loaded Sm_2O_3-OX and Eu_2O_3 Catalysts[a]

Run	Catalyst[c]	Temp. (K)	Conv.[b](%)		Yield[b](%)					(mmol·h^{-1})
			C_2H_6	O_2	C_2H_4	C_3H_6	C_3H_8	CO	CO_2	H_2
19	Sm_2O_3-OX	873	16.5	89	9.8	0.4	2.2	4.9	5.8	1.3
20	LiBr / Sm_2O_3-OX	873	13.0	70	5.9	0.1	0.5	4.6	5.1	1.2
21	NaBr / Sm_2O_3-OX	873	11.0	66	6.2	0.1	0.5	5.1	4.1	0.9
22	KBr / Sm_2O_3-OX	873	11.9	62	7.1	0.1	0.5	4.5	3.7	0.7
23	Eu_2O_3	973	31.3	90	27.4	0.8	2.1	4.1	3.2	1.2
5	Eu_2O_3	923	23.2	96	17.4	0.7	3.2	5.6	3.3	1.0
24	KF / Eu_2O_3	973	28.7	93	23.3	0.9	2.6	4.1	2.5	1.0
25	KF / Eu_2O_3	923	15.0	71	11.9	0.4	2.2	3.5	3.7	0.8
26	KCl / Eu_2O_3	923	12.0	46	10.1	0.2	1.0	2.8	1.7	0.5
27	KBr / Eu_2O_3	923	16.6	65	12.5	0.3	1.0	4.4	2.2	0.7

[a] Amount of catalyst = 0.10 g, C_2H_6 feed rate = 7.5 mmol·h^{-1}, W/F = 1.2 g·h·mol^{-1}, $CH_4 : C_2H_6 : O_2 : He = 18 : 3 : 1 : 10$ (molar ratio).

[b] Based on ethane feed and oxygen feed.

[c] Alkali metal halide was loaded 10 mol% to the rare earth oxide.

Table 4. Effects of Pretreatment of the Catalyst on Oxidative Methylation of Ethane with Methane at 873 K[a]

Run	Catalyst	Yield (%)[b] C_3H_6	C_3H_8	C_2H_4	CO	CO_2
28	KBr(10 mol%)/La_2O_3-OX	0.3	2.0	7.8	4.1	4.4
29[c]	KBr(10 mol%)/La_2O_3-OX	0.2	1.1	7.4	4.2	4.4
30	La_2O_3-OX	0.1	0.7	5.0	5.8	5.7
31[c]	La_2O_3-OX	0.1	0.9	6.5	6.0	7.3
32[c]	KBr	0.0	0.0	0.1	0.0	0.0
33[c]	KBr(20 wt.%)/SiO_2	0.0	0.0	3.8	2.7	0.3

a Amount of catalyst = 0.10 g, C_2H_6 feed rate = 7.5 mmol·h^{-1}, W/F = 1.2 g·h·mol^{-1}, CH_4 : C_2H_6 : O_2 : He = 18 : 3 : 1 : 10 (molar ratio).

b Yields in the initial reaction period (20 - 40 min) based on ethane feed.

c Without pretreatment.

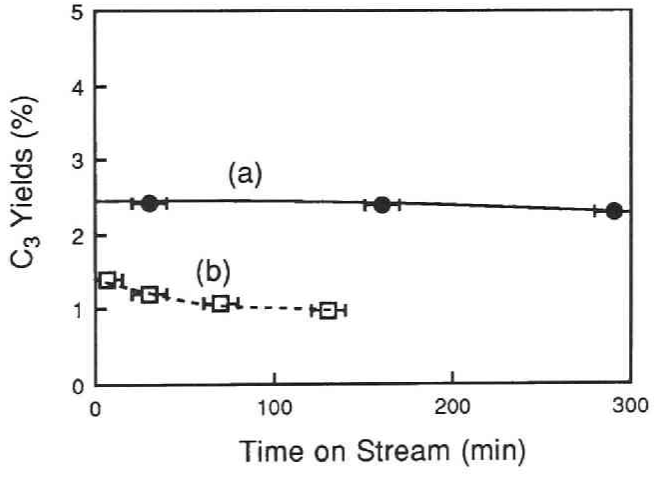

Figure 5. Changes in the yields of the products in the prolonged run at 873 K over the KBr (10 mol%) loaded La2O3-OX catalysts. W/F, C_2H_6 feed rate, reaction gas composition were the same as shown in Figure 1. (a) After pretreatment of the catalyst at 873 K for 2h, (b) fresh catalyst.

of pretreated one. The yields of C_3 compounds further decreased in the course of the reaction as shown in Figure 5, while the yields of ethene and carbon oxides were almost unchanged. Lower activities for C_3 formation by the lack of pretreatment seem not to be due to the deactivation of the parent oxides, since La_2O_3-OX showed the same C_3 yield whether with or without the heat treatment. Therefore with the halide loaded catalysts, the active sites, which selectively produce C_3 compounds, would be formed during activation in an air stream.

We performed the reaction with KBr powder and the silica supported KBr catalyst, in order to examine activity of KBr itself. Both KBr and silica supported KBr gave none of C_3 compounds. These results again suggest that KBr has an effect only to improve activities of the parent oxides which themselves have activities for the cross-coupling reaction, as described in a previous chapter.[14]

There are several reports concerning roles of halide additives. With the alkali metal chloride loaded oxide catalysts, Otsuka and Komatsu[19] proposed formation of compounded oxides active for oxidative coupling of methane on the surface of the halide loaded catalysts. Residual chlorine on the surface would be responsible for the promotion of dehydrogenation of ethane to ethene. Burch et al.[20] studied oxidative coupling of methane on a potassium-promoted manganese oxide catalyst. They reported that the selectivity for C_2 compounds was greatly enhanced by an injection of a single pulse of dichloromethane and it was maintained for a long period even after most of chlorine on the catalyst seemed to be lost. Their results were interpreted in terms of the surface modification by added chlorine. We have proposed one possible role of halides loaded on the catalysts in the study of oxidative methylation of toluene in a previous chapter.[13,14] Alkali or alkaline earth metals supplied from their halides seem to exist in the form of oxides during the reaction. The halogen should have a role of suppressing complete oxidation of reactants, intermediates and/or the C_8 products.

In addition, in the present study, loading of alkali and alkaline earth metal halides greatly enhanced catalytic activity of the La_2O_3-OX catalyst, but not those of Sm_2O_3-OX and Eu_2O_3. Furthermore, KBr itself did not show any activity for C_3 formation. These results indicate that the strong interaction between the surface of the parent oxide and additives induced the formation of active sites. The results shown in Table 4 and Figure 5 revealed that stable active sites for C_3 formation were formed

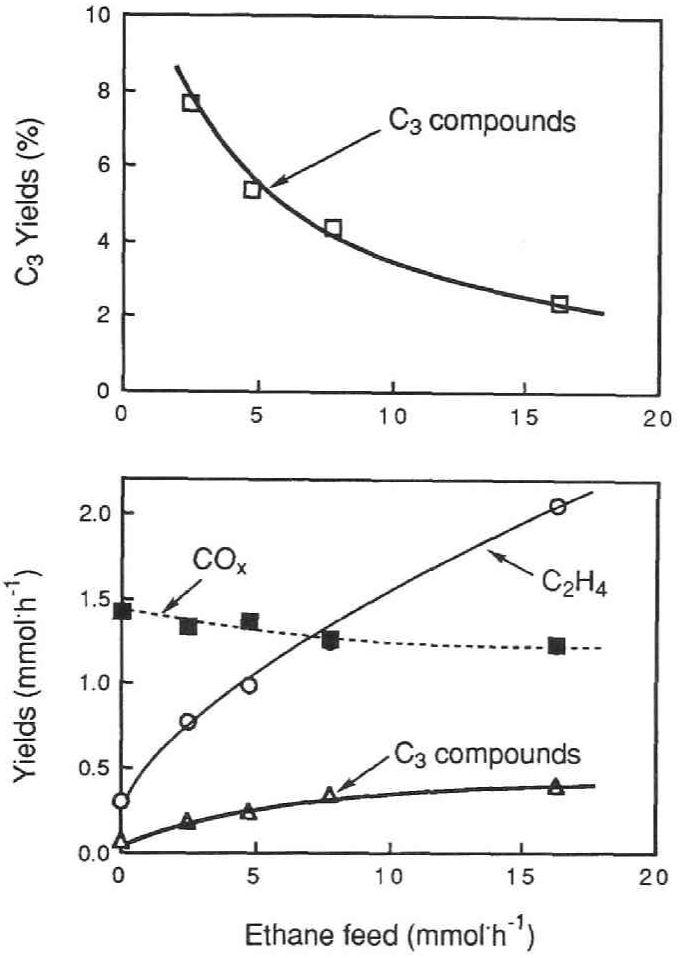

Figure 6. Effects of the amount of ethane in the feed gas on Eu_2O_3-OX catalyst at 923 K. W/F was the same as shown in Figure 1.
Methane feed rate = 45 mmol·h^{-1}, oxygen feed rate = 2.5 mmol·h^{-1}.
(△) absolute amounts of C_3 products, (○) C_2H_4, (■) CO + CO_2,
and (□) C_3 yield based on ethane feed.

during calcination in a stream of air just before the reaction. Most part of halide additives is assumed to be lost during the high temperature treatment in the presence of molecular oxygen, as we have demonstrated in chapter 6.[14] Thus a very small amount of residual additives, which interacts strongly with the oxide surface would be precursors to the stable active sites, although the nature of these sites is still unclear.

Effects of Reaction Conditions

As described above, Eu_2O_3-OX gave the maximum yield of C_3 products under the selected reaction conditions. In order to get informations on the reaction path, effects of the reaction conditions on the product distribution were investigated using the Eu_2O_3-OX catalyst.

Figure 6 shows effects of the amount of ethane in the feed gas on the product yields. Feed rates of methane, oxygen, and balance (helium) were fixed, thus the ratio of ethane to methane increased with increasing the amount of ethane. The absolute amounts of C_3 compounds gradually increased with increasing the amount of ethane. On the other hand, the apparent yield of C_3 compounds based on the ethane feed reached the maximum value of 7.7% with a smaller amount of ethane in the feed, 2.5 $mmol \cdot h^{-1}$. It should be noted that C_4 hydrocarbons were formed in fairly high yield of 0.9% when a larger amount of ethane (16 $mmol \cdot h^{-1}$) was fed.

Effects of oxygen feed between 0.9 $mmol \cdot h^{-1}$ and 6.8 $mmol \cdot h^{-1}$ on the Eu_2O_3-OX catalyst were examined, with methane and ethane feed being kept at 45 $mmol \cdot h^{-1}$ and 7.5 $mmol \cdot h^{-1}$, respectively. Results are shown in Figure 7. Although formation of C_3 compounds was leveled off at a higher feed rate of O_2, the yields of ethene and carbon oxides increased continuously with an increase in the O_2 feed. A oxygen feed rate of 2 - 3 $mmol \cdot h^{-1}$ seems to be optimum for C_3 formation.

We accomplished the experiments without methane or ethane to determine the reaction path. As shown in Table 5, the reaction without methane on La_2O_3 and Eu_2O_3 afforded mainly ethene and carbon oxides. Very small amounts of C_3 compounds were detected compared to that with both methane and ethane. When the reaction gas did not contain ethane, only trace amounts of C_3 compounds were formed (see Figure 6).

Figure 8 shows effects of W/F on the yields of the products by changing the amounts of the Eu_2O_3-OX catalyst at 923 K and of the KBr(10 mol%) loaded La_2O_3-OX at 873 K. The reaction at 873 K with quartz glass

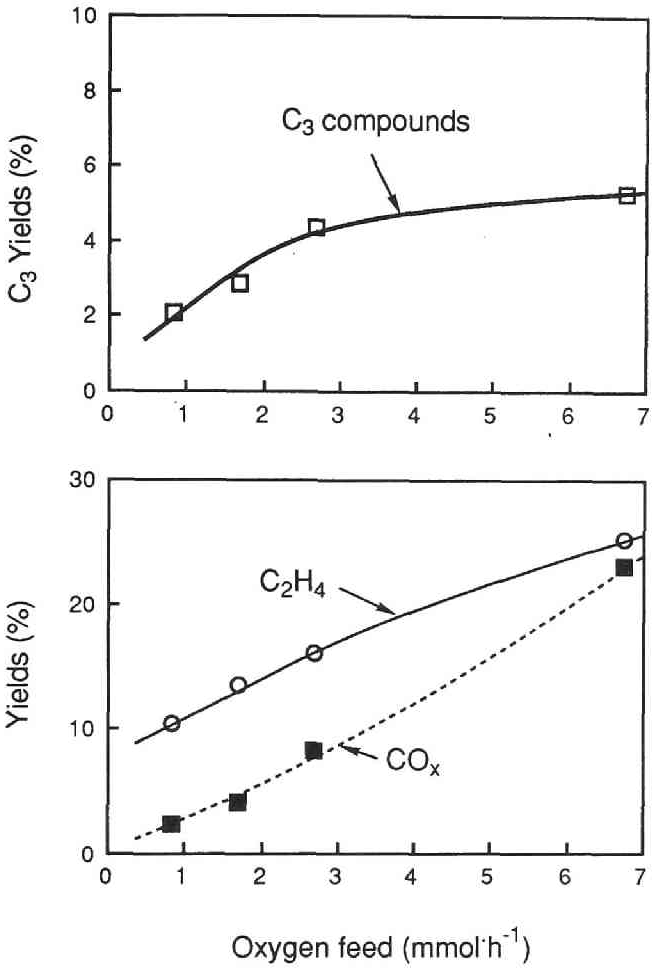

Figure 7. Effects of the amount of oxygen in the feed gas on Eu_2O_3-OX at 923 K. W/F = 1.2 g·h·mol^{-1}, methane feed rate = 45 mmol·h^{-1}, ethane feed rate = 7.5 mmol·h^{-1}. (□) C_3, (○) C_2H_4, (■) CO + CO_2 yields.

Table 5. Reaction with or without Methane[a]

Run	Catalyst	CH_4 Feed ($mmol \cdot h^{-1}$)	Products ($mmol \cdot h^{-1}$)					
			C_2H_4	C_3H_6	C_3H_8	CO	CO_2	H_2
1	La_2O_3	45	0.46	0.01	0.11	0.65	0.52	0.6
34	La_2O_3	0	0.70	0.02	0.02	0.73	0.83	0.7
5	Eu_2O_3	45	1.35	0.05	0.25	0.87	0.50	1.0
35	Eu_2O_3	0	1.42	0.03	0.02	0.72	0.50	0.6

[a] Reaction temperature = 923 K, amount of catalyst = 0.10 g, W/F = 1.2 $g \cdot h \cdot mol^{-1}$, C_2H_6 feed rate = 7.5 $mmol \cdot h^{-1}$, O_2 feed rate = 2.5 $mmol \cdot h^{-1}$, balance = He.

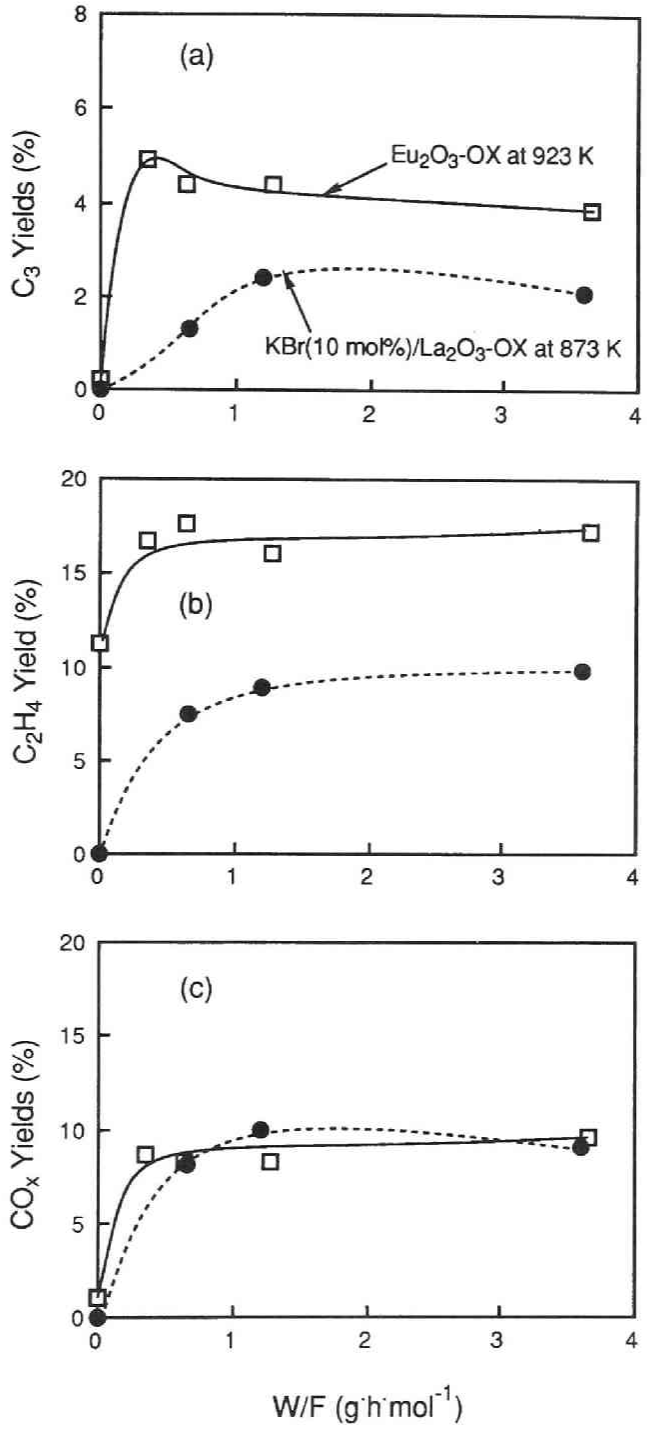

Figure 8. Effects of W/F by changing the amount of the catalyst.
(□) Eu_2O_3-OX at 923 K and (●) KBr (10 mol%)/La_2O3-OX at 873 K.
Reaction gas composition was the same as shown in Figure 1.
(a) C_3, (b) C_2H_4, (c) CO + CO_2 yields.

wool plug alone which was used for holding the catalyst bed yielded almost none of the products, but a fair amount of ethene at 923 K. Propane and propene were not formed both at 873 K and 923 K. This indicates that dehydrogenation from ethane to ethene could proceed above 923 K even in the absence of the catalyst, whereas the cross-coupling reaction between methane and ethane did not occur. With only 0.029 g of the Eu_2O_3-OX catalyst at 923 K (W/F = 0.35 $g \cdot h \cdot mol^{-1}$), the highest C_3 yield of 4.9% was achieved, and the conversion of oxygen reached nearly 100%. The C_3 yields then gradually decreased with increasing W/F. The reaction with further decreasing W/F was not performed, since packing of a smaller amount of the catalyst in uniform layer was not possible. The yields of ethene and carbon oxides were unchanged regardless of W/F above 0.35 $g \cdot h \cdot mol^{-1}$. These results indicate that the Eu_2O_3-OX catalyst is active enough to complete the reaction with only about 0.030 g of the catalyst. With further increasing W/F, a part of the catalyst would not fully work due to the lack of molecular oxygen. Oxidation of C_3 compounds by the lattice oxygen of Eu_2O_3-OX catalyst might occur to a small extent, resulting in slight decreases in the C_3 yields with a larger amount of catalyst. On the other hand, the C_3 yields showed the maximum at W/F of 1.2 $g \cdot h \cdot mol^{-1}$ (amount of the catalyst; 0.10 g) for the KBr loaded La_2O_3-OX catalyst at the lower temperature of 873 K, suggesting that higher W/F is required to achieve the maximum C_3 yield due to the smaller reaction rate.

From these findings we may draw some informations on the reaction mechanism. The oxidative coupling reaction seems to be initiated with abstraction of hydrogen from methane and ethane to form methyl and ethyl radical species, as shown in eqs. (1) and (2).

The surface oxygen species, which selectively abstract hydrogen from alkanes, have been proposed to be O^- anion radicals by Lunsford et al. on oxidative coupling of methane with the Li doped MgO catalyst.[2] On the other hand, Otsuka et al. reported that O_2^{2-} species should be responsible for the formation of methyl radicals on the Sm_2O_3 catalyst.[21] Our results presented in this paper, however, gave only obscure informations about the active surface oxygen species.

The results without methane or ethane indicate that C_3 compounds are mainly produced via cross-coupling of methyl and ethyl radical species, as shown in eq.(3). Abstraction of one more hydrogen from ethyl radical species (eq.(4)) to form ethene might compete with the cross-

coupling reaction. Thus formation of ethene would consequently suppress the yields of C_3 compounds. Above 923 K, a considerable amount of ethene may be formed thermally in the gas phase, since ethene was formed even in the absence of the catalyst (eq. (5), and see Figure 8). When the reaction gas included a large amount of ethane, C_4 hydrocarbons (butane and butenes) were formed in relatively high yields. They would form via homo-coupling of ethyl radical species. This suggests that the ratio of methyl to ethyl radical species on the surface depends on the ratio of methane to ethane in the gas phase. Activation of methane and ethane might proceed competitively on the surface active centers. The reaction of ethane, which was formed by oxidative coupling of methane, with methane in the feed is also possible to give small amounts of C_3 compounds. Furthermore, as indicated by the results in the reaction without methane, a very small part of C_3 compounds seemed to be formed by a cracking of butane (eq.(6)). Formation of C_3 products via addition of methane to ethene, a dehydrogenated product from ethane, has been ruled out on the basic oxide catalysts by Otsuka et al.[16]

$$CH_4 + [O] \longrightarrow CH_3\cdot + [O]\text{-}H \quad (1)$$

$$C_2H_6 + [O] \longrightarrow C_2H_5\cdot + [O]\text{-}H \quad (2)$$

$$CH_3\cdot + C_2H_5\cdot + M \longrightarrow C_3H_8 + M \quad (3)$$

$$C_2H_5\cdot + [O] \longrightarrow C_2H_4 + [O]\text{-}H \quad (4)$$

$$C_2H_6 \longrightarrow C_2H_4 + H_2 \quad (5)$$

$$2C_2H_5\cdot + M \longrightarrow C_4H_{10} \longrightarrow C_3H_6 + CH_4 \quad (6)$$

where [O] = surface oxygen species,
M = media.

References

1 P. Pitchai and K. Klier, *Catal. Rev.-Sci. Eng., 28 (1)*, **1986**, 13.

2 G. Keller and M. Bhasin, *J. Catal., 73,* **1982,** 9.

3 T. Ito, J.X. Wang, G.H. Lin and J.H. Lunsford, *J. Am. Chem. Soc., 107,* **1985**, 5062.

4 K. Otsuka, K. Jinno and A. Morikawa, *Chem. Lett.,* **1985**, 499.

5 K. Aika, T. Moriyama, N. Takasaki and E. Iwamatsu, *J. Chem. Soc., Chem. Commun.,* **1986**, 1210.

6 K. Asami, S. Hashimoto, T. Shikada, K. Fujimoto and H. Tominaga, *Chem. Lett.,* **1986**, 1233.

7 T. Moriyama, N. Takasaki, E. Iwamatsu and K. Aika, *Chem. Lett.,* **1986**, 1165.

8 Kh.E. Kcheyan, O.M. Revenko and A.N. Shatalova, *Proc. -World Pet. Congress., 11(4),* **1984**, 465.

9 N. Yakovich, L.P. Bokareva and A.G. Kostyuk, *Pr-va Krupnotonnazhn, Prouktov Neftekhimii, M.,* **1979**, 37 in *Chem Abstr., 93,* **1980**, 7755d.

10 Y. Osada, K. Enomoto, T. Fukushima, S. Ogasawara, T. Shikada and T. Ikariya, *J. Chem. Soc., Chem. Commun.,* **1989**, 1156.

11 Y. Osada, S. Ogasawara, T. Fukushima, T. Shikada and T. Ikariya, *J. Chem. Soc., Chem. Commun.,* **1990**, 1434.

12 Y. Osada, N. Okino, S. Ogasawara, T. Fukushima, T. Shikada and T. Ikariya, *Chem. Lett.,* **1990**, 281.

13 T. Suzuki, K. Wada and Y. Watanabe, *Appl. Catal., 53,* **1989**, L19 (Chapter 6).

14 T. Suzuki, K. Wada and Y. Watanabe, *Ind. Eng. Chem. Res., 30,* **1991**, 1719 (Chapter 6).

15 T. Sodesawa, M. Matsubara, S. Satoh and F. Nozaki, *Chem. Lett.,* **1987**, 1513.

16 K. Otsuka et al. reported oxidative methylation of ethane with methane on the basic oxide catalysts in the 66th anual meeting of the Catalysis Society of Japan, in Nagasaki, **1990**.

17 T. Suzuki, K. Wada and Y. Watanabe, *Appl. Catal., 59,* **1990**, 213 (Chapter 5).

18 K. Fujimoto, S. Hashimoto, K. Asami and H. Tominaga, *Chem. Lett.,* **1987**, 2157.

19 K. Otsuka and T. Komatsu,
J. Chem. Soc., Chem. Commun., **1987**, 388.
20 R. Burch, G.D. Squire and S.C. Tsang, *Appl. Catal., 46,* **1989**, 69: R. Burch, E.M. Crabb, G.D. Squire and S.C. Tsang, *Catal. Lett.*, **1989**, 249: R. Burch, S. Chalker, G.D. Squire and S.C. Tsang, *J. Chem. Soc., Faraday Trans., 86 (9),* **1990**, 1607.
21 K. Otsuka, *Sekiyu Gakkaishi, 30 (6),* **1987**, 385.

Concluding Remarks and List of Publications

Concluding Remarks

New methodology for direct conversion of light alkanes via selective partial oxidation using various solid metal oxide catalysts was described in this thesis.

Part I dealt with photocatalytic selective oxidation of methane, ethane, propane and propene to oxygen-containing chemicals over the supported oxide catalysts and unsupported solid oxide semiconductor catalysts at around 450 - 550 K.

In chapter 1, results of selective partial oxidation of methane in the presence of a supported molybdenum oxide catalyst under UV irradiation, using a fluidized bed flow-type reaction system, were described. With 0.025 g of the silica supported MoO_3(4.4 wt.%) prepared by the usual impregnation method, methanal was formed in the highest yield of 19 $\mu mol \cdot h^{-1}$ at around 503 K, CH_4 flow rate of 7.5 $mmol \cdot h^{-1}$ and the ratio of CH_4 : O_2 : He at 6 : 2 : 25. Six $\mu mol \cdot h^{-1}$ of carbon monoxide was also formed. The yield of methanal depended on the loading levels of MoO_3 and the reaction temperature. At an ambient temperature, only a trace amount of methanal was formed. Partial oxidation of ethane and propane was also examined in the similar reaction system. The highest yield of ethanal (60 $\mu mol \cdot h^{-1}$) together with methanal (22 $\mu mol \cdot h^{-1}$) was achieved in photo-oxidation of ethane over the MoO_3(2.5 wt.%)/SiO_2 catalyst under the reaction conditions as follows: Reaction temperature; 493 K, C_2H_6 flow rate; 19 $mmol \cdot h^{-1}$, C_2H_6 : O_2 : He; 15 : 2 : 11. The amount of total carbon oxides was *ca.* 5 $\mu mol \cdot h^{-1}$. Photo-oxidation of propane using the same catalyst under the similar conditions afforded propanal, acetone and ethanal (total yield; 60 $\mu mol \cdot h^{-1}$). The combined selectivity for these chemicals reached 95%. UV irradiation was indispensable for the all reactions. The active surface species responsible for the activation of alkanes seems to be photoactivated charge transfer complexes on the surface, such as Mo^{5+}-O^-.

Chapter 2 dealt with photo-oxidation of light alkanes over the solid metal oxide semiconductors, such as ZnO and TiO_2 using a fixed bed flow-type reaction apparatus at around 500 K. Reaction conditions were as follows: amount of the catalyst; 0.25 g, alkane feed rate; 7.5 $mmol \cdot h^{-1}$. alkane : O_2 : He; 3 : 1 : 10. Activity of zinc oxide catalysts for photo-oxidation of ethane and propane greatly enhanced with an increase in the

reaction temperature. Ethanal was formed in the yield of 84 $\mu mol \cdot h^{-1}$ with the selectivity more than 70%. Photo-oxidation of propane over the same catalyst yielded propanal and acetone (ca. 1 : 1) in the combined yield of 113 $\mu mol \cdot h^{-1}$ (selectivity; 76%). Photo-oxidation of methane afforded a small amount of methanal (4.7 $\mu mol \cdot h^{-1}$). As far as we know, this is the first example of selective formation of methanal by photocatalytic oxidation of methane over solid semiconductors. But the principal product of methane oxidation was carbon dioxide, and the selectivity for methanal was low (less than 10%). All the reactions required UV irradiation and elevated reaction temperatures to give oxidation products. Catalytic activity depended on characteristics of zinc oxide. Photo-oxidation of methane on TiO_2 predominantly gave carbon oxides, and the yields of the products increased with an increase in the reaction temperature. On the other hand, in the reaction with ethane and propane, the yield of carbon oxides decreased at elevated temperatures.

Chapter 3 described improving effects of molybdenum oxide loading on the zinc oxide catalyst on the selectivity for photo-oxidation of methane. The reaction with the MoO_3(2.0 wt.%)/ZnO catalyst at 548 K yielded methanal in the yield of 8.0 $\mu mol \cdot h^{-1}$ with the high selectivity, whereas the parent ZnO catalyst mainly produced carbon dioxide. UV irradiation and catalyst bed temperatures above 400 K were indispensable. Loading of MoO_3 on ZnO, however, markedly decreased the catalytic activity for photo-oxidation of ethane and propane.

In chapter 4, studies on photocatalytic oxidation at elevated temperatures were extended to propene using the ZnO, MoO_3/ZnO and MoO_3/SiO_2 catalysts. Propenal, ethanal and carbon dioxide were predominantly formed over ZnO. On the other hand, MoO_3 loaded ZnO gave propanal in addition to ethanal, whereas formation of propenal and carbon dioxide was suppressed. With silica supported molybdenum oxide similar product yields were obtained to those with MoO_3/ZnO. The active species over MoO_3/ZnO seemed to be provided from the loaded molybdenum species.

Part II dealt with the investigations on oxidative homo-coupling of methane, and cross-coupling of toluene and ethane with methane over various basic metal oxide catalysts.

Chapter 5 described effects of the use of carbon dioxide as a reactive diluent for oxidative coupling of methane to C_2 compounds (ethane and ethene) over group IIA and IIIB metal oxide catalysts prepared by several

methods. Alkaline earth metal oxide based catalysts prepared from their oxalates exhibited higher C_2 space time yields than commercial ones. The multicomponent catalyst, Sm_2O_3(15 wt.%)/MgO-OX, which was prepared from the decomposition of oxalates at 1173 K, showed the highest catalytic activity. When the diluent of the reactant gas was changed from He to CO_2, the C_2 yield and selectivity increased significantly with magnesium oxide based catalysts. Optimum partial pressure of carbon dioxide in the feed greatly depended on alkaline earth metal oxide and the reaction temperature. Deactivation of the catalyst during a prolonged run was suppressed in carbon dioxide atmosphere, probably due to preventing from coke deposition.

Chapter 6 dealt with oxidative methylation of toluene with methane to styrene and ethylbenzene (C_8 compounds) over various metal oxide catalysts at 973 1023 K. Several group IIIB metal oxides and calcium oxide were found to be active and selective catalysts. The activities and selectivities of these catalysts could be improved by addition of alkali and alkaline earth metal halides. Sodium bromide promoted lanthanum oxide exhibited the highest C_8 yield of 23.9 % and the C_8 selectivity of 40.2 %. The optimum conditions were as follows: reaction temperature; 1023 K, partial pressure of methane; 4 9 kPa, methane, oxygen and toluene molar ratio of 50 : 5 : 1.7. The reaction was proved to proceed predominantly via oxidative cross-coupling of methane and toluene through the studies using toluene-d_8. The essential role of the halides was assumed to provide active and selective sites on the surface of oxide based catalysts.

In chapter 7, studies on oxidative methylation of ethane with methane were described. Propane and propene (C_3 compounds) were produced together with a large amount of ethene. Several rare earth oxides showed fair catalytic performances. Among them, europium oxide gave the C_3 products in the highest yield of 7.7% at 973 K (amount of catalyst; 0.10 g, ethane feed rate; 2.5 mmol·h^{-1}, the molar ratio CH_4 : C_2H_6 : O_2 : He; 18 : 1 : 1 : 12). The alkali and alkaline earth halides loaded lanthanum oxide catalysts showed higher activities than the parent oxide catalyst, whereas addition of theses halides on europium oxide completely suppressed its catalytic activity.

In summary, several novel methodology of direct conversion of light alkanes, especially methane, in both photocatalysis and heterogeneous thermal catalytic reactions were explored, and details of the reactions were investigated extensively. Through these studies, selective oxidation

of methane to methanal, and effective utilization of methane as a source for carbon-carbon bond formation to give valuable hydrocarbons such as styrene or propene were achieved.

Finally the present author believes that the investigation in the present thesis would contribute widely for development of heterogeneous catalysis in the alkane conversion technology.

List of Publications

Chapter 1 manuscript under preparation.

in short communications,
J. Chem. Soc., Chem. Commun., **1990**, 1059.
Appl. Catal., 74, **1991**, L1.

Chapter 2 manuscript under preparation.

Chapter 3 manuscript under preparation.

parts of chapters 2 and 3 are published
in following short communication,
J. Chem. Soc., Chem. Commun., **1991**, 726.

Chapter 4 manuscript under preparation.

Chapter 5 *Appl. Catal., 59*, **1990**, 213.

Chapter 6 *Ind. Eng. Chem. Res., 30*, **1991**, 1719.

in short communication,
Appl. Catal., 53, **1989**, L19.

Chapter 7 *Appl. Catal.,* under contribution.